**DESIGN OF 4X4 BUTLER SMART ANTENNA ARRAY FOR 5G COMMUNICATION SYSTEM**



By

**MAKY MOHAMMED SADIQ MAKY**

**Thesis Submitted to the School of Graduate Studies, Universiti Putra Malaysia, in Fulfilment of the Requirements for the Degree of Doctor of Philosophy**

**February 2024**

**FK 2024 34**

Abstract of thesis presented to the Senate of Universiti Putra Malaysia in fulfilment of the requirement for the degree of Doctor of Philosophy

**DESIGN OF 4X4 BUTLER SMART ANTENNA ARRAY FOR 5G COMMUNICATION SYSTEM**

By

**MAKY MOHAMMED SADIQ MAKY**

**February 2024**

**Chairman : Associate Professor Nasri bin Sulaiman, PhD**
**Faculty : Engineering**

This thesis responds to the escalating demand for high-performance wireless communication networks by introducing an innovative antenna system that merges a 4x4 Butler matrix with a 1x4 linear array antenna. This cutting-edge system incorporates machine learning algorithms deployed on an embedded control chip, fostering optimized performance and adaptability to meet the requirements for faster data rates, higher capacity, and improved coverage.

The exploration begins with the scrutiny of three distinct antenna designs for comparison and selection to construct the antenna array within the Butler Matrix network. The first design involves a printed Meander Line Antenna (MLA) tailored for LTE mobile terminals, showcasing a bandwidth of 57 MHz, compact dimensions (32 × 28 × 1.1) mm³, and a frequency of 2.5 GHz. The second design features a Multiband Hand-Held Antenna with E-shaped Monopole Feeding, validated through simulation and measurements. The third design adopts an inverted U slot antenna for

a 5G antenna array, demonstrating low reflection coefficient, gain, and omni-directional radiation patterns at 28 GHz.

Following the individual designs, the multi-beam antenna array is established, achieving matching at 50Ω and high gain with four beams directed at specific angles. The Butler matrix, reduced in size and components, generates four beams with high isolation and transmission coefficients. The final design's compact size (23 mm × 20.5 mm) facilitates integration with other devices, outperforming traditional designs with up to 11 dB gain.

The ultimate proposal introduces an intelligent antenna system amalgamating a multi-beam antenna for 5G at 28 GHz, a 4x4 modified Butler matrix, a 1x4 linear array antenna, and the Random Forest Decision algorithm implemented on an embedded control chip. This advanced system allows dynamic beam steering and adaptive beamforming, vital for efficient 5G communication, adapting to network needs based on user demand and environmental factors.

Simulation studies and experimental results comprehensively analyze the proposed antenna system, focusing on beamforming, spatial diversity, interference mitigation, and the effectiveness of machine learning algorithms. The system exhibits superiority over conventional antennas, showcasing potential applications in IoT devices, mobile communication networks, and scenarios requiring adaptive antenna systems. The integration of machine learning algorithms on the embedded control chip equips the system to tackle diverse challenges associated with these applications.

This work significantly contributes to the ongoing endeavors in miniaturizing Butler Matrix Networks while preserving, and even enhancing, their performance. This work also contributes to addressing a pertinent issue in traditional antenna systems, which often consume substantial power regardless of the receiver's actual requirements. Our modeling approach incorporates innovative power conservation mechanisms. This addition responds to the growing concern of energy efficiency in wireless communication networks. By intelligently adapting power consumption based on the communication scenario and environmental factors, the proposed system aligns with contemporary efforts to create sustainable and eco-friendly communication technologies.

**KEYWORDS:** 5G Technology, Butler-Matrix, Multi-Beam Antenna, Slot Antenna Array, Wideband.

**SDG:** GOAL 9: Industry, Innovation, and Infrastructure

**SDG:** GOAL 11: Sustainable Cities and Communities

Abstrak tesis yang dikemukakan kepada Senat Universiti Putra Malaysia sebagai memenuhi keperluan untuk ijazah Doktor Falsafah

**REKA BENTUK 4X4 BUTLER SMART ANTENNA ARRAY UNTUK SISTEM KOMUNIKASI 5G**

Oleh

**MAKY MOHAMMED SADIQ MAKY**

**Februari 2024**

**Pengerusi : Profesor Madya Nasri bin Sulaiman, PhD**
**Fakulti : Kejuruteraan**


Tesis ini merupakan maklumbalas kepada permintaan yang semakin meningkat untuk rangkaian komunikasi tanpa wayar berprestasi tinggi dengan memperkenalkan sistem antena inovatif yang menggabungkan matriks Butler 4x4 dengan antena tatasusunan linear 1x4. Sistem canggih ini menggabungkan algoritma pembelajaran mesin yang digunakan pada cip kawalan terbenam, lantas mencipta prestasi yang optimum dan kebolehsuaian bagi memenuhi keperluan untuk kadar data yang lebih pantas, kapasiti yang lebih tinggi, dan liputan yang lebih baik.

Penerokaan bermula dengan penelitian tiga reka bentuk antena berbeza untuk perbandingan dan pemilihan bagi membina tatasusunan antena dalam rangkaian Butler Matrix. Reka bentuk pertama melibatkan Antena Talian Meander (MLA) bercetak yang disesuaikan untuk terminal mudah alih LTE, dengan lebar jalur 57 MHz, dimensi padat (32 × 28 × 1.1) $mm^3$, dan frekuensi 2.5 GHz. Reka bentuk kedua menampilkan Antena Tangan Berbilang Jalur dengan Suapan Monopole berbentuk E, disahkan melalui simulasi dan pengukuran. Reka bentuk ketiga

menggunakan antena slot U terbalik untuk tatasusunan antena 5G, dengan pekali pantulan rendah, perolehan dan corak sinaran omni-arah pada 28 GHz.

Mengikut reka bentuk individu, tatasusunan antena berbilang rasuk diwujudkan, mencapai padanan pada 50Ω dan pencapaian tinggi dengan empat rasuk diarahkan pada sudut tertentu. Matriks Butler, dikurangkan dalam saiz dan komponen, menghasilkan empat rasuk dengan pekali pengasingan dan penghantaran yang tinggi. Saiz kompak reka bentuk akhir (23 mm × 20.5 mm) memudahkan penyepaduan dengan peranti lain, mengatasi reka bentuk tradisional dengan peningkatan sehingga 11 dB.

Cadangan muktamad memperkenalkan sistem antena pintar yang menggabungkan antena berbilang rasuk untuk 5G pada 28 GHz, matriks Butler yang diubahsuai 4x4, antena tatasusunan linear 1x4, dan algoritma Random Forest Decision yang dilaksanakan pada cip kawalan terbenam. Sistem canggih ini mencipta stereng rasuk dinamik dan pembentukan rasuk adaptif, yang mana penting untuk komunikasi 5G yang cekap, yang boleh disesuaikan dengan keperluan rangkaian berdasarkan permintaan pengguna dan faktor persekitaran.

Kajian simulasi dan hasil percubaan menganalisis secara komprehensif sistem antena yang dicadangkan, dengan fokus ke atas pembentukan pancaran, kepelbagaian ruang, pengurangan gangguan, dan keberkesanan algoritma pembelajaran mesin. Sistem ini lebih unggul berbanding antena konvensional, mempamerkan potensi aplikasi dalam peranti IoT, rangkaian komunikasi mudah alih, dan senario yang memerlukan sistem antena penyesuaian. Penyepaduan algoritma pembelajaran mesin

pada cip kawalan terbenam melengkapkan sistem untuk menangani pelbagai cabaran berkaitan aplikasi ini.

Kajian ini memberi sumbangan signifikan kepada usaha berterusan dalam mengecilkan Butler Matrix Networks sambil mengekalkan, malah meningkatkan prestasinya. Kajian ini juga menangani isu penting dalam sistem antena tradisional, yang mana sering menggunakan kuasa besar tanpa mengira keperluan sebenar penerima. Pendekatan pemodelan kami menggabungkan mekanisme penjimatan kuasa yang inovatif. Penambahan ini adalah maklumbalas kepada kebimbangan yang semakin meningkat mengenai kecekapan tenaga dalam rangkaian komunikasi tanpa wayar. Dengan menyesuaikan penggunaan kuasa secara bijak berdasarkan senario komunikasi dan faktor persekitaran, sistem yang dicadangkan adalah sejajar dengan usaha kontemporari untuk mencipta teknologi komunikasi yang mampan dan mesra alam.

**Kata kunci:** antena berbalas multi-peluru, jalur lebar, matriks Butler, selamba antena slot, Teknologi 5G.

**SDG:** Matlamat 9: Industri, Inovasi, dan Infrastruktur

**SDG:** Matlamat 11: Bandar dan Komuniti Mampan

## ACKNOWLEDGEMENTS

Firstly, I would like to thank the chairman of the supervisory committee, Assoc. Prof. Dr. Nasri Bin Sulaiman for his support, encouragement, patience and dedication throughout the duration of my study. This work would not have been possible without his guidance and input.

I would also like to thank the members of the supervisory committee, Prof. Dr. Mohd Nizar Bin Hamidon and Prof. Dr. Maryam Binti Mohd Isa, who had helped me during times of difficulty.

Special thanks to my parents for their prayers and support which have kept me going during my study.

Most of all, I wish to thank my wife and my sons, Mustafa, Zahraa, Yusif, and Lozan to whom without their support and patience, this work would not have been possible to complete.

Finally, I would like to thank all those who have helped me to solve any related technical problems.

This thesis was submitted to the Senate of Universiti Putra Malaysia and has been accepted as fulfillment of the requirement for the degree of Doctor of Philosophy. The members of the Supervisory Committee were as follows:

**Nasri bin Sulaiman, PhD**
Associate Professor
Faculty of Engineering
Universiti Putra Malaysia
(Chairman)

**Maryam binti Mohd Isa, PhD**
Associate Professor
Faculty of Engineering
Universiti Putra Malaysia
(Member)

**Mohd Nizar bin Hamidon, PhD**
Professor
Faculty of Engineering
Universiti Putra Malaysia
(Member)

______________________________

**ZALILAH MOHD SHARIFF, PhD**
Professor and Dean
School of Graduate Studies
Universiti Putra Malaysia

Date: 16 May 2024

## TABLE OF CONTENTS

## LIST OF TABLES

## LIST OF FIGURES

# LIST OF ABBREVIATIONS

| | |
|---|---|
| 1 G | First Generation |
| 2 G | Second Generation |
| 3 G | Third Generation |
| 3 GPP | 3rd Generation Partnership Project |
| 4 G | Fourth Generation |
| 5 G | Fifith Generation |
| CPW | Coplanar Waveguide |
| CST | Computer Simulation Technology |
| WLAN | Wireless Local Area Network |
| mm-wave | Millimeter-wave |
| BFN | Beamforming network |
| IFA | Inverted-F Antenna |
| QoS | Quality of Service |
| BM | Butler Matrix |
| dB | Decibel |
| DCS | Digital Cellular System |
| DGS | Defected Ground Structure |
| FDD | Frequency Division Duplex |
| FTP | File Transfer Protocol |
| GPRS | General Packet Radio Service |
| GSM | Global System Mobile Communication |
| SWI | Substrate Integrated Waveguide |
| BCS | Broadside Coupled Stripline |
| LTCC | Low-temperature co-fired ceramics |
| EM | Electromagnetic |

| | |
|---|---|
| SAS | Smart Antenna Networks |
| SWR | Standing Wave Ratio |
| LTE | Long Term Evolution |
| MLA | Meander Line Antenna |
| PIFA | Planar Iinverted F Antenna |
| Q-Factor | Quality Factor |
| RF | Radio Frequency |
| SAR | Specific Absorption rate |
| FFT | Fast Fourier Transform |
| HBLC | Hybrid branch-line couplers |
| AI | Artificial intelligence |
| ML | Machine learning |
| SMS | Short Message Service |
| TDD | Time Division Duplex |
| UE | User Equipment |
| UL | Uplink Peak Data rate |
| UMTS | Universal Mobile Telecommunication System |
| VoIP | Voice over Internet Protocol |
| Wi-Fi | Wireless Fidelity |
| IEWS | Information and Electronic Warfare Systems |
| GRU | Gated Recurrent Unit |
| LSTM | Long-Short Term Memory |
| IoT | Internet of Things |
| HFSS | High-frequency structure simulator |
| ADS | Advanced Design System |
| FPGA | Field-programmable gate array |

## LIST OF SYMBOLS

| | |
|---|---|
| U | Radiation Severity in Watts Per Steradian |
| $P_{acc}$ | Accepted Power in Watts Entering |
| $P_{incident}$ | Incident Power in Watts |
| $P_{rad}$ | Radiated Power in Watts |
| U(θ , φ) | Radiation Intensity in Watts Per Steradian |
| \|E\| | E-field Magnitude |
| $\eta_\circ$ | Intrinsic Impedance of Free Space |
| Re | Real Part of a Complex Number |
| A | Complex Modal Excitation Specified |
| $S_{11}$ | Reflection Coefficient of the Antenna |
| A | Union of all Port Boundaries in the Model |
| Q | Reactance to Resistance in the Device |
| $R$ | Ohmic Resistance |
| $X$ | Reactance or Stored Energy |
| $\omega$ | Angular Frequency (rad / sec) |
| $W$ | Time-Averaged Energy |
| $\eta_a$ | Radiation Efficiency |
| $Rr$ | Radiation Resistance of the Antenna |
| $Rm$ | Ohmic Losses in the Antenna Structure and Any Matching Device |
| $\omega_c$ | Cutoff Angular Frequency |
| $\omega_0$ | Resonance Angular Frequency |
| $f_c$ | Cutoff Frequency |

# CHAPTER 1

# INTRODUCTION

## 1.1 Research Background

In an era marked by an insatiable demand for high-performance wireless communication networks, the imperative to innovate has never been more pressing [1]. Communication networks have evolved from rudimentary point-to-point connections to sophisticated, globally interconnected systems. Each generation of communication networks represents a significant leap in terms of technology, architecture, and capabilities. These generations have been characterized by distinct attributes such as data rates, latency, coverage, and the types of services they can support [2]. This thesis explores the blend of technology and the increasing need for faster data, more capacity, and wider coverage. Our response to this imperative is an avant-garde antenna system that seamlessly integrates a 4x4 Butler matrix with a 1x4 linear array antenna. What sets this system apart is its infusion with machine learning algorithms meticulously orchestrated on an embedded control chip, promising not just optimized performance but also unparalleled adaptability.

The trajectory of our exploration unfolds with a meticulous examination of three distinctive antenna designs, each meticulously crafted for comparison and, ultimately, selection to construct the antenna array within the Butler Matrix network. The first design introduces a printed Meander Line Antenna (MLA), precisely tailored for LTE mobile terminals. With a bandwidth of 57 MHz, compact dimensions measuring $(32 \times 28 \times 1.1)$ $mm^3$, and operation at a frequency of 2.5

GHz, this design caters to the dynamic needs of mobile communication with an emphasis on efficiency and versatility.

Our second design venture features a Multiband Hand-Held Antenna endowed with E-shaped Monopole Feeding. The validation of this design through simulation and precise measurements attests to its accuracy and practical viability.

The third design introduces an exploration into 5G antenna arrays, incorporating an inverted U slot antenna distinguished by its low reflection coefficient, significant gain, and omni-directional radiation patterns at the crucial 28 GHz frequency.

Integrating individual designs into a multi-beam antenna array results in a harmonious culmination, characterized by achieving matching at 50Ω, high gain with precisely directed beams, and a streamlined Butler matrix in both size and components, generating four beams with exceptional isolation and transmission coefficients. The compact final design, measuring (23 mm × 20.5 mm), stands as a testament to innovation and surpasses traditional designs with a remarkable gain increase of up to 11 dB.

The zenith of our proposal introduces an intelligent antenna system, a fusion of a multi-beam antenna for 5G at 28 GHz, a 4x4 modified Butler matrix, a 1x4 linear array antenna, and the formidable Random Forest Decision algorithm orchestrated on an embedded control chip [3]. This integrated system is not merely advanced; it heralds a new era in wireless communication, enabling dynamic beam steering and adaptive beamforming. This adaptability is not a mere feature but rather a necessity for the efficient orchestration of 5G communication, adapting dynamically to network needs, user demands, and the ever-shifting environmental factors [4].

The subsequent chapters of this thesis delve into a comprehensive analysis of the proposed antenna system, focusing on critical aspects such as beamforming, spatial diversity, interference mitigation, and the efficacy of machine learning algorithms. The results and insights derived showcase the superiority of our proposed model over conventional antennas, paving the way for potential applications in diverse scenarios, from IoT devices to mobile communication networks. Moreover, this work is not confined to technological innovation alone; it significantly contributes to ongoing endeavors in miniaturizing Butler Matrix Networks without compromising their performance. Furthermore, it addresses a pressing concern in traditional antenna systems, i.e., power consumption. Our modeling approach incorporates innovative power conservation mechanisms, responding adeptly to the growing imperative of energy efficiency in wireless communication networks. By intelligently adapting power consumption based on the communication scenario and environmental factors, our proposed system aligns seamlessly with contemporary efforts to create sustainable and eco-friendly communication technologies. This thesis, therefore, is not merely a contribution to technology; it is a blueprint for the future of wireless communication.

## 1.2 Generations of Mobile Networks

1. First Generation (1G): Emerged in the late 1970s and early 1980s, based on analog technology (AMPS). Enabled basic voice communication with limited capacity and security features. Transitioned to subsequent generations for higher capacity and improved reliability [5].

2. Second Generation (2G): Shifted from analog to digital communication with technologies like GSM and CDMA. Allowed more efficient spectrum use, introduced text messaging (SMS), and laid the foundation for mobile data services [6].

3. Third Generation (3G): Introduced higher data rates and the transmission of both voice and data at reasonable speeds. Technologies like UMTS and CDMA2000 enabled mobile internet access, video conferencing, and multimedia services [7].

4. Fourth Generation (4G): Based on LTE technology, marked by high data rates, low latency, all-IP architecture, and advanced modulation techniques. Facilitated seamless streaming of high-definition video, online gaming, and mobile apps [8].

5. Fifth Generation (5G): Represents a new era with ultra-high data rates, extremely low latency, and massive device connectivity. Goes beyond personal communication to enable IoT, industrial automation, AR, and VR. Utilizes technologies like millimeter-wave frequencies, massive MIMO, and network slicing [9].

The successive evolution of these generations symbolizes an ongoing quest for enhanced performance and groundbreaking services, influencing the manner in which connectivity and the digital world are experienced. Table 1.1 summarizes the differences between these generations

**Table 1.1 : Technology and Characteristics for Mobile Networks**

| Generation | Technology and Characteristics |
|---|---|
| 1G | Analog technology (e.g., Advanced Mobile Phone System - AMPS), basic voice communication, limited capacity, susceptible to interference, lacked security features. Transition driven by the need for higher capacity, improved voice quality, and enhanced reliability. |
| 2G | Digital technology (e.g., Global System for Mobile Communications - GSM, Code Division Multiple Access - CDMA), more efficient use of frequency spectrum, introduced text messaging (SMS), laid the foundation for mobile data services at modest speeds. |
| 3G | Mobile Data and Broadband, technologies like Universal Mobile Telecommunications System (UMTS) and CDMA2000, higher data rates, capability to transmit voice and data at reasonable speed, enabled mobile internet access, video conferencing, and multimedia services. |
| 4G | LTE (Long-Term Evolution) technology, high data rates, low latency, all-IP architecture, advanced modulation techniques, facilitated streaming of high-definition video, online gaming, and mobile apps. Contributed to enhanced user experiences and growth of the mobile ecosystem. |
| 5G | Ultra-high data rates, extremely low latency, massive device connectivity, supports Internet of Things (IoT), industrial automation, augmented reality (AR), and virtual reality (VR). Utilizes millimeter-wave frequencies, massive MIMO (Multiple-Input, Multiple-Output), and network slicing. Represents a new era in connectivity and innovation. |

## 1.3 Motivation of Thesis

The motives of this thesis can be summarized in six main points:

1. Spectrum Efficiency: With the exponential growth in the number of wireless devices and the ever-increasing demand for high-speed data services, efficiently utilizing the limited radio frequency spectrum has become a critical concern. An intelligent antenna system can dynamically adapt to changing signal environments, thereby improving spectrum efficiency and accommodating more users within the same frequency band.

2. Enhanced Communication Quality: Traditional antenna systems often suffer from interference and signal degradation, leading to poor communication

quality. An intelligent antenna system that incorporates a 4x4 Butler Matrix and a 1x4 linear array antenna can effectively reduce interference and enhance signal quality, ensuring a more reliable and robust wireless communication experience for users.

3. Adaptive Performance: The integration of machine learning-based embedded control chips allows the antenna system to learn from its environment and autonomously optimize its performance. This adaptability is crucial for handling diverse and dynamic network conditions, ensuring consistent and high-quality communication links even in challenging scenarios.

4. Increased Capacity: By minimizing interference and optimizing the signal's direction, intelligent antenna systems can support a higher number of simultaneous users, resulting in increased network capacity. This is essential for meeting the growing demands of modern wireless communication systems, including the Internet of Things (IoT) and 5G networks.

5. Energy Efficiency: Directional radiation patterns of intelligent antenna systems lead to reduced power consumption, as the signal energy is focused towards the intended users rather than being dispersed over a wide area. This energy efficiency is critical for achieving sustainable wireless networks and prolonging the battery life of mobile devices.

6. Future-Proofing Wireless Networks: As wireless communication technologies continue to evolve, incorporating machine learning and intelligent antenna systems will become increasingly important to ensure the adaptability and scalability of future networks. This thesis not only addresses current challenges, but also lays the foundation for future advancements in wireless communication systems.

## 1.4 Problem Statement

The problem statement for this thesis involves investigating, designing, and implementing a smart antenna system that can adapt to varying signal environments, reduce interference, and enhance communication quality. Furthermore, the integration of machine learning-driven embedded control chips will enable the system to optimize its performance autonomously and adapt to changing network conditions, ultimately leading to improved wireless communication and system efficiency. The problem statement is summarized in the following points:

1- The increasing demand for high-quality wireless communication services require the development of more advanced antenna systems. Traditional antenna systems, such as omnidirectional and sectored antennas, often result in inefficient use of the spectrum, interference, and limited network capacity. To solve the issue, it is necessary to develop a smart antenna system. This advanced system seeks to address the challenges posed by traditional antenna systems and improve the overall performance and efficiency of wireless communication networks [10].

2- The compact design should be easily integrable with other devices through innovative design techniques leading to a substantial reduction in size of the Butler Matrix without compromising performance.

3- Addressing signal degradation attributed to reflections, interference, and fluctuating signal strengths, the application of beamforming technology is pivotal in our pursuit to overcome these challenges and enhance reception quality [11].

4- In the realm of traditional antenna systems, notable power consumption is observed, independent of the actual requirements of the receiver. The integration of an embedded control chip and AI algorithm in this context facilitates dynamic adjustments in power consumption, aligning with the specific needs of the receiver [12].

## 1.5 Objectives of Thesis

The primary objective of this thesis is to design, simulate, and analyze an innovative intelligent antenna array system, integrating a Butler Matrix with embedded control chips enhanced by the AI-based Random Forest Decision algorithm. This research aims to achieve the following specific to:

1. To design a Mini Microstrip Antenna Array for Smart Antenna System operating at 28GHz.
2. To design the feed network using a Structure of the Butler Matrix Network.
3. To develop a Beamforming Antenna Array.
4. To propose an intelligent antenna and test the algorithm depending on the data collected from our system.

By accomplishing these objectives, this thesis seeks to propel the field of intelligent antenna arrays forward by presenting an innovative model that leverages the power of embedded control chips and AI algorithms within the context of a Butler Matrix-integrated system. The proposed intelligent antenna array holds the promise of revolutionizing wireless communication by enhancing signal quality, optimizing power utilization, and providing a roadmap for future advancements in the field.

## 1.6 Scope of Work and Study Limitations

This research focuses on integrating a 4x4 Butler Matrix with a 1x4 linear array antenna and control chip by machine learning algorithms, and exploring the synergies between these components to enhance wireless communication networks.

The primary goal is to have an antenna that keeps power consumption under control and is small in size, allowing it to integrate easily with other devices.

Despite the potential benefits of the study findings, there are certain limitations and challenges associated with the research, including:

1- Antenna Size Reduction Challenges:

- Challenges exist in maintaining full antenna performance as size reduction may lead to decreased radiation efficiency and signal reception.
- Size reduction can limit the frequency range with effective interaction, posing a challenge for designing antennas meeting diverse frequency band needs.

2- Balancing Performance and Size:

- Striking a balance between maintaining Butler Matrix performance and reducing attached antenna size is challenging.
- It is crucial to find ways to enhance performance without adversely impacting the overall volume.

3- Integration Complexity:

- Integrating a 4x4 Butler Matrix with a 1x4 linear array antenna and implementing machine learning on an embedded control chip introduces hardware integration complexity.
- Ensuring seamless coordination between these components poses a significant challenge.

4- Dataset Challenges for Machine Learning:**

- Machine learning algorithms require extensive datasets for training and validation.

- Generating or obtaining relevant and diverse datasets for antenna behavior under various conditions is a crucial challenge.

5- Translation of Simulation Results:

- Translating simulation results into practical, real-world implementations can be challenging.
- Validating the proposed antenna system's performance through extensive experiments and ensuring reliability in diverse scenarios is crucial.

## 1.7 Thesis Organization

This thesis comprises five chapters. In the current chapter, the needs, problem statement, motivation, and objective of smart antenna systems for 5G mobile applications are presented.

Chapter 2 presents an extensive review of the relevant literature, focusing on previous studies and research addressing the same topic. Additionally, the chapter offers a comprehensive analysis of the methodologies employed by researchers to address the problem and achieve their objectives. Also, this chapter presents the underlying principles and theoretical background of the Antenna, Beamforming techniques, and Butler Matrix, as well as the challenges and trade-offs associated with their combination. Additionally, it elucidates the suitability of the machine learning algorithms for real-time optimization and adaptability in various scenarios.

Chapter 3 presents the research methodology. Firstly, it presents the design of the three types of antennas namely the Meander Line Antenna based on defected ground structure, the open slot antenna supplied by an E-shaped monopole for use with mobile and wireless LAN services, and the rectangular patch antenna with inverted U slot to easily resonate the antenna at 28GHz. The chapter then explains the design of a 1x4 linear array antenna for the 28 GHz frequency band without mutual coupling for wireless communication systems. Next, it explains the novel approach for intelligent antennas using an embedded control chip with the AI-based Random Forest Decision algorithm.

Chapter 4 presents the results of the design and the fabrication of a uniquely miniaturized 4x4 Butler Matrix Network integrated with a 1x4 linear array antenna for the 28 GHz frequency band. The chapter thoroughly discusses the design strategies to validate this innovative system. Next, it presents the advancements in intelligent antenna systems, showcasing the potential of embedded control chips and AI algorithms in signal selection and power management.

Chapter 5 concludes the thesis by summarizing the key findings and contributions of the research. It also identifies potential avenues for future work, aiming to further refine and optimize the proposed intelligent antenna system based on the embedded control chip. The concluding remarks emphasize the potential of the developed model to revolutionize wireless communication systems and pave the way for next-generation connectivity solutions.

# CHAPTER 2

# LITERATURE REVIEW

## 2.1 Introduction

Millimeter-wave (mm-wave) has been considered in recent years for enhancing the spectrum efficiency of 5G communication systems which increases the bandwidth with a higher data speed rate. In addition, the small-sized device operates on mm-wave communications [13]. Despite all the features offered by 5G technology, it still has a higher loss from congestion and overlapping signals, which results in lower Quality of Service (QoS) [14]. Moreover, with the increasing number of mobile users, 5G must deal with more traffic at a higher speed. This has led to a significant number of studies in the field of beamforming networks with the goal of solving this issue and enhancing the quality of communication links even in unfavorable circumstances. To maintain appropriate cell coverage without overlapping and decreasing path loss, a multi-beam antenna will be utilized to facilitate the 5G system. Microstrip antenna with beamforming technology has attracted many researchers to implement multi-beam antenna designs.

Patch antennas and patch antenna arrays played a significant role in the evolution of antenna technology. Their development was driven by the need for compact, efficient, and versatile radiators in various communication systems, including wireless communication, satellite communication, and radar systems.

As wireless communication systems evolved, there was a growing demand for antennas that could operate across multiple frequency bands and support various communication standards. Researchers and engineers developed techniques to broaden the bandwidth of patch antennas, leading to the creation of multiband and wideband designs. Techniques such as stacked patches, parasitic elements, and metamaterial-based structures allowed patch antennas to cover a broader frequency range without sacrificing performance.

In an era marked by the incessant quest for faster, more reliable, and efficient wireless communication systems, beamforming technology has emerged as a cornerstone solution to meet the escalating demands of the modern world. Among the many beamforming techniques, the Butler Matrix has distinguished itself as a versatile and indispensable component in enabling precise control over electromagnetic wave propagation.

Beamforming, the process of steering and shaping electromagnetic waves in a specific direction, has evolved significantly over the years, playing an instrumental role in revolutionizing wireless communication systems. The Butler Matrix, a key innovation in this evolution, provides a powerful tool for achieving advanced beamforming capabilities. As the demand for high-speed data transfer, reduced interference, and enhanced connectivity continues to grow, it becomes imperative to embark on a comprehensive journey through the history, development, and application of the Butler Matrix beamforming technology. In a passive beamforming network (BFN) design, the antenna elements type and type of BFN structure are essential [15]. As the direction of a PAA system's beams frequently depends on the phase and differences between them, multibeam antennas are typically used [16]. In order to get the desired results, modern wireless communication systems rely heavily on multi-beam and beam-scanning antennas. The multi-beam antenna concept has already been implemented in many applications, including WLANs [17], base stations, satellite communications [18], and even auto motive radars [19], in order to provide wide-angle coverage. The benefits of beamforming can be summarized in four general points [20]:

- A multi-beam antenna, often known as a phased array antenna, is a switched-beam antenna. It is an antenna array that, based on predetermined weights assigned to each received signal, forms a large number of fixed beams in various directions.
- Beams direct in certain fixed discrete directions. One beam will turn on or be guided towards the targeted user among numerous others. A switch is used to pick the optimal beam for receiving a specific signal, resulting in the highest possible received strength. In short, the desired signal beam follows the user's movements.
- Simple: To choose a certain beam, all that is required is a beam forming network, an RF switch, and control circuitry.
- Economical: Because all processing takes place in the RF domain, just one signal needs to be translated to baseband and processed there. This is a significant benefit because down conversion circuits are among the most expensive components in today's wireless systems.

In recent years, there has been a surge in research pertaining to the design and manufacturing of Butler Matrix Networks and linear array antennas, specifically in the 28 GHz frequency band, catering to the advancements in 5G and beyond. In 2019, researchers devised and proposed a Butler Matrix-based four-directional switching beamforming antenna system that was implemented in a two-layer hybrid stack-up substrate. Two layers make up the hybrid stack-up substrate, and each of these layers has unique electrical and thermal characteristics. Adding two-layer hybrid stack up substrate causes more complexity and incurs more cost for structure. Moreover, this approach failed to reduce complexity [21]. In the same year, Prachin et al. developed the beamforming system using another strategy, i.e., phased-array beamforming system. It can constantly steer a beam in any direction, but because it requires complex beamforming circuitry with accurate phase shifters, variable gain blocks, and switches, the complexity and expense of system implementation necessarily increased [22]. After one year, Campo et al. lens antenna was used as another method. When a lens is activated by several feeds at various points, the focusing or reflecting function of the lens can vary the direction in which the electromagnetic wave propagates, producing multiple radiation beams. Reflector-based and lens-based multibeam antennas, while typically adequate for millimeter wave frequencies, suffer from huge dimensions and are therefore unsuitable for sub-6 GHz base station applications. Nevertheless, this technique was not successful due to complexity management [23]. In 2020, Zhou et al. presented a research study on the design of a compact 4X4 Butler Matrix using substrate integrated waveguide technology for 28 GHz 5G applications [24]. The paper emphasized the advantages of this technology in terms of size reduction and improved performance. In 2021, Imani and others departed from the traditional design of the Butler Matrix network in order to obtain a smaller size. The final structure for the proposed BM also contains four directional couplers, two −45o phase shifters, and one crossover, but the dimensions are still big whereby the total size of the BM is 37 mm X 47 mm [25]. Zubaida et al (2021) used the SIW technique. They proposed a 3X3 multibeam antenna at 28GHz, where the BM was introduced through SIW, but the cost and complexity of the SIW technique led to usage restrictions [26]. In the same year, M. Jeon et al fabricated a conventional structure of a multi-beam antenna. Due to the conventional BM comprising the four hybrid couplers, 2 phase shifters, and two crossovers, the transmission line may be adding unwanted effects such as side lobes and insertion loss. Therefore, modification and reduction of the elements in the Butler Matrix are required [27]. After one year, Alsirhani et al. modified the 4X4 Butler matrix (BM) to decrease the side loop effect and increase the gain of each beam but at the expense of adding more auxiliary elements, which is more complex for structure [28]. Temga et al. (2022) proposed a compact 2-D phased array based on a compact 4x4 Butler Matrix without crossover designed in Broadside Coupled Stripline (BCS) technology for Sub-6GHz 5G applications. The proposed 4×4 Butler Matrix (BM) is composed of only four 3dB/90° broadside couplers and two 45° phase shifters [29]. A comprehensive study was conducted by Nam et al. (2022) on a new topology that can reduce the size of the Butler Matrix without removing or modifying components, such as couplers, shifts, and crossovers. To realize the proposed topology, a Butler Matrix was implemented with a multi-layer substrate using low-temperature co-fired ceramics (LTCC). To verify the proposed structure, a 4 × 4 Butler Matrix operating at 28 GHz was fabricated and measured [30]. In 2023, Abdulbari et al. presented a design of BM with size reduction and improved bandwidth of up to 836 MHz compared to the traditional BM [31]. Finally, TEMGA et al. (2023) proposed a new Beamforming Network (BFN) realized in Broadside Coupled Stripline (BCS) to feed 1 × 4 and 2 × 2 arrays antenna at 28 GHZ-Band. The new BFN is composed only of couplers and phase shifters. It does not require any crossover compared to the conventional Butler Matrix (BM) which requires two crossovers. The tight coupling and low loss characteristics of the BCS allow for a compact and wideband BFN design [32].

While these studies provide significant insights into the design and manufacturing of Butler Matrix Networks with linear array antennas, there is still a need for further research into the miniaturization of these systems, particularly in the 28 GHz frequency band. This thesis aims to contribute to this area of research by presenting a unique design that is the smallest of its kind.

The development in the beamforming did not stop to this extent; intelligent antenna technologies have emerged as a promising high-performance solution that keeps pace with the rapid development of communications connections. A wide range of 'smart' antenna technologies have been offered as viable solutions to improve modern wireless communications in recent years [33]. The antenna is a crucial component of both civil and military radio systems, serving as an electromagnetic (EM) transducer by converting guided waves into free space waves and vice versa. Antennas can be used to increase or decrease the quantity of energy supplied or received in specific directions, depending on the application. A well-designed antenna may help minimize system requirements while increasing overall system performance [34]. Historically, wireless systems have either used omnidirectional or sectored antenna systems. The downside of such antenna systems is that the electromagnetic energy needed by a particular user in a particular direction is needlessly disseminated across the cell, producing interference for other users. Smart antenna systems have been explored and developed in order to mitigate this form of interference and guide energy to the intended user [35]. Smart Antenna Networks

(SAS) have swiftly become one of the most important technologies for achieving high efficiency and improved wireless communication systems. The SAS has received a lot of attention in recent decades because it can dynamically enhance system capacity by adjusting interference and targeting the intended user. Intelligent antenna technology has a significant impact on spectrum efficiency, service quality optimization, network configuration reduction, and operational transparency across multi-technology wireless grids when used in communication systems [36]. Intelligent antennas maximize power efficiency. Depending on the clever antenna employed in a communication system, the clever antenna does not always cover an area while waiting for new members. A single user beam can be sent by intelligent antennas. A smart antenna, on the other hand, is not perfect because some signals sent to users can heavily interfere with other signals bouncing off nearby physical structures. Machine learning has gained a lot of attention as a way to identify better answers in several fields, and it is expected to play a big role in our future technology. With its omnidirectional uses in automating complex and long processes with specialized detailing, it has become a go-to tool for science and engineering [37]. Despite still being in its infancy, it has become a phenomenon in the technology business, with machine-learning users altering the foundations of hundreds of industries and research projects, particularly in the field of antennas. In this era of Big Data, machine learning (ML) has emerged as a major player and there has been a notable increase in research focusing on utilizing machine learning for the design of adaptive antennas, specifically to accommodate the advancements in 5G and future wireless technologies. ML is also showing promise in antenna optimization by estimating antenna behavior and speeding up the optimization process with accuracy and efficiency.

In 2019, Masood et al proposed a novel approach for predicting the propagation characteristics of wireless signals in three-dimensional (3D) space using machine learning techniques. The authors collected real-world data from measurement campaigns, which include various input parameters such as antenna height, frequency, and building density. They utilized this dataset to train a machine learning model that can learn the complex relationships between the input parameters and the resulting signal propagation characteristics, such as path loss and delay spread [38]. A year later, Gampala et al highlighted the importance of antenna design optimization in achieving desired performance metrics such as radiation pattern, gain, and bandwidth. They discussed how traditional optimization methods can be time-consuming and computationally intensive, leading to significant design iterations [39]. In 2021, Wei Panpan et al. proposed different algorithms and techniques for beamforming and spatial signal processing in MIMO/smart antenna arrays. These techniques aim to improve signal quality, enhance interference rejection, and optimize the performance of the handheld device in varying wireless environments [40]. In the same year, Mohsin et al addressed the challenge of sidelobe levels in smart antenna arrays, as high sidelobes can cause interference and reduce the overall performance of the system. They proposed the use of a cultural algorithm, which is a computational intelligence technique inspired by cultural evolution, to optimize the antenna array's configuration and minimize the sidelobe levels [41]. Chen, Joy, and Lu-Tsou Yeh in 2021 addressed the need for efficient and reliable wireless energy transmission in IoT systems, where numerous devices require power in a wireless and energy-efficient manner. They proposed the use of adaptive array processing techniques to enhance the energy transmission process [42]. A year later, Pirapaharan et al proposed a smart beam steering technique that leverages the advantages of both analog and digital beamforming. The technique utilizes a hybrid approach, where analog beamforming is performed at the RF (Radio Frequency) level, and digital beamforming is carried out at the baseband level. This combination enables fast and efficient beam steering while reducing the memory requirements [43]. In the same year, El-Khamy et al. highlighted the importance of wideband antennas in modern wireless communication systems and the need for adaptive beamforming to improve signal reception and transmission. They proposed the use of a thinned Eisenstein fractal geometry, which offers a compact and efficient antenna array design [44]. In 2023, Senapati, Anupama et al. presented a paper on the need for smart antennas in 5G networks to improve signal quality, increase capacity, and enhance overall system performance. The authors discussed the array synthesis methods, which involve determining the antenna element positions and weights to achieve desired radiation patterns and beamforming characteristics [45].

These prior works have made significant contributions to the field of intelligent antenna systems, utilizing AI algorithms and various machine learning techniques for signal selection and return loss reduction. They provide valuable insights into the design, optimization, and performance evaluation of intelligent antenna systems. However, these studies do not address practical constraints associated with implementing MIMO/smart antenna arrays in handheld devices. Factors such as power consumption, size, cost, and manufacturing feasibility are critical considerations for handheld devices. Providing insights into how these constraints can be effectively addressed in our proposed design would have enhanced the practicality and applicability of the research.

## 2.2 Antenna

Antennas constitute a vital component of any radio system, as they facilitate the conversion of electromagnetic waves in open space into electrical voltages and currents on a transmission line, and conversely, the conversion of these electrical signals back into electromagnetic waves [46]. This transformation must be highly efficient, especially given that the power density of propagating electromagnetic waves typically diminishes significantly over extended distances. Consequently, substantial effort is dedicated to the design of antennas and their associated circuitry, commonly referred to as feed networks.

Electromagnetic waves radiate outward from their source in a radial fashion. When observing these waves from a considerable distance represented by "r", the radiating source is often treated as a point, and the resulting electromagnetic fields are considered real. To measure the power density flow, the method employed involved using the Poynting vector, defined as the cross product of the electric and magnetic fields.

$$S = E \times H^{*} \ ( W/ m^{2} )$$

Envision an optimal point source uniformly emitting radiation in all directions. When considering a spherical surface surrounding this point source, the power passing through it maintains uniformity across the entire sphere. As the radius "r" of this sphere increases, the surface area of the sphere expands at a rate proportional to $r^2$. Consequently, the power density decreases at a rate inversely proportional to $1/r^2$ because the same overall power (represented by the Poynting vector) now spreads over a larger area. This inverse relationship, known as the inverse-square law, is a well-known phenomenon found in various natural laws, including gravity, electrostatics, and acoustics [47].

[47] proposed that an ideal antenna should efficiently radiate all incoming power, originating from a transmission line, precisely in the intended directions and with the desired polarization. However, in practical scenarios, antennas emit some energy in all directions, similar to the point source discussed earlier. Consequently, a portion of this energy propagates in unintended directions and is consequently lost. A parameter employed to quantify the portion of energy emitted in a specific direction by an antenna is known as the beam or radiation pattern. It is worth noting that the term "radiation pattern" is a broader concept that can encompass both field and power patterns. However, for the purposes of this study, our focus is solely on the power pattern, which is typically represented in decibels as a function of angular space [48].

When categorizing antenna radiation patterns, they generally fall into one of three major classes:

1. Isotropic: An isotropic antenna pattern radiates energy equally in all directions. It is essential to understand that isotropic radiation patterns are purely theoretical constructs. Nevertheless, they are frequently employed for the analysis of antenna arrays. This choice is advantageous because it allows for the examination of array characteristics independently of the individual antenna element's radiation traits, such as side-lobes, half-power beam-width (HPBW), and so on.

2. Omnidirectional: An omnidirectional antenna pattern radiates energy uniformly in a specific plane.

3. Directional: In contrast, directional antennas emit energy predominantly in one specific direction.

Notably, though termed a "radiation pattern", antennas exhibit reciprocity, indicating their ability to capture energy similarly to how they emit it. In the subsequent subsections, a comprehensive discussion of well-established antenna elements will be presented, laying the groundwork for an exploration of antenna arrays and the concept of beamforming.

As their composition is uncomplicated, inexpensive, and simple in appearance, planner antennas have been proven to be well-suited for modern communication systems (GSM 890-960 MHz, DCS 1710-1880 MHz, PCS 1850-1990 MHz, UMTS 1920-2170 MHz, WLANs 2400-2484 MHz). Additionally, planner antennas are compatible with LTE (Long Term Evolution) in the 700 MHz band (758-798 MHz) [49]. for wireless and 5G, it is the latest cellular network technology standard for high-speed wireless communication, and it was globally rolled out by cellular providers in 2019. This technology builds upon the foundation of 4G networks, which currently enable connectivity for the majority of modern smartphones.

According to the definitions provided by IEEE, antennas, or aerials, are described as devices used for emitting or capturing radio waves. They serve as an intermediary for electromagnetic energy transfer between free space and a guided medium. Various antenna types exist, such as wire antennas, aperture antennas, reflector antennas, and lens antennas. Among these, microstrip patches stand out as exceptionally versatile, conformal, and easy to manufacture. In wireless applications, achieving a good antenna design is crucial for attaining reliable range and stable data throughput. This becomes particularly vital in scenarios with limited space for antennas, as is often the case in compact and low-power designs. To achieve the desired antenna performance, users must possess a fundamental understanding of antenna functionality and the associated design parameters. These parameters encompass selecting the appropriate antenna type, tuning the antenna, achieving impedance matching, managing gain and losses, and determining the required radiation pattern.

### 2.2.1 Types of printed antenna

Common printed antennas are typically employed in embedded applications including Microstrip Lines/Patch antennas, Planar Inverted 'F' (PIFA) antennas, and Meander Line (MLA) antennas, among others. Microstrip lines, which are an extension of monopole antennas, can be easily manufactured by etching a copper strip onto the radio circuit board. Their performance is constrained by the nearby electronics on the circuit board, making them a cost-effective option. Microstrip monopoles typically operate at a single frequency. Patch antennas, on the other hand, are suitable for systems requiring a focused beam pattern in a specific direction. They are created using square or round copper patches on the upper surface of the circuit board, and their radiation pattern is perpendicular to the board's surface. PIFA antennas have a distinctive "F" shape, resembling the letter "F" lying on its side. The shorter sections of the "F" serve as feeding points, while the earth and the "tail" facilitate surface radiation [52]. PIFA antennas are well-suited for embedded applications due to their somewhat omnidirectional radiation pattern and the ability to cover multiple frequency bands. They are easily integrated into wireless phones, offering a low-profile design. Typically, PIFAs are used in conjunction with the ground plane, often the cellular phone's circuit board ground plane. Another type of radiating element is the Meander Line Antenna (MLA), which combines a loop antenna with frequency-tuning meander lines. The electrical length of MLA is primarily determined by the delay characteristics of the meander line rather than the length of the radiating structure itself. MLAs can be designed to exhibit broadband capabilities, allowing operation across various frequency bands. For base stations, classical dipoles are commonly employed. These dipoles are efficient radiators and are created by bending the end of an open-circuit two-wire transmission line into a "T" shape, where the top of the “T” serves as the radiating section, with its length corresponding to the wavelength of the signal. In some applications, monopole antennas with lengths of λ/2 or λ/4 mounted over a ground plane are used. For specialized applications like perimeter security systems, tunnels, and interior zones of cellular or 802.11 systems, special antenna constructions may be necessary. One approach to cover a large but defined area with RF energy involves using an RF-leaky feeder cable to provide controlled radiation [54].

#### 2.2.1.1 Microstrip patch antenna

A simplified microstrip antenna consists of a dielectric substrate sandwiched between two conducting surfaces: the antenna plane and the ground plane.

Figure 2.1 illustrates a basic microstrip patch antenna configuration. These antennas primarily radiate due to the fringing fields between the edges of the patch and the ground plane. They operate in a quasi-TEM mode because the electromagnetic fields propagate in both the substrate and free space. The dimensions of the patch are typically represented by (a) for the length and (b) for the width.

The thickness of the substrate is denoted as "h". Microstrip antennas are commonly fed using various techniques, including Microstrip Line feed [55], Coaxial feed [56], Proximity coupled, and Aperture coupled techniques, each having its own set of advantages and disadvantages as depicted in Figure 2.2 [50].

Microstrip antennas, despite their advantages, come with certain drawbacks [58]. These drawbacks encompass limited bandwidth, reduced efficiency, low gain, unintended spurious radiation, and susceptibility to surface wave excitation. Although measures like optimizing feed mechanisms and substrate thickness can mitigate pseudo radiation and surface wave issues, the primary challenges revolve around addressing the constraints of bandwidth and radiation efficiency. To enhance these aspects, increasing the substrate thickness is a viable approach, but it carries the risk of triggering surface wave problems.

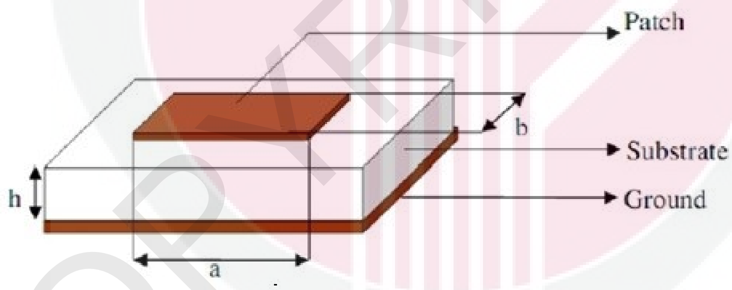


**Figure 2.1 : Microstrip Antenna [55]**

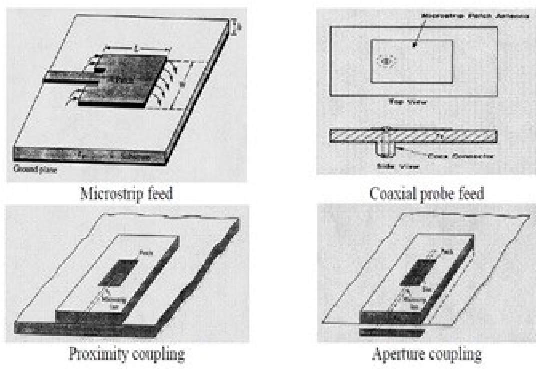


**Figure 2.2 : Microstrip Antenna Feeding Methods**

#### 2.2.1.2 Planar inverted F antenna

Planar inverted F antennas (PIFAs) have gained popularity for portable wireless devices because of their compact, low-profile design, and integrated structure [59]. They offer advantages such as easy fabrication, cost-effectiveness, and simplicity [60]. In comparison to conventional patch antennas, PIFAs typically exhibit a broader inherent bandwidth, thanks to their utilization of a thicker air substrate. Conventional PIFAs typically have bandwidths ranging from 4% to 12% for a -10 dB return loss [61]. A basic PIFA comprises a ground plane, a top plate element, a feed wire responsible for feeding the resonating top plate, and a DC shorting plate that connects the ground and the top plate at one end of the resonating patch. This configuration is depicted in Figure 2.3.

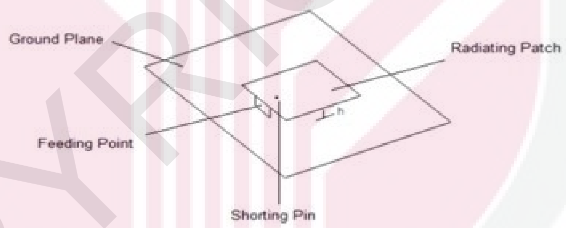


**Figure 2.3 : Planar Inverted F Antenna**

The inverted-F design of a PIFA results in the creation of a remarkably consistent 3D signal sphere, effectively generating an omnidirectional signal field.

#### 2.2.1.3 Meander Line Antenna

The Meander Line Antenna (MLA) is a type of printed antenna that achieves size reduction by incorporating a wire structure on a dielectric substrate. Initially developed by BAE SYSTEMS, formerly a part of Lockheed Martin Company, MLA technology was created for Information and Electronic Warfare Systems (IEWS), where high-performance antennas were needed for both satellite and terrestrial communications. Recently, these antennas have found applications in mobile handsets, wireless data networking for laptops, PC cards, and access points. In its basic form, MLA combines features of traditional wire antennas and planar strip lines. Its advantages include a straightforward configuration, easy integration into wireless devices, cost-effectiveness, and the potential for low Specific Absorption Rate (SAR) characteristics. SAR measures the rate at which energy is absorbed by the body when exposed to a radio frequency (RF) electromagnetic field and is expressed in watts per kilogram. MLA offers twice the surface area compared to other antennas, ensuring high antenna efficiency for improved transmission and reception. This sets it apart from other popular two-dimensional antenna types like Inverted-F Antennas (IFA) and Planar Inverted F Antennas (PIFA), which generate a 3D signal due to their cubic structure. In the Meander Line Antenna (also known as a rampart line antenna), the radiating element is constructed from a meandering microstrip line that consists of a series of right-angled compensated bends, as illustrated in Figure 2.4. In this configuration, the fundamental element is comprised of four right-angled bends, and radiation primarily occurs at the discontinuities, particularly at the bends of the structure. To minimize the susceptance caused by the right-angled discontinuities for impedance matching, these right-angle bends are chamfered or compensated. Within each half-wavelength segment, the direction of the current changes, and this design incorporates more than four half-wavelength changes. Depending on the dimensions of the meander line antenna, the radiation from these bends combines to produce the desired polarization.

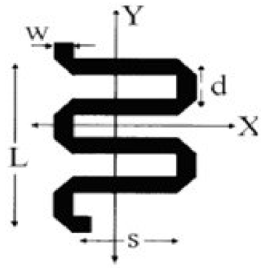


**Figure 2.4 : The Fundamental Section of the Meander Line Antenna**

### 2.2.2 Electrically Small Antenna

The fundamental constraints on the performance of compact antennas have been explored extensively in the literature. [62] conducted a study on how the effective volume of an antenna affects its radiation efficiency and bandwidth, characterizing an electrically small antenna as one whose maximum physical dimension is significantly smaller than the wavelength (radian length), with the radian length being defined as a distance equal to $\lambda/2$. This definition is appropriate because a sphere with a diameter equal to the radian length encompasses a greater portion of the stored near-field energy of the electrically small antenna. In 1987, Fujimoto authored the monograph "Small Antennas" which, along with the work of [63], summarized various approaches used in the design of electrically small antennas (ESA). More recently, [64] established an exact lower limit for antenna performance and addressed apparent errors in the derivation of Q.

#### 2.2.2.1 Fundamental limitations

Electrically small antennas (ESAs), due to their inherent size constraints, possess a minimum value of Q-factor; resultantly, there is a limit on their maximum achievable impedance bandwidth [65]. It is important to note that antennas operating at frequencies outside their natural operating range, characterized by their Q-factor (Quality Factor), are generally of limited practical utility. Both electrically small and low-profile antennas face performance limitations due to their reduced size. These antenna categories typically exhibit low efficiency and pose challenges in terms of impedance matching with transmission lines, primarily because of their low input resistance and high input reactance. Furthermore, ESAs often feature narrow impedance bandwidth, which is a crucial parameter in the antenna design process.

#### 2.2.2.2 Limit on radiation efficiency

The Q Factor is generally defined as the ratio of the energy stored in the resonator to the energy lost in one cycle [66]:

$$\mathbf{Q = 2\pi \frac{Energy\ Stored}{Energy\ Dissipated\ Per\ Cycle}} \tag{2.11}$$

Usually, Q factor is used to describe the ratio of reactance to resistance in the device. Therefore, the equation (2.11) can be written as:

$$\mathbf{Q = \frac{2\pi X}{R}} \tag{2.12}$$

In the above formula, X is the reactance or stored energy, and R is the ohmic resistance. Analogously, Chu defines the radiation Q for an antenna as:

$$\mathbf{Q = \frac{2\omega W}{P_{rad}}} \tag{2.13}$$

In the above given formula, "ω" represents the radian frequency, "Prad" denotes the radiated power, and "W" represents the time-averaged, non-propagating, stored electric or magnetic energy, whichever is greater. Electrically small antennas typically exhibit a high reactance input resistance and a low resistance. As a result, they have a high Q factor and a limited frequency bandwidth. Additionally, ESAs tend to have low radiation efficiency.

$$\eta_a = \frac{R_r}{R_r + R_m} \tag{2.14}$$

In the provided formula, "Rr" stands for the radiation resistance of the antenna, and "Rm" refers to the ohmic losses within the antenna structure and any matching device. Radiation efficiency (ηa) describes the portion of the energy delivered by the antenna to free space that reaches the load or receiver [66]. Every small-sized antenna can be equivalently represented as a lumped reactance component, specifically a capacitor, inductor, or a combination of both. The electric dipole, or dipole antenna, functions as a capacitor, while the magnetic dipole, or loop antenna, behaves like an inductor. Antennas can also be represented by a combination of reactive and resistive lumped elements. In this equivalent circuit, reactance represents the portion of input energy stored in the near field of the antenna, while the resistive element signifies the radiation resistance of the antenna. Wheeler's models depict the magnetic dipole as a series of inductance and resistance and the electric dipole as a shunt capacitance and susceptance. This representation aligns with the concept of circuit duality, and both equivalent circuits are illustrated in Figure 2.5.

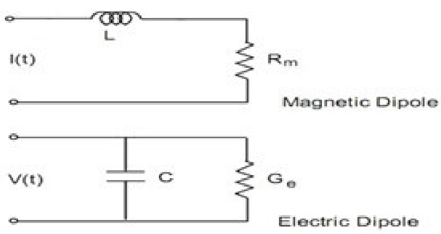


**Figure 2.5 : Equivalent Circuits of a Magnetic and Electric Dipole**

### 2.2.3 Antenna Arrays

In the previous section, the features of a lone planar antenna were examined. Typically, a single antenna element exhibits a relatively wide radiation pattern, resulting in modest values of directivity and gain. However, many commercial applications demand antennas with highly directive attributes and substantial gains, often exceeding 10dB, to meet the demands of long-distance communication. Achieving such performance levels necessitates increasing the electrical dimensions of the antenna. Enlarging the size of individual antenna elements is a common approach to enhance their directive characteristics. Alternatively, there is a method to expand the electrical dimensions of the antenna without necessarily increasing the dimensions of each individual element. This approach involves arranging multiple radiating elements in a specific geometric and electrical configuration. This innovative antenna structure, composed of multiple elements, is commonly known as an array [67]. Typically, the array elements are identical, although it is not a strict requirement; however, it simplifies the design and enhances practicality. The individual elements within an antenna array can take various forms, such as wires, microstrips, or apertures. The overall field radiated by the antenna array results from the vector addition of the fields radiated by the individual elements. This assumes that the current in each antenna element is the same as that of an isolated antenna, neglecting coupling. This is an ideal scenario, and the array's performance depends on the separation between its elements. To achieve highly directive radiation patterns, it is crucial that the fields emitted by the elements within the array interfere constructively in the desired directions while interfering destructively in other spatial regions. Several key factors influence the shape and overall radiation pattern of the antenna array, including:

1. The geometric arrangement of the antenna array (e.g., linear, rectangular, circular, spherical).
2. The relative displacement between the antenna elements.
3. The amplitude excitation of each individual antenna element.
4. The phase excitation of each individual antenna element.
5. The radiation pattern of each individual antenna element.

## 2.3 The Butler Matrix

The Butler Matrix is a specialized beamforming network or matrix used in antenna systems, particularly in phased array antennas. Its primary function is to efficiently steer and control the direction of electromagnetic waves radiated or received by an array of antenna elements. Named after its inventor, W. L. Butler [68], the Butler Matrix is a crucial component in various applications, including radar systems, wireless communication networks, and satellite communication. The primary purpose of the Butler Matrix is to provide phase shifting and amplitude weighting to the signals feeding individual antenna elements within an array. This manipulation of phase and amplitude allows the array to shape its radiation pattern, enabling beam steering in specific directions and beamforming to focus or nullify signals.

Key features and functions of the Butler Matrix include:

1. Phase Shifting: The Butler Matrix introduces controlled phase shifts to the signals applied to each antenna element. These phase shifts are precisely adjusted to align the wavefronts from different elements, resulting in constructive interference in the desired direction.

2. Amplitude Control: It also provides amplitude weighting to the signals, allowing for fine-tuned control over the strength of the radiated or received signals in different directions. This capability helps shape the beam pattern, enhancing signal reception or transmission in target areas while reducing interference from other directions.

3. Beam Steering: By varying the phase and amplitude coefficients applied to each antenna element, the Butler Matrix can steer the main beam of the antenna array to different angles without physically repositioning the individual elements. This dynamic beam steering is valuable in applications like tracking targets or connecting to multiple satellites.

4. Multi-Beam Formation: In addition to steering the main beam, the Butler Matrix can also create multiple beams simultaneously, providing the antenna array with the ability to serve multiple communication links or track multiple targets independently.

5. Low Loss: To ensure efficient energy transfer and minimal signal loss, Butler Matrices are designed to have low insertion loss, making them suitable for high-frequency applications.

6. Compact Design: The compact and planar design of Butler Matrices makes them well-suited for integration into phased array antennas, reducing space requirements and improving overall system efficiency.

The Butler Matrix represents a pivotal advancement in antenna technology, enabling the precise control and manipulation of electromagnetic waves in antenna arrays. Its application extends across various fields, including military radar systems, satellite communication, and 5G wireless networks, where beamforming and beam steering are essential for optimizing signal strength and coverage.

### 2.3.1 Concept

In essence, the number of beams (N) in the Butler Matrix is directly proportional to the number of antenna elements, where N equals 2m, with 'm' being a positive integer. As asserted by [69], the Butler Matrix can be viewed as an implementation of the Fast Fourier Transform (FFT), making it the most computationally efficient option among various implementations involving power combiners, splitters, and phase shifters. However, it is worth noting that one limitation of this BFN is that its beams are fixed and cannot be dynamically adjusted.

### 2.3.2 Butler Matrix Structure

Analog passive BFN is the simplest and easiest RF power distribution circuit to feed the antenna array elements, which is used to provide a multi-beam rectenna system design. BFN is an RF power combining network, with N input port and N output port, where N is the same number of feeds in the array also a number of generated beams. The power passing from one of the input ports is distributed with equal amplitude between the output ports, but at different phases with a fixed phase difference angle which passively controls by BFN components. Various types of BFN has been implemented such as Rotman lens, Nolen and Blass matrix, but the Butler Matrix configuration is the simplest and easiest to implement than the other types [70]. Figure 2.6 illustrates the architecture of a conventional N X N Butler Matrix, which is composed of several hybrid branch-line couplers, crossover, and phase shifters.

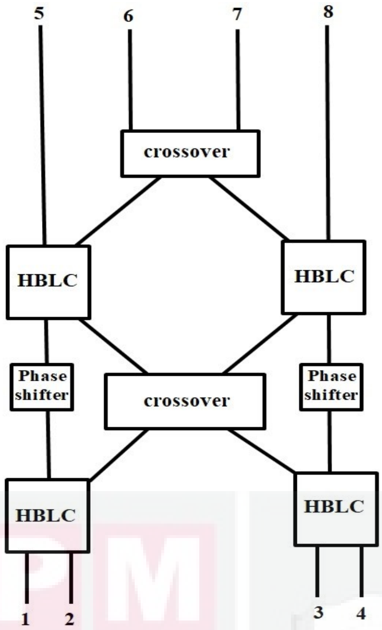


**Figure 2.6 : The architecture of a conventional 4 ×4 butler matrix**

Hybrid branch-line couplers (HBLC), also known as 90o branch-line coupler, is a microwave component utilized to combine power passively. HBLC is a special case of the directional coupler circuit (called a 3dB directional coupler) that has four ports with two input ports and two output ports. The power passing into any port is separated with equal amplitude and 90o phase difference between output ports. The number of HBLC utilized in BFN configuration is selected according to ((N/2) * log2 N). Figure 2.7 shows the HBLC structure design and also dimensions of transmission lines.

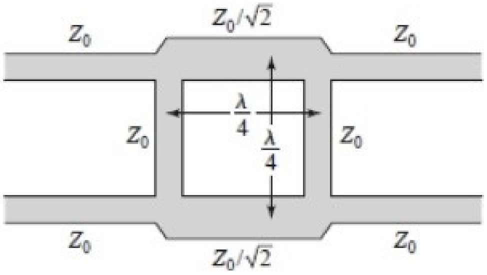

**Figure 2.7 : The architecture of a Hybrid branch-line coupler [71]**

By virtue of [71], the scattering matrix of 90o HBLC is given as follows:

$$[S]=\frac{-1}{\sqrt{2}}\begin{bmatrix} 0 & j & 1 & 0 \\ j & 0 & 0 & 1 \\ 1 & 0 & 0 & j \\ 0 & 1 & j & 0 \end{bmatrix} \quad (2.14)$$

A crossover circuit is a cascade of two HBLC. The crossover is utilized to pass the signals to the second stage without loss and with 0dB insertion loss. The scattering matrix of crossover is given as follows:

$$[S]=\begin{bmatrix} 0 & 0 & j & 0 \\ 0 & 0 & 0 & j \\ j & 0 & 0 & 0 \\ 0 & j & 0 & 0 \end{bmatrix} \quad (2.15)$$

Phase shifters are required to complete the Butler Matrix configuration. The phase shifter controls the phase difference between the output ports of the Butler Matrix. The phase shifter circuit consists of two coupled transmission lines folded at one of its edges.

## 2.4 Smart Antenna

Smart antennas rely on electronic beam scanning, or switching, as a key component of sophisticated wireless systems [72]. Satellite communications, intersatellite linkages, radars, sensor systems, mobile communications (5G and beyond), local area networks (LANs), GNSS, and wireless power transmission all rely on smart antennas, also known as adaptive arrays or intelligent antennas. Electronic beam scanning, or switching, is one of the most significant elements of a smart antenna. Smart antennas allow wireless devices to achieve optimal performance and channel throughput by electronically directing their maximum emission in the required directions while creating nulls against interfering sources [73]. The system of intelligent antennas is based on spatial processing. The area of coverage and transmission quality have expanded as a result of the rising number of users and demands; smart antennas help to meet all of these needs. When it comes to our human body systems, the functionality of smart antenna systems is well understood [74]. A human signal processor, the brain calculates where the speaker is coming from depending on the time delay between the sound waves heard by each ear. The brain determines the sound's direction by combining the strength of the signals received from each ear. When there are several speakers, the brain is able to block out the background noise and concentrate only on the topic at hand. In order for a listener to respond in the same direction as the intended speaker, they must point their transmitter (mouth) toward the speaker. Similar to human ears, except instead of ears, two antennas are used in smart antenna systems. Instead of the brain, a digital signal processor is used. The antennas' weights are adjusted to drive the main lobe in a certain direction while nulls are positioned in interference directions, using smart antenna design [42] [75]. Figure 2.8 shows the stretcher of Smart Antenna:

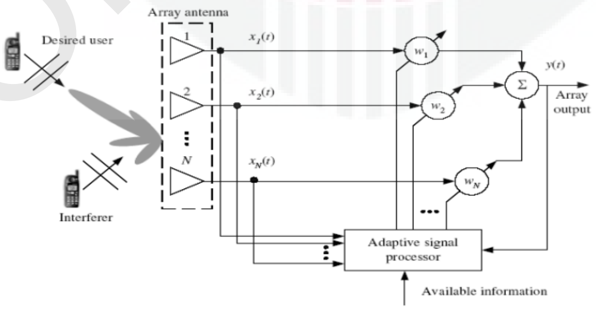


**Figure 2.8 : The stretcher of Smart Antenna [10]**

The first smart antenna systems were developed for military uses, where they were used to reduce interfering or jamming signals from the adversary. In FDMA, TDMA, and CDMA networks, these smart antenna systems often have active multi-beam technology and give significant performance increases [10].

### 2.4.1 Smart Antenna System Features and Benefits

This system has many advantages that radiate its use in the field of communications and can be summarized as follows [36]:

- To achieve interference rejection, an antenna pattern is directed towards co-channel interfering sources, therefore boosting the signal-to-interference ratio of received signals by a factor of two. As a result, there is an increase in capacity.
- As the radio environment changes, Spatial Division Multiple Access adjusts to the new conditions by providing each user with the highest quality uplink and downlink signals possible, and by distributing frequencies based on which users are most concentrated in a given geographic region. RF pollution and interference are reduced as a result of lower power usage (ease health hazard).
- The use of Smart Antennas in cellular communication might result in a considerable reduction in fuel use.

### 2.4.2 Configurations for Smart Antennas

It is possible to get reuse signal gain by combining the inputs from many antennas in order to enhance the amount of power available to cover a given region. To achieve interference rejection, an antenna pattern is directed towards co-channel interfering sources, improving the signal-to-interference ratio of received signals [73]. As a result, the capacity is increased. Spatial Division Multiple Access (SDMA) adjusts to the radio environment by giving each user the finest quality uplink and downlink signals and, owing to Smart Antenna, is capable of changing frequency allocation to the place where the greatest number of users are located. RF pollution and interference are reduced as a result of reduced power usage (a health hazard). The adoption of Smart Antenna in cellular connectivity will dramatically minimize diesel usage. Figure 2.9 shows the types of configurations for Smart Antennas.

These two types of research are thought to be among the most fertile ground for researchers to conduct and expand their work. Table 2.1 shows the most important differences between these two configurations and how they work:

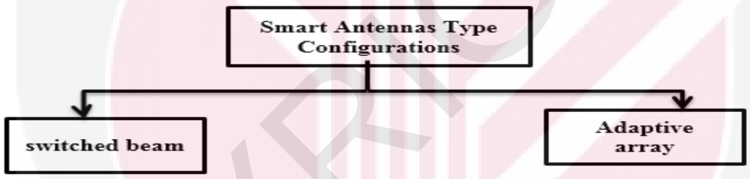


**Figure 2.9 : Types of  Configurations for Smart Antennas [76]**

**Table 2.1 : Most Important Differences between Switched Beam and Adaptive Array [42] [77]**

| Switched Beam Antennas | Adaptive Array Antenna |
|---|---|
| Definition: A multi-beam antenna, often known as a phased array antenna, is a switched-beam antenna. It is an antenna array that, based on predetermined weights assigned to each received signal, forms a large number of fixed beams in various directions. | Definition: Adaptive array antennas calculate user arrival directions, set beam former weights accordingly, and optimize the signal-to-interference ratio (S/I) and signal-to-noise power ratio (S/N). These antennas offer flexibility as the beam pattern adjusts with user movements. The null beam targets interferers, balancing interference, while the main beam focuses on the desired user. |
| **Example**: The antenna array, illustrated below, demonstrates beams directed in specific fixed directions. A switch selects the optimal beam to receive a signal from a targeted user among several others. This dynamic beam adjustment aligns with the user's movements.<br>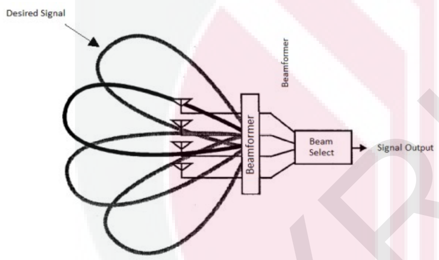<br> | **Example.** The figure below illustrates an adaptive array antenna's beam pattern, demonstrating the Direction of Arrival method to estimate the beam direction and effectively cancel interfering signals.<br>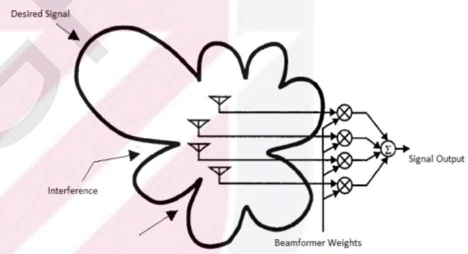<br> |
| **Benefit**: 1. Simplicity: Selecting a specific beam requires a beam forming network, an RF switch, and control circuitry. The process is streamlined.<br>2. Economical: Conducting all processing in the RF domain reduces the need for multiple translations to baseband, a cost-saving advantage given the expense of down conversion circuits in contemporary wireless systems. | Benefit: 1. Increased Service Users: Smart antennas enable frequency reuse, accommodating more users and reducing operational costs for network operators.<br>2. Range Expansion: Concentrating gain on connected devices extends coverage, potentially reducing the need for additional antennas or base stations.<br>3. Safety and Security: Smart antennas enhance security by not broadcasting signals omnidirectionally.<br>4. Reduced Interference: Directional radiation reduces interference, promoting frequency reuse and expanding system range.<br>5. Broadband Expansion: Frequency reuse and adaptive arrays increase available bandwidth. |
| **Non-Benefit**: 1. Limited Flexibility: The primary beam can only be focused in specific set directions, potentially limiting the gain in the user's actual direction. | **Non-Benefit**: 1. Complexity: Smart antennas are intricate, making flaw detection and troubleshooting more challenging. |

**Table 2.1 : Continued**

| | |
|---|---|
| 2. Limited Interference Reduction: Switched-beam antennas may not be optimal for SDMA applications where interference suppression is critical. The inability to form nulls in arbitrary directions limits their effectiveness in interference reduction. | 2. Higher Cost: Advanced processing technology increases the cost of smart antennas compared to standard antennas.<br>3. Larger Dimensions: The use of antenna arrays results in larger systems, potentially affecting aesthetics in social settings.<br>4. Placement Challenges: Smart antennas require strategic placement, which may differ from locations suitable for standard antennas. |

Switched beam antennas offer simplicity and cost-effectiveness in beam selection, making them suitable for certain applications. However, their limitations in flexibility and interference reduction need consideration based on the specific requirements of the wireless system in use. Meanwhile, adaptive array antennas offer enhanced capabilities but come with challenges related to complexity, cost, size, and placement considerations. Therefore, the antenna design proposed in this thesis combines the good advantages of both types while reducing the problems arising from them.

### 2.4.3 Machine Learning in Smart Antenna

Machine learning is an application of artificial intelligence (AI) that enables users to gather and evaluate data from their surroundings. Machine learning enables software to progressively learn and adapt to a given job without human intervention, allowing it to make data-driven judgments [37]. Machine learning works through statistical techniques, among other methods. Over the last decade, antenna designs have been extensively examined and used machine learning (ML) techniques because they can learn from antenna data collected or simulated through a training process, and subsequently assist in speeding up the entire antenna design process [78].

### 2.4.4 Evolution in Machine Learning

In order to calculate predation efficiency, statistical measures have been employed [79]:

1. Mean absolute percentage error (MAPE) based on equation (2.16)
2. Root mean square error (RMSE) based on equation (2.17)
3. Mean absolute error (MAE) according to equation (2.18)

For performance evaluation of LSTM and GRU deep learning algorithms, performance indexes were used to compare target values with actual values. These metrics have a single value to calculate the accuracy of machine learning algorithms. Different approaches to measuring the results of machine learning models are:

$$\mathbf{MAPE} = \frac{\mathbf{1}}{\mathbf{n}}\sum_{\mathbf{t=1}}^{\mathbf{n}} \mathbf{e_t^2} \qquad (\mathbf{2.16})$$

$$\mathbf{RMSE} = \sqrt{\frac{\mathbf{1}}{\mathbf{n}}\sum_{\mathbf{t=1}}^{\mathbf{n}} \mathbf{e_t^2}} \qquad (\mathbf{2.17})$$

$$\mathbf{MAE} = \frac{\mathbf{1}}{\mathbf{n}}\sum_{\mathbf{t=1}}^{\mathbf{n}} |\mathbf{e_t}| \qquad (\mathbf{2.18})$$

### 2.4.5 Machine Learning Models in Smart Antenna

Machine learning is based on data-driven algorithms without using rules-based programming [80]. It can generally be split into three main categories: supervised learning, non-controlled learning, and strengthened learning. Other less often used scenarios include: semi-supervised, transudatory, online, and active education [81].

The various learning algorithms in each category have been included. A model captures the core of the discovered knowledge in some formulation. Using a model will assist in our understanding of the world. Models may also be used to make predictions. Data mining can be quite rewarding for the data miner to discover new knowledge and build models that correctly predict the future, which is entirely used in smart antennas. The common steps thus include data planning, data mining, pattern validation, and the representation of information. Any important preprocessing of data is introduced during the data preparation stage, so the implementation of the data mining algorithms is most successful. Knowledge patterns are then extracted using the relevant machine learning algorithm [82]. In the phase of pattern analysis, the goal is to measure the achievable patterns of information and to minimize and summarize those patterns obtained to only the patterns of affective knowledge, thus collecting all the knowledge necessary for implementation. Knowledge production is about developing the required information in a form that is convenient for the needs of users, which should be easy to understand, test, and use in other applications if appropriate [78].

### 2.4.6 Approaches in Smart Antenna

The fundamental research criterion in smart antennas is to identify spatial signatures. Then, the intelligent antenna calculates beam forming vectors using these spatial signatures, which are used to track and locate a moving or target antenna beam. Two approaches are used in intelligent antennas: switched beam systems and adaptive systems [83]. A switched beam antenna contains several predefined radiation patterns, and a system requirement is based upon the appropriate radiation beam pattern. While the antenna spatial dimension is used, the primary ray occasionally cannot accurately indicate the interest signal (SoI), as illustrated [74]. The pattern of the beam is designed by altering the excitability of the individual antenna elements in a comparatively adaptive antenna system that offers beam orientation in all directions. Furthermore, these excitations might be adjusted in the direction of no interest (SNoI) to decrease radiation (b). Thus, the intelligent antenna can maximize spatial utility through adaptive beam shaping. The most frequent applications for intelligent antenna systems are acoustic signal processing, radar track and scan, and cellular systems like 5G and LTE. The primary distinction between reconfigurable antennas and intelligent antennas is that reconfigurable antennas are antennas with single elements instead of antenna arrays [11]. In spite of the tireless efforts of researchers, the key challenge of smart antennas with data learning and analysis remains unsolved. One of the major reasons for this outcome is that it recognized the most significant signal of interest for further analysis within a reasonable time and cost [34].

The primary benefit of smart antenna systems is their ability to simultaneously increase the amount of usable signal received and decrease the degree of interference, thus increasing the SIR ratio in densely populated areas. In essence, intelligent antennas can filter out background noise generated by other system users, allowing for the clear transmission and reception of critical signals. Furthermore, because smart antennas are more focused than omnidirectional and sectored antennas, they may be able to direct their energy in non-essential directions toward the intended users rather than squandering it in non-essential directions. This enables base stations to be further split, such as in less densely populated regions.

This application of smart antenna can be created by using different simulation tools to study microscopically and monoscopically different conditions. Table 2.2 gives a summary of these simulators to produce and analyze real-life scenarios.

**Table 2.2 : Smart Antenna Tools [84]**

| **Tools** | **Descriptions** | **Programming language and operating system** |
|---|---|---|
| Yagi Calculator | Calculate the dimensions of the antenna components using this online calculator. | Windows |
| VHF/UHF Yagi Antenna Design | The term "antennas for VHF UHF bands" refers to antennas for the VHF and UHF radio bands. | Java script |
| Antenna Scatterers Analysis Program | Antenna analysis software for numerical electromagnetic antenna design, modeling, and analysis is available for free. | Windows |
| 4NEC2 antenna modeller | For both the beginning and seasoned antenna modeller, 4nec2 is a fully free Nec2, Nec4, and Windows-based program for constructing, evaluating, optimizing, and testing 2D and 3D type antenna geometry structures, as well as generating, displaying, and/or comparing near/far-field radiation patterns. | Windows |
| Antenna Designer | Interactively construct, visualize, and analyze antennas in the Antenna Toolbox library. Using this application Choose antennas depending on their overall characteristics or their antenna performance. | MATLAB |

### 2.4.7 Conception of SA and Previous Studies

Nowadays, demand for antennas for applications is expanding dramatically as virtually every electronic instrument uses wireless signals. This means changeable functions, smart antennas, and the smallest possible size. An antenna design must, therefore, be intelligent and efficient. One of the most difficult components for future wireless communication and sensing is the antenna, which serves as a vital interface between propagating electromagnetic waves and electrical signals processed or created by integrated circuits [85]. The need for ever-shrinking physical size and weight for actual IoT applications, adequate efficiency for power and thermal concerns, and sufficient bandwidth for optimal data rate and sensor resolution are only a few of the competing factors in antenna design. Consider a common smartphone [78]. To build the data set for antenna designs, numerical simulations for various inputs and combinations can be used extensively. The geometric characteristics of intelligent technology utilizing a microstrip antenna must be studied design goals (e.g., resonance frequency, orientation, and efficiency) (e.g., slot and gap). Table 2.3 shows the most popular studies in antenna research.

**Table 2.3 : Most popular studies**

| Ref | Description | Limitation | Result |
|---|---|---|---|
| **[82] 2015** | The article explores various classification approaches and machine learning algorithms for categorizing network traffic. Nine classifiers, including BayesNet, Logistic, IBK, J48, PART, JRip, Random Tree, Random Forest, and REPTree, were selected for evaluation. Additionally, the study examined the performance of machine learning techniques such as Boosting, Bagging, and Blending (Stacking). | Out of the nine algorithms assessed, only two were tested in a mini-experiment, and demonstrated superior performance. Based on this limited experiment, they were identified as the most effective. Additionally, for ease of classification, a pre-existing classification tool is recommended. | The higher the quires (91.523) in random forest, the higher the precision (0.962) in Bayes net. |
| **[75] 2016** | The proposed system introduces three successful adaptive blind beam | The proposed system has not been evaluated by | The KW-CMA, when contrasted with previous blind beam formation |

**Table 2.3 : Continued**

| | | | |
|---|---|---|---|
| | formers for smart antenna systems, utilizing the constant modulus approach, particularly the constant modulus algorithm (CMA). Additionally, to mitigate side lobe levels (SLL), the system employs three different windows—hanning, hamming, and kaiser—resulting in algorithms named H-CMA, HW-CMA, and KW-CMA. | any classification methods, i.e., on the percentage of accuracy, error, or precision. | algorithms, excels in reducing PSLL significantly while ensuring swift convergence. Furthermore, it stands out for its energy efficiency, attributed to the elimination of side lobes. |
| **[86] 2017** | This paper addresses challenges in ultra-wideband radio transmission interferometry with Doppler radar, specifically when multiple targets share similar Doppler velocities in the same range bin, leading to visual anomalies. To tackle this issue, the paper proposes a combination of Doppler interferometry and Capon techniques. The technique, validated through numerical calculations and tests, notably enhances performance across diverse scenarios, offering a solution to challenges related to visual anomalies in the presence of multiple moving targets. | In order to improve accuracy, this approach requires a lot of flying. | When compared to an image acquired using a combination of the UWB Doppler radar interferometry imaging technique and the false image rejection method, the recommended methodology has a high accuracy of 26 mm and improves imaging accuracy by 47 percent. |
| **[87] 2019** | This study introduces a methodology employing Support Vector Machines (SVMs) with low-degree polynomial kernels. The SVMs are trained on datasets generated through diverse sampling procedures. Validation involves simulations with random array configurations, progressively increasing the number of components. | The influence of a single element on the amplitude of the far-field pattern diminishes as the size of an arbitrary array increases. This means that for large antenna arrays with thousands of components, the current SVM technique may be | The following setups yielded SVM kernel results: (a) 25 element dense regular array, 326 classes, (b) 18 element irregular array, 988 classes, and (c) 25 element irregular array, 326 classes, 8 element dense regular array, 988 classes. |

**Table 2.3 : Continued**

| | | | |
|---|---|---|---|
| | The objective is to assess the viability of the proposed SVM approach for large antenna arrays. | unable of detecting even a single faulty element. | |
| **[42] 2021** | This proposed system enhances wireless energy transfer efficiency in IoT applications through adaptive array processing algorithms. The approach employs a simple channel model and cost-effective estimate methods to minimize computational costs. Energy transmission occurs simultaneously with a common clock using continuous tones. The energy harvester calculates the optimal Received Signal Strength Indicator (RSSI) signal, with visual representations depicting average harvested power, gain convergence, and average RSSI statistics across multiple antennas with varying iteration and distance ranges. | The proposed system relied on listing its results only on the plans without addressing the details of the scheme. | A test is configured to function at 915 MHz with the help of the Universal Software Radio Peripheral (USRP), and energy is sent at that frequency. |
| **Proposal** | To construct a unified system facilitating the receiver's efficient selection of the optimal signal, characterized by minimal return losses and maximal gain, a novel modeling approach for intelligent antennas is suggested. This approach is grounded in an embedded control chip incorporating the Random Forest Decision (AI) algorithm. | The intelligent antenna system relies on an embedded 3 control chips to make real-time decisions using the Random Forest Decision algorithm. | The algorithm employed in the system aids in power conservation by dynamically adjusting the antenna settings based on the receiver's requirements. The intelligent antenna system leverages the embedded control chip, which facilitates real-time decision-making using the Random Forest Decision algorithm. |

The findings from Table 2.3 can be summarized as follows:

**Table 2.4 : Summary of previous studies**

| Refers | Year | ML | DL | Traditional antenna | Smart antenna | Single antenna | Multiple antennae |
|---|---|---|---|---|---|---|---|
| **[82]** | 2015 | ✓ | ☒ | ✓ | ☒ | ☒ | ✓ |
| **[75]** | 2016 | ✓ | ☒ | ☒ | ✓ | ☒ | ✓ |
| **[86]** | 2017 | ☒ | ☒ | ☒ | ✓ | ☒ | ✓ |
| **[87]** | 2019 | ✓ | ☒ | ✓ | ☒ | ✓ | ☒ |
| **[42]** | 2021 | ✓ | ☒ | ☒ | ✓ | ☒ | ✓ |

The appropriate ML method can be used (e.g., nearest neighbor, linear regression clustering, neural networks, etc.). This is the most crucial stage involving data processing and extracting information that can tie the output modification to the change in the input mode. This helps build a behavioral model that predicts or explains a specific numerical value based on several previous data [80]. The next generation of antenna technology and production technology could be inspired to carry out future work to enhance the IoT industry [42]. The projected results can enable automatic and robust design and production of future antennas for several wireless, medical, and aeronautical applications [88]. Table 2.5 displays a summary of current machine learning solution proposed for Smart Antenna.

**Table 2.5 : Summary of Machine Learning Solution in Smart Antenna**

| Author | ML methods | Scope |
|---|---|---|
| **Proposal work** | Random Forest Decision (AI) algorithm. | Reduce power consumption. |
| **A. Aoad [90]** | DTR, DFE, ANN | Improve efficiency and accuracy, also simulated directivity, half-power beamwidth, and VSWR are compared with measured results. |
| **Gampala and Reddy [91]** | Algorithm for optimizing generic machine learning with the Global Response Search Method (GRSM) | Built with a slotted patch antenna for GPS applications.<br>The use of machine learning enables the antenna designer to generate trained mathematical model that replicates the original antenna design and then apply optimization on the trained model. |
| **El Misilmani and Naous [37]** | ANN + Full-Wave analysis | Generic Antenna |
| **Wu et al [34]** | Artificial neural networks (ANN) and support vector machines (SVM) | Radar Antenna |
| **JP Geers [95]** | ML | Smart antenna to build a multi-agent system that enables a smart antenna grid to obtain an optimal solution. |

### 2.4.8 Antenna Array

Increasing an antenna's electrical dimensions can be accomplished by combining the radiating components in the geometric and electrical design, rather than increasing the size of each individual element. The elements of the array are mostly the same. It is not required, but it is more straightforward, more practical, and more convenient. In a single antenna array, the constituent elements could be of any kind (wires, microstrip, apertures, etc.). When the current in each antenna is equal to the current in the isolated antenna, which implies that the antennas are not coupled, the vector addition of the fields radiated by each element establishes the wide range of the antenna array. When the current in each antenna is equal to the current in the isolated antenna, it implies that the antennas are not coupled. This is the best-case scenario, and the performance is reliant on the manner in which the components come together and split from one another. Construction-wise, interfering fields from elements in the array should be used to produce directed radiation patterns and to demolish all other elements and objects in the surrounding space. The application of antenna array is summarized in Table 2.6:

**Table 2.6 : Machine Learning Approach in Antenna Array**

| Papers | Reference | ML methods | Performance |
|---|---|---|---|
| **de Lange et al.** | [87] | CNN | Prediction for Antenna parameters |
| **Gampala and Reddy** | [91] | Generic ML with Global Response Search Method (GRSM) optimization algorithm | Suited for GPS use and slotted patch antenna |
| **El Misilmani and Naous** | [37] | ANN + Full-Wave analysis | Generic Antenna |
| **Wu et al.** | [34] | Artificial neural networks (ANN) and support vector machines (SVM) (ANNs) | Radar Antenna |
| **Mahdi et al.** | [93] | NN | Forecast the opening antenna form |
| **Liu et al.** | [94] | ANN | |
| **Geers** | [95] | ML | Smart antenna |

## 2.5 Summary

In this chapter, the historical evolution of patch antennas and arrays is explored, highlighting their significance in various communication systems. As communication systems advanced, the demand for antennas operating across multiple frequency bands grew. Techniques like stacked patches and metamaterial-based structures were developed to broaden the bandwidth of patch antennas.

The chapter introduces beamforming technology, focusing on the versatile Butler Matrix. Beamforming plays a crucial role in steering electromagnetic waves precisely, addressing the need for high-speed data transfer, reduced interference, and improved connectivity. The Butler Matrix, in a passive beamforming network (BFN) design, is discussed by emphasizing its impact on the direction of beams in phased-array antenna (PAA) systems.

The section then transitions to recent research on Butler Matrix Networks and linear array antennas, specifically in the 28 GHz frequency band for 5G. Various studies are presented, each proposing different strategies to improve the efficiency and reduce the size of Butler Matrices. The evolution from traditional designs to compact, size-reduced structures is traced, acknowledging the challenges and advancements in each approach.

The chapter concludes by introducing the emergence of intelligent antenna technologies. 'Smart' antennas, including SAS, have become vital for efficient wireless communication systems. Machine learning's role in enhancing antenna performance and adapting to 5G technologies is highlighted. Several studies are cited, showcasing how machine learning aids in predicting signal propagation characteristics, optimizing antenna designs, and addressing challenges such as sidelobe levels and efficient wireless energy transmission.

While acknowledging the contributions of prior research, the chapter emphasizes the need for further exploration, particularly in miniaturizing systems, and introduces the thesis's unique design aimed at being the smallest of its kind in the 28 GHz frequency band. The chapter concludes by noting that practical constraints associated with implementing MIMO/smart antenna arrays in handheld devices need further attention for comprehensive research.

# CHAPTER 3

# RESEARCH METHODOLOGY

## 3.1 Introduction

This section describes the main stages of the practical aspect of the thesis and the methodology used to construct the proposed system. The proposed method includes several stages to achieve an intelligent antenna system.

## 3.2 System Description

This work aims to design an intelligent antenna system amalgamating a multi-beam antenna for 5G at 28 GHz, a 4x4 modified Butler Matrix, a 1x4 linear array antenna, and the Random Forest Decision algorithm implemented on an embedded control chip which not only meets the performance requirements of the 28 GHz band, but also aligns with the size constraints of modern devices. The Butler Matrix Network, known for its exceptional beamforming capabilities, and the 1x4 Linear Array Antenna are ingeniously combined in our design to enhance the overall performance and spatial diversity of the system. The compactness of the design allows for a high level of integration, making it an ideal candidate for modern communication systems where space constraints and weight are critical factors. However, reducing the size of the Butler Matrix without compromising its performance is a challenging task, and manufacturing such a device to function efficiently at the 28 GHz band introduces another layer of complexity. We introduce a modified conventional BM for a 5G system by removing one of the crossovers elements, and four orthogonal beams are formed. The beam is directed at four different directions, thus reducing interference from the nearby user, which means the scanning of a wider coverage area. The 1X4 slotted antenna array is simulated and then incorporated into the single-layer planer with a BM circuit designed. Therefore, a multi-beam radiation is achieved and simulated by using the Ansoft HFSS simulator. This chapter also thoroughly discusses the design strategies and the unique fabrication process. The innovative design stands out for its compactness, making it the smallest of its kind, while also maintaining high performance at a frequency band of 28 GHz, a key range in the 5G wireless communication spectrum. Figure 3.1 shows the structure of the general methodology of the thesis.

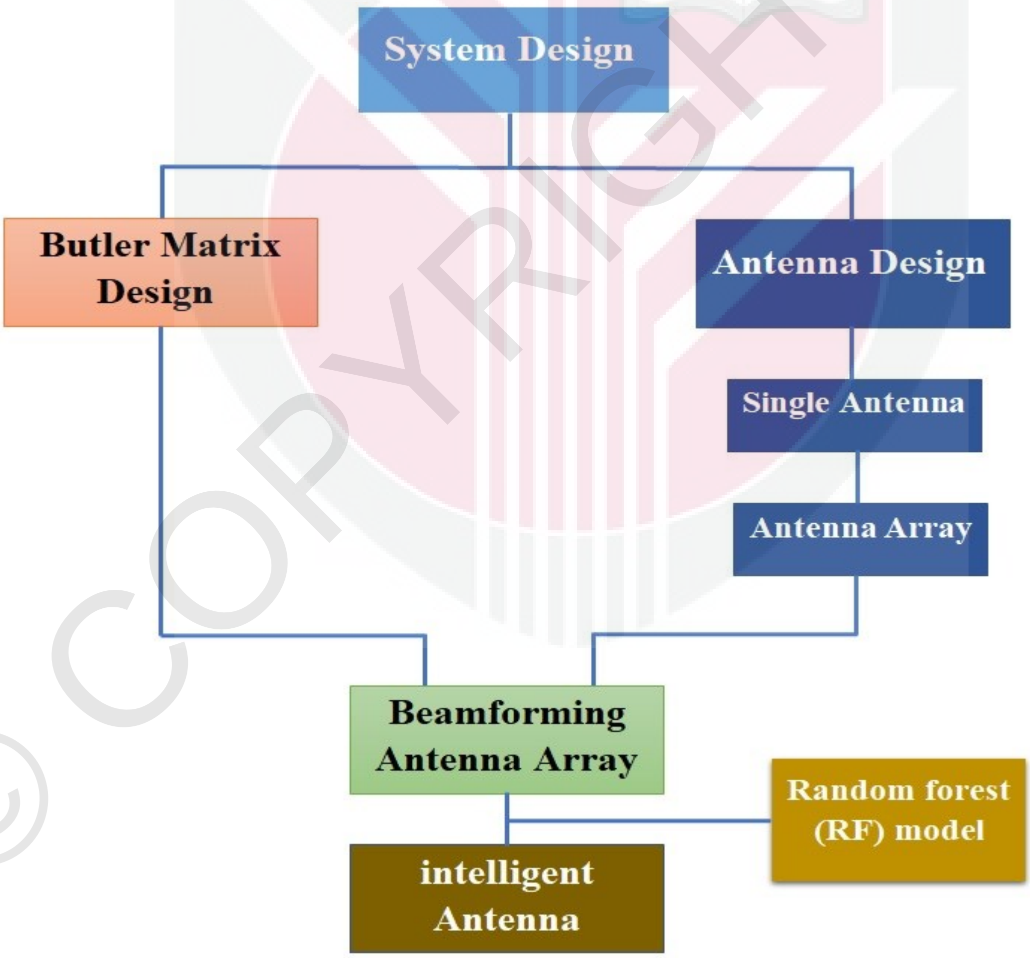


**Figure 3.1 : The General Methodology of the Thesis**

Three single antenna designs were studied to compare them and to choose the best design to form the antenna array, which will later be integrated with the Butler Matrix network. In this chapter, the methodology used in designing each of these three antennas will be discussed and their characteristics revealed.

Firstly, a design and simulation process is initiated for a printed Meander Line Antenna (MLA) tailored to meet the specifications of LTE mobile terminals. The designed MLA has a compact size of $(32 \times 28 \times 1.1)\ mm^3$ and operation frequency of 2.5 GHZ.

Secondly, a Multiband Hand-Held Antenna with E-shaped Monopole Feeding is meticulously designed, simulated, and fabricated utilizing the CST 2014 program for simulation.

The designed E-shaped has a compact size of $(42 \times 33.8 \times 1.5)\ mm^3$ and operation frequency of 2.4 GHZ.

Then, a new and compact Microstrip-Feed planar monopole antenna featuring invert U-slots is designed to cover a range of applications, including WiFi, Bluetooth, LTE, and 5G. The core structure of this antenna element is a rectangular patch, designed to operate in higher frequency ranges, with the aim of reducing the overall circuit dimensions. To achieve wideband performance, U-slots have been incorporated into the rectangular patch, serving as resonance pathways, followed by a linear antenna array comprising four planar monopole elements featuring invert U-slots. Assessments of all pertinent parameters are conducted, simulated, and scrutinized.

This work aims to design and fabricate a uniquely miniaturized 4x4 Butler Matrix Network integrated with a 1x4 linear array antenna for the 28 GHz frequency band, which not only meets the performance requirements of the 28 GHz band, but also aligns with the size constraints of modern devices.

To demonstrate the multibeam performance of the above components, direct incorporation between a slotted array antenna with a proposed BM is investigated. All the realized components have been arranged on the same layer and printed on the Roger-Ro4003, a dielectric material with 0.0022 tangent loss and a thickness of 0.305mm. Ansoft HFSS is used for implementation. The final design with all dimensions has a total size of 23mm X 20.5mm. Each BM's output port serves as a feeding line for the antenna array elements connected to them.

Finally, following the integration of the antenna with the Butler Matrix Network and the formation of a beamforming antenna array, an intelligent system is achieved through the utilization of a random forest model with three control chips (Ports-Controlled). Figure 3.2 shows the structure of the proposed system and its components.

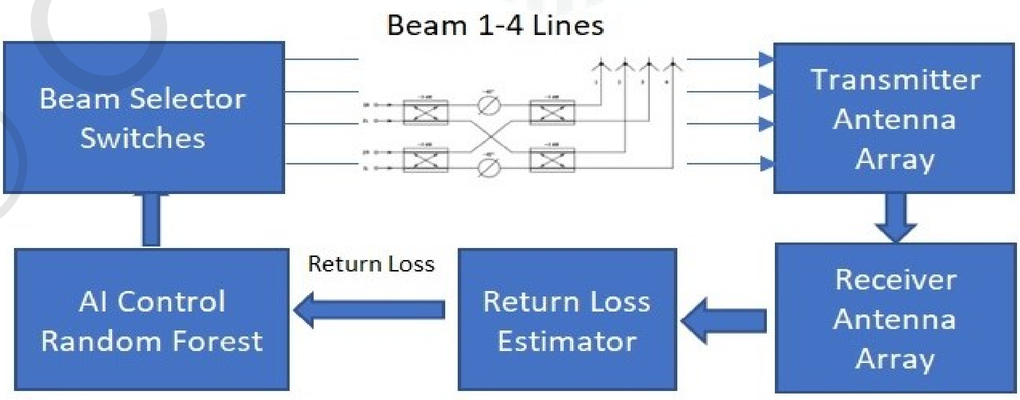


**Figure 3.2 : General diagram of proposed system**

The methodology of each part is explained in detail in the following sections.

### 3.3 Antenna Design

In Chapter 2, a comprehensive exploration of Multiple Linear Array (MLA) configurations tailored for LTE and 5G applications was undertaken. This current chapter redirects the focus towards the meticulous analysis and design of an antenna structure, specifically crafted to provide high gain and bandwidth performance. The emphasis is on applications within mobile communication and the Internet of Things (IoT).

A microstrip patch antenna composed of a dielectric substrate with a ground plane on the opposite side serves as the foundation for our design. This antenna type possesses several advantages, including its light weight, low-profile planar configuration, cheap manufacturing costs, and compatibility with microwave integrated circuits technology. Consequently, microstrip patch antennas find suitability in a wide range of applications, spanning wireless communication systems, cellular phones, pagers, radar systems, and satellite communication systems [50].

The selection of antenna dimensions is a critical aspect in antenna design, and several parameters are considered to ensure optimal performance. Firstly, the operating frequency is a fundamental parameter, as it dictates the size of the antenna elements based on the wavelength. Matching the dimensions to the desired frequency is crucial for efficient signal transmission or reception.

Secondly, the antenna type and design requirements influence dimensions. For instance, a patch antenna's dimensions are determined by the resonant frequency and substrate characteristics, while a dipole antenna's length is a function of the operating frequency.

The third parameter is the desired radiation pattern. The shape and size of the antenna play a role in steering the radiation pattern. For directional antennas, such as Yagi-Uda or parabolic antennas, dimensions are tailored to achieve specific beamwidths and gain.

Impedance matching is another crucial consideration. The dimensions of the antenna elements and the feed structure must be carefully chosen to achieve the desired impedance, ensuring efficient power transfer between the antenna and the transmission line.

Moreover, the physical size and form factor are important for practical deployment. In many applications, especially in mobile devices, compactness is a key criterion. Thus, dimensions are often constrained to meet space requirements while maintaining adequate performance.

In summary, antenna dimensions are determined by a combination of factors, including operating frequency, antenna type, radiation pattern requirements, impedance matching, and practical considerations related to size and form factor. The optimization of these parameters collectively ensures the antenna's effectiveness in its intended application [96].

### 3.3.1 Design MLA for Operating Frequency at 2.5 GHz Based on Defected Ground Structure

Because of their advantages of being lightweight, small, conformal, and having a high bandwidth, the compact printed antennas have become more widely utilized in wireless communication systems [97]. The Meander Line Antenna is a type of printed antenna in which the wire structure is embedded on a dielectric substrate to achieve downsizing in size; it is a combination of conventional wire and planer strip line in its most basic form. In this section, we propose an antenna design by using Defected Ground Structure (DGS) [98] instead of coplanar waveguide [99] to lower the size of the antenna by half, compared to the traditional design.

#### 3.3.1.1 Methodology

The proposed antenna specifications feature a compact size of (34 × 28 × 1.1) $mm^3$. All the dimensions are labelled in Table 3.1. A partial ground loaded with a defected ground structure (DGS) is utilized instead of a coplanar waveguide line, as depicted in Figure 3.3. Figure 3.4 illustrates the proposed ground structure. The substrate, with εr = 4.5 and a thickness of 1.1 mm, is employed in the proposed DGS antenna, which comprises 6 branches. The integration of a Defected Ground Structure (DGS) with an antenna yields numerous benefits. This includes the improvement of the radiation pattern, ensuring directed signal emission, and the broadening of bandwidth. DGS acts as an effective shield, mitigating electromagnetic interference and enhancing the signal-to-noise ratio. It contributes to size reduction, maintaining compactness without compromising performance. Additionally, DGS enhances gain and directivity, augments signal quality, and allows for frequency-selective characteristics. By controlling surface waves, it optimizes antenna performance and facilitates tailored impedance matching for optimal power transfer. Overall, the strategic use of DGS significantly optimizes the operational characteristics of the antenna, making it a versatile and efficient component in wireless communication systems.

**Table 3.1 : Proposed Antenna**

| **Parameter** | W | L | W2 | W3 | H | G | a | D | S |
|---|---|---|---|---|---|---|---|---|---|
| **dimensions in mm** | 28 | 32 | 28 | 15 | 13 | 23 | 3.6 | 2 | 0.4 |

The dimensions specified in the table achieved the highest gain and lowest return losses, and the impedance matching is 50 Ω.

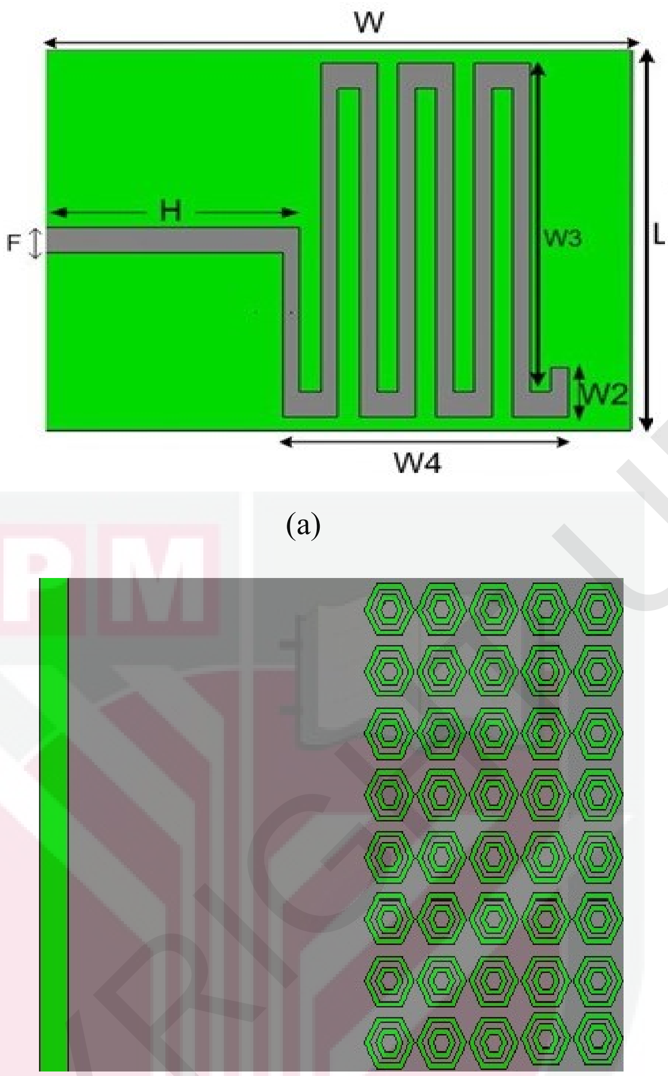


(a)

(b)

**Figure 3.3 : Geometry of the proposed antenna (a) Front and (b) Back**

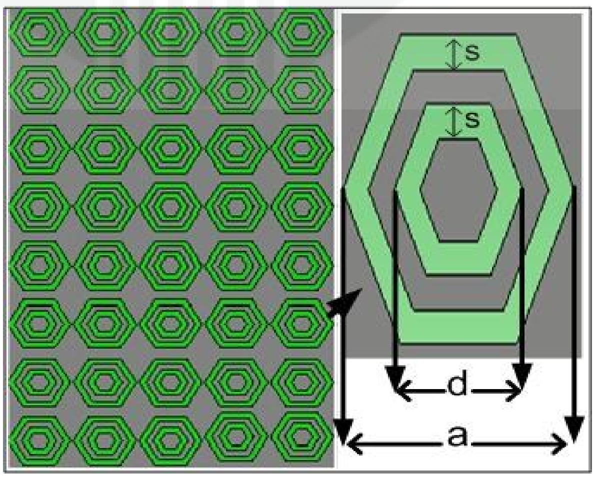


**Figure 3.4 : Geometries of DGS**

#### 3.3.1.2 Impedance Matching

The substrate and feed line thickness have been determined to suit the resistance required 50Ω. The impedance calculation software, as shown in Figure 3.5, was used to calculate impedance with respect to the height of the substrate and width of the feed line of MLA. Table 3.2 shows the results.

**Table 3.2 : Impedance Calculation**

| H mm | W mm | $\varepsilon$ | Impedance Ω |
|---|---|---|---|
| 1.5 | 2 | 4.5 | 58.4 |
| 1 | 1.5 | 4.5 | 54.23 |
| 1.1 | 2 | 4.5 | 50 |

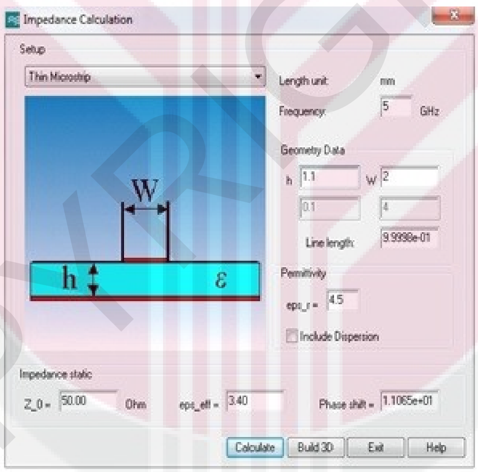


**Figure 3.5 : Impedance calculation**

### 3.3.2 Design Multiband Hand Held Antenna with E-Shaped Monopole Feeding

The development of a multiband hand-held antenna featuring an E-shaped monopole feeding mechanism represents a notable achievement in antenna design. The incorporation of the E-shaped monopole feeding structure not only ensures efficient impedance matching, but also enhances the antenna's bandwidth and radiation characteristics. This chapter delves into the intricate details of the antenna's design, simulation, optimization, and practical implementation.

#### 3.3.2.1 Methodology

The proposed antenna is a planar printed antenna with compact dimensions of $(42 \times 33.8 \times 1.5) mm^3$. The antenna can be easily integrated in small and sleek mobile devices. All the labelled dimensions are tabulated in Table 3.3. A prototype of the antenna is designed over FR4 substrate (ε_r= 4.5), with a thickness of 1.5 mm and loss tangent of 0.025, to obtain a compact radiation structure that meets the demanding bandwidth specification. Figure 3.6 shows the geometry of the proposed antenna.

The proposed antenna is composed of two planar E-shaped monopole and three branch lines. The first branch line acts as a monopole radiator at 900 MHz and at the same time acts as a cavity resonator fed by the E-shaped monopole that radiates in the upper frequency bands. The second and third branch lines increase the path over which the surface current flows and that eventually results in lowering the resonant frequency. The electrical length of the first line with 61.25 mm is optimized to resonate at 900MHz (869-993 MHz), while the electrical length of the second and third line is optimized to resonate at 700MHz (650-750 MHz) with a length of 83.85 mm and 89.8 mm, respectively.

**Table 3.3 : Parameters of the proposed antenna (all dimensions in mm)**

| | | | | | | | |
|---|---|---|---|---|---|---|---|
| **Parameter** | **L1** | **L2** | **L3** | **L4** | **L5** | **L6** | **L7** |
| **Value** | **36** | **27.5** | **18.5** | **4.5** | **14.5** | **12.9** | **10** |
| **Parameter** | **Ls** | **Lg** | **W1** | **W2** | **W3** | **W4** | **W5** |
| **Value** | **6** | **4** | **15.5** | **14.5** | **12** | **8** | **33.8** |
| **Parameter** | **W7** | **W8** | **Wg** | **Wf** | **W6** | **Lf** | |
| **Value** | **20.8** | **14.8** | **45** | **2.8** | **28.8** | **19** | |

The values in the previous table were adopted because they achieved the highest gains and lowest return losses and operate efficiently at the required frequency.

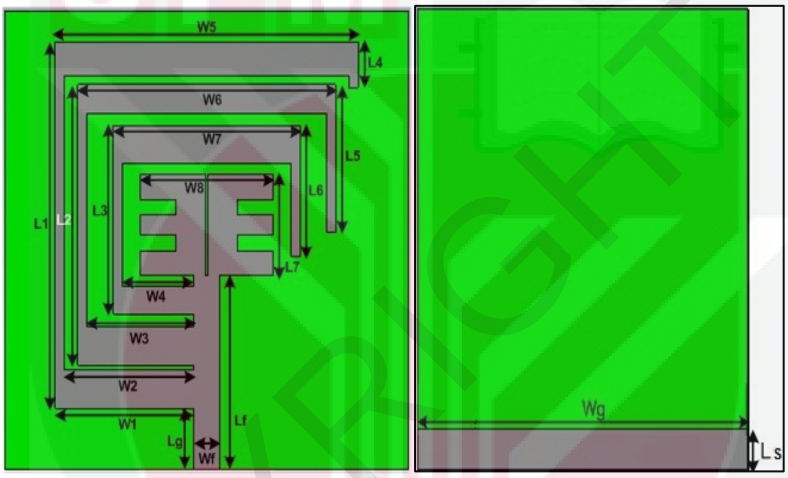


(a) Front (b) Back

**Figure 3.6 : Geometry of the Proposed Antenna (a) Front and (b) Back**

### 3.3.3 Design Novel Planar Monopole Antenna with Invert U-Slots

The design of a novel planar monopole antenna with invert U-slots represents a significant advancement in antenna technology [100]. This novel design holds great promise for a wide range of applications, including wireless communication systems and emerging 5G networks where versatile and efficient antennas are in high demand. This chapter delves into the intricacies of the design, simulation, and characterization of this ground breaking planar monopole antenna. The methodology employed for the design of the single antenna is depicted in Figure 3.7.

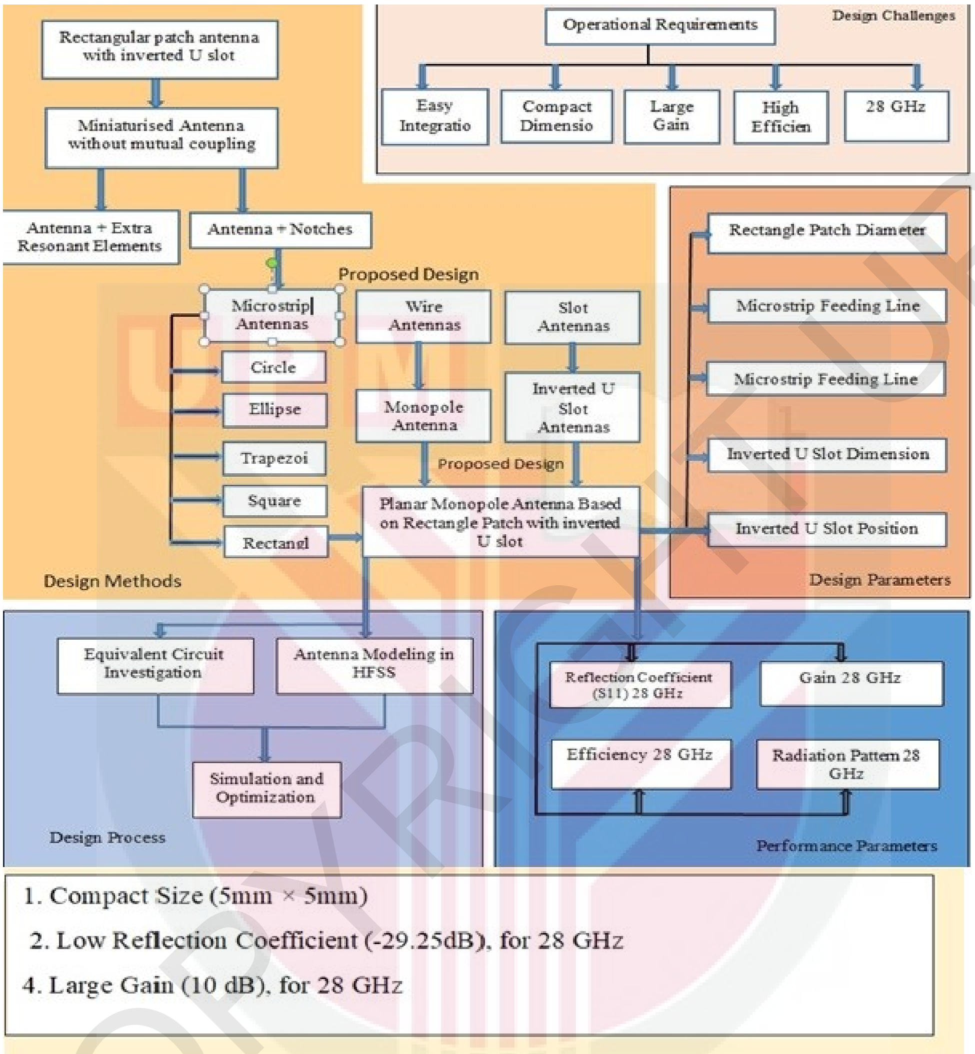


**Figure 3.7 : Investigation of Planar Monopole Antenna with Invert U-Slots**

### 3.3.3.1 Antenna Structure Design

Research indicates that among various shapes for printed antenna radiating patches, the rectangular configuration offers smaller dimensions relative to the operating frequency. The antenna is designed to produce 28 GHz. The following formulas are used to determine the antenna’s dimension [101].

$$w_p = \frac{v_0}{2f_r}\sqrt{\frac{2}{\varepsilon_r+1}} \tag{3.1}$$

The length of the patch is calculated:

$$L = L_f - 2\Delta L \tag{3.2}$$

The effective length, $L_f$ is calculated using this formula:

$$L_f = \frac{v_0}{2f_r\sqrt{\varepsilon_{rf}}} \tag{3.3}$$

$$\Delta L = 0.412h\,\frac{(\varepsilon_{rf}+0.3)\,\left({}^{w}/_{h}+0.264\right)}{(\varepsilon_{rf}-0.258)\,\left({}^{w}/_{h}+0.8\right)} \tag{3.4}$$

To calculate the effective dielectric constant $\varepsilon_{reff}$

$$\varepsilon_{rf} = \frac{\varepsilon_r+1}{2} + \frac{\varepsilon_r-1}{2} \tag{3.5}$$

Calculations are made and is optimized in the optimization technique in HFSS. The results are tabulated in Table 3.4.

**Table 3.4 : Dimension of the antenna**

| Parameter | Value (mm) |
|---|---|
| Length of patch, $w$ | 2.863 |
| Width of patch, $l$ | 2.5 |
| Length of substrate, $w_s$ | 5 |
| Width of substrate, $l_s$ | 5 |
| Length of feed line, $l_f$ | 1.85 |
| Width of feed line, $w_f$ | 0.4 |
| Length of slot Ls | 0.1 |
| Width of slot Ws | 0.1 |

The performance of the antenna at these dimensions is high in terms of gains and return losses, as well as matching the impedance of 50 ohms, which is the most important condition that must be met in order for the antenna to be able to transmit the signal at the required frequency, to reach the final size of the antenna at (5 × 5) mm$^2$, which is the desired goal due to its small size and high efficiency, as illustrated in Figure 3.8.

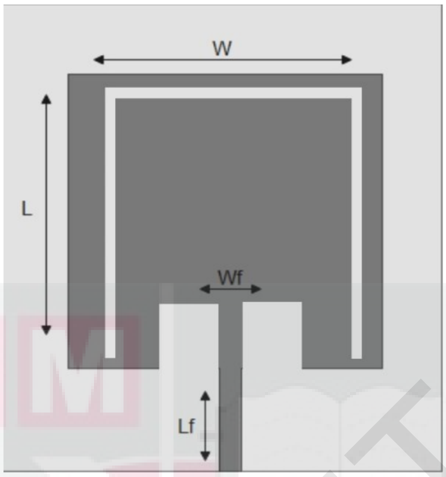


**Figure 3.8 : Geometry of the Proposed Antenna**

The proposed antenna is designed and simulated using high-frequency structure simulator (HFSS) software. The dimension of the antenna is 5 mm × 5 mm by using Roger-Ro4003 with a dielectric constant of 0.0027 and thickness of 0.305 mm. The ground dimension is the same as the substrate of 5 mm × 5 mm using copper with thickness of 0.035 mm. The width of feed line, $w_f$ and length of feed line, $L_f$ are 0.4 mm × 1.85 mm, respectively. 50 Ω matching is achieved by using quarter waveguide feed line.

### 3.3.4 5G Antenna Array Design

Connecting to the proposed BFN, a straightforward patch array antenna operates at 28 GHz. This setup involves four rectangular slotted patch antennas, each measuring 5mm × 18.5mm. The design employs the inverted U-slot for easy resonance at the operating frequency without mutual coupling. The methodology employed for the design of the single antenna is depicted in Figure 3.9. Adopting a uniform linear array ensures physical alignment with the modified BM. The substrate material is RogerRo4003 with a thickness of 0.305mm, and the dimensions are tabulated in Table 3.5. For antenna feeding, a multi-microstrip feed is chosen for its suitability in direct integration with the BM. Figure 3.10 shows the proposed design, and the dimensional parameters of the design are indicated in the caption.

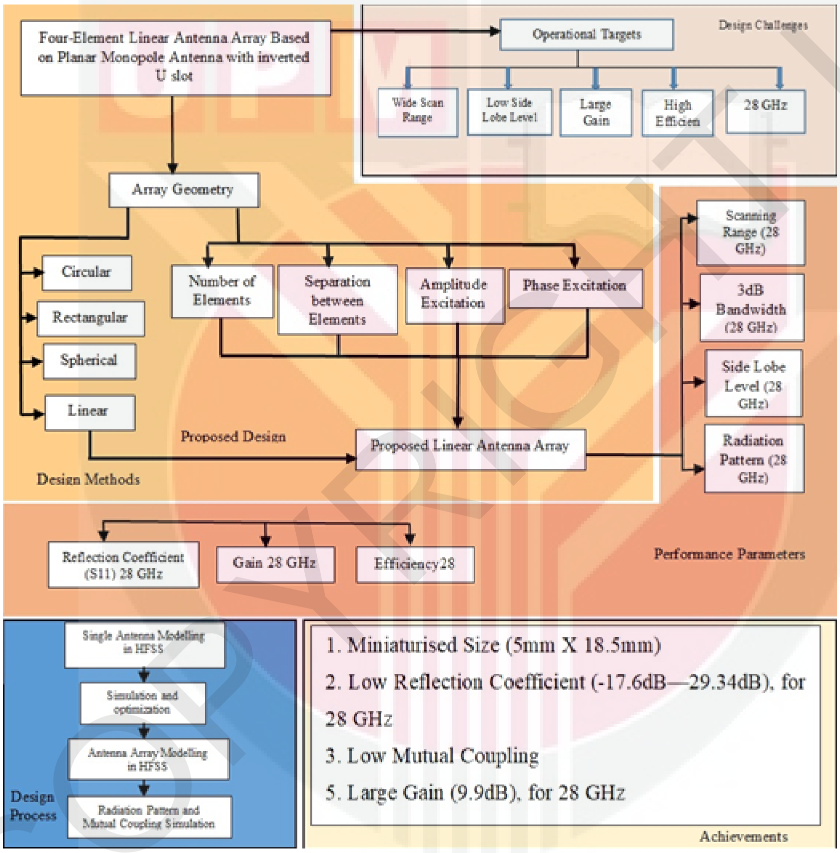


**Figure 3.9 : Investigation of Four-Element Linear Antenna Array**

**Table 3.5 : Dimensions of the antenna**

| Dimensions | Value (mm) |
|---|---|
| Patch length | 2.83 |
| Patch width | 2.5 |
| Feed line length | 1.5 |
| Feed line width | 0.4 |
| Slot width | 0.1 |
| Space between elements | 4.5 |

The antenna exhibits excellent performance at these specified dimensions, delivering high gains, low return losses, and effective impedance matching at 50 ohms. Meeting this crucial condition is essential for the antenna to efficiently transmit signals at the required frequency. Further details on this performance will be discussed in Chapter 4.

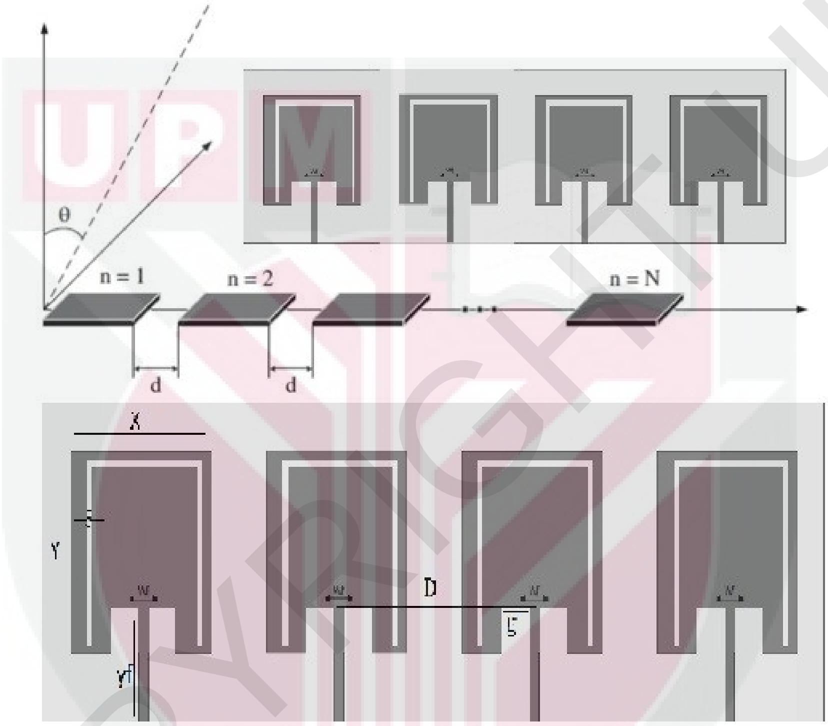


**Figure 3.10 : The schematic of the 5G antenna array proposed, with dimensions of (X=2.5, Y=2.83, xf=0.4, yf=1.5, D=4.5, g=0.35, s=0.1) mm**

Array factor can be determined by:

$$\mathbf{AF} = \sum_{n=1}^{N} \boldsymbol{exp\, j\, (n = 1)\psi} \quad \mathbf{(3.6)}$$

$$\boldsymbol{\psi = kdcos(\theta) + \beta} \quad \mathbf{(3.7)}$$

Where k is the propagation number (k= $\frac{2\pi}{\lambda}$ ), n is an array element number, and θ represents the scan angle of the array. The d has a significant role; it should be large enough to avoid the mutual coupling between the elements, but should not be too large in order to avoid the grating lobe.

## 3.4 5G-BM Structure Design

The proposed configuration for a 4-beam Butler Matrix includes hybrid branch-line couplers, one crossover, and two phase shifters, which were designed and optimized using Keysight ADS software from Agilent Technologies. The investigations of BMN geometry are shown in Figure 3.11.

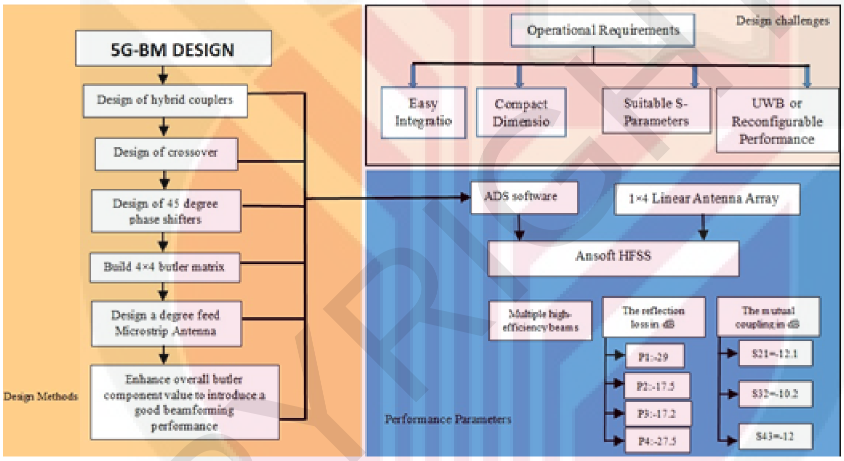


**Figure 3.11 : The investigations of Butler Matrix Network**

The Butler Matrix elements consist of transmission lines, and the lengths of these elements are calculated using microstrip feed line equations. Constructed on a Roger-Ro4003 substrate layer (0.305 mm thickness, dielectric constant of 3.55, and a loss tangent of 0.0022) with perfect conductor (copper) strips, the design isolates Butler Matrix elements from the ground plane. The schematic structure of the adopted Hybrid Branch Line Coupler design is illustrated in Figure 3.12 within the

ADS schematic window, featuring HPLC built-in components, microstrip line connectors, input ports, and a power probe for output power measurement.

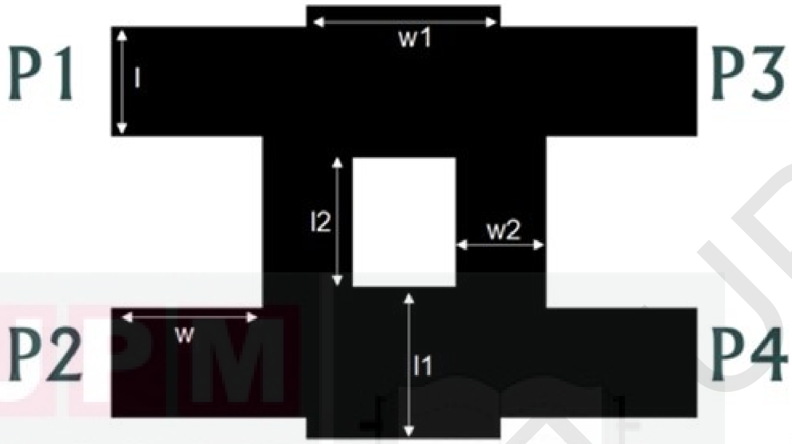


**Figure 3.12 : The HBLC structure (l=0.936, w=1.28, l1=0.876, w1=1.29, l2=1.09, w2=0.758) mm**

The simulated phase difference is near to the theoretical 90o phase difference by an average of ±5° over the frequency range of (20-30) GHz. By virtue of the scattering matrix of HBLC is given as follows [102]:

Even mode:

$$\begin{bmatrix} K & L \\ M & N \end{bmatrix} = \begin{bmatrix} 1 & 0 \\ jY_L & 1 \end{bmatrix} \begin{bmatrix} 0 & jZ_K \\ jY_K & 0 \end{bmatrix} \begin{bmatrix} 1 & 0 \\ jY_L & 1 \end{bmatrix} \quad (4.1)$$

$$\Gamma_e(S11) = \frac{K + L - M - N}{K + L + M + N} = 0 \quad (4.2)$$

$$R_e(S21) = \frac{2}{K + L + M + N} = -\frac{(1+j)}{\sqrt{2}} \quad (4.3)$$

Odd mode:

$$\begin{bmatrix} K & L \\ M & N \end{bmatrix} = \begin{bmatrix} 1 & 0 \\ -jY_L & 1 \end{bmatrix} \begin{bmatrix} 0 & jZ_K \\ jY_K & 0 \end{bmatrix} \begin{bmatrix} 1 & 0 \\ -jY_L & 1 \end{bmatrix} \quad (4.4)$$

$$\Gamma_0(S11) = \frac{K + L - M - N}{K + L + M + N} = 0 \quad (4.5)$$

$$\mathbf{R_0(S21)} = \frac{2}{\mathbf{K+L+M+N}} = -\frac{(1-j)}{\sqrt{2}} \qquad \mathbf{(4.6)}$$

Having characteristic admittance of the conventional branch-line coupler $Y_K = \frac{1}{Z_K}$ and $Y_L = \frac{1}{Z_L}$, where $R_e$, $\Gamma_e$ and $R_0$, $\Gamma_0$ represents transmission and reflection coefficients of the even and odd modes, respectively. Therefore, for an ideal matching condition, the scattering parameter matrix of the standard BLC is:

$$[S]=\begin{bmatrix} S_{11} & S_{12} & S_{13} & S_{14} \\ S_{21} & S_{22} & S_{23} & S_{24} \\ S_{31} & S_{32} & S_{33} & S_{34} \\ S_{41} & S_{42} & S_{43} & S_{44} \end{bmatrix} = \frac{1}{\sqrt{2}}\begin{bmatrix} 0 & j & 1 & 0 \\ j & 0 & 0 & 1 \\ 1 & 0 & 0 & j \\ 0 & 1 & j & 0 \end{bmatrix} \qquad \mathbf{(4.7)}$$

A crossover can be formed by combining two HBLCs. Figure 3.13 illustrates the configuration of the crossover. The crossover is utilized to pass the signals to the second stage without loss and with 0dB insertion loss. The scattering matrix of the crossover is given as follows [16]:

$$[S]=\begin{bmatrix} 0 & 0 & j & 0 \\ 0 & 0 & 0 & j \\ j & 0 & 0 & 0 \\ 0 & j & 0 & 0 \end{bmatrix} \qquad \mathbf{(4.8)}$$

For the conventional transmission line section, the KLMN matrix is given by:

$$\begin{bmatrix} K & L \\ M & N \end{bmatrix}_{\frac{\lambda}{4}} = \begin{bmatrix} \cos\theta & jz\sin\theta \\ \frac{j}{z_0} & \cos\theta \end{bmatrix}\begin{bmatrix} 0 & jZ_0 \\ \frac{j}{z_0} & 0 \end{bmatrix} \qquad \mathbf{(4.9)}$$

Finally, the scattering parameters are given as:

$$s_{11} = \frac{s_{11}^e + s_{11}^o}{2} \qquad \mathbf{(4.10)}$$

$$s_{21} = \frac{s_{21}^e + s_{21}^o}{2} \qquad \mathbf{(4.11)}$$

$$\mathbf{s_{31}} = \frac{\mathbf{s_{31}^e + s_{31}^o}}{\mathbf{2}} \quad (4.12)$$

$$\mathbf{s_{41}} = \frac{\mathbf{s_{41}^e + s_{41}^o}}{\mathbf{2}} \quad (4.13)$$


**Figure 3.13 : The crossover structure**

Figure 3.14 gives the configuration of the schematic structure of the shifter designed. We analyzed the operation of a phase shifter, specifically focusing on its performance at a frequency of 28 GHz. Our experimental results show a noteworthy correspondence with theoretical expectations, particularly in the aspect of the phase shift value.

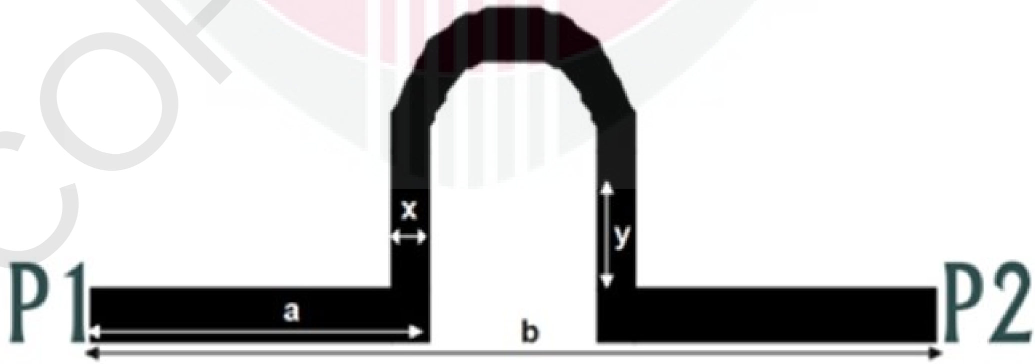


**Figure 3.14 : The phase shifter with its schematic (a=3.08 b=8.71 x=0.4 y=1.2) mm**

All relevant components are seamlessly integrated to construct a modified Butler Matrix (BM) network, implemented through a microstrip transmission line. The schematic structure and symbol of the overall adopted 4×4 BM design are depicted in Figure 3.15 within the ADS schematic window. The layout design clarifies that ports 1 to 4 serve as input ports, whereas output ports 5 to 8 are linked to the antenna network as depicted in Figure 3.16. The designated purpose of the BM is to uniformly feed all elements in the antenna array with equal amplitudes and phase shifts that vary uniformly. Upon exciting different input ports, theoretically distinct phase shifts are achieved (-135º, -45º, 45º, and 135º) [103]. Consequently, the beam can be switched in different directions. The overall size is 15mm x 17mm, approximately (1.4x1.58)$\lambda c^2$, where $\lambda c$ represents the wavelength at 28 GHz.

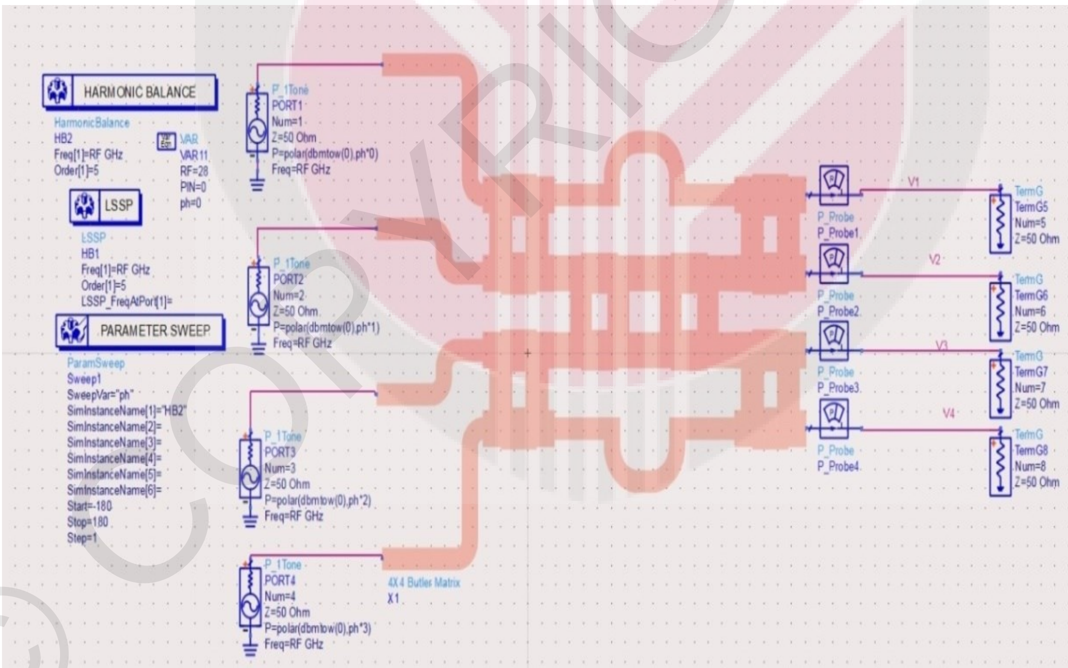


**Figure 3.15 : The schematic of the 4X4 Butler Matrix proposed**

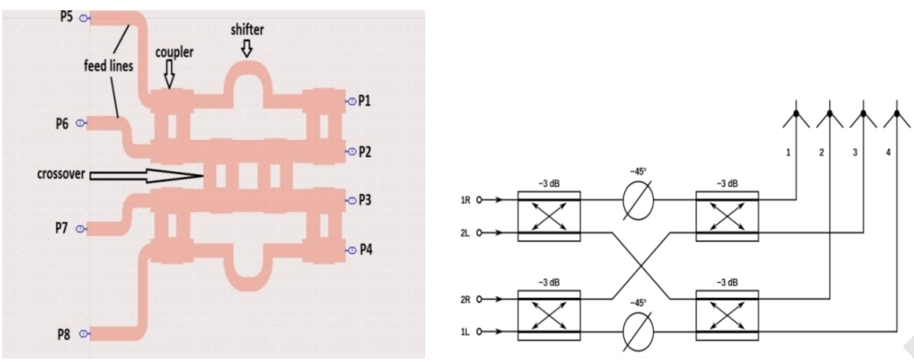


(A) (B)

**Figure 3.16 : The layout design of (a) the 4X4 Butler Matrix proposed and (b) the Butler Matrix construction**

## 3.5 5G Beamforming Antenna Array

Finally, to demonstrate the multibeam performance of the above components, direct incorporation between a slotted array antenna with a proposed BM is investigated. All the realized components are arranged on the same layer and printed on the Roger-Ro4003, a dielectric material with 0.0022 tangent loss and a thickness of 0.305mm. Ansoft HFSS is used for implementation. As illustrated in Figure 3.17, the schematic of the final design with all dimensions has a total size of 23mm X 20.5mm. Each BM’s output port serves as a feeding line for the antenna array elements connected to them.

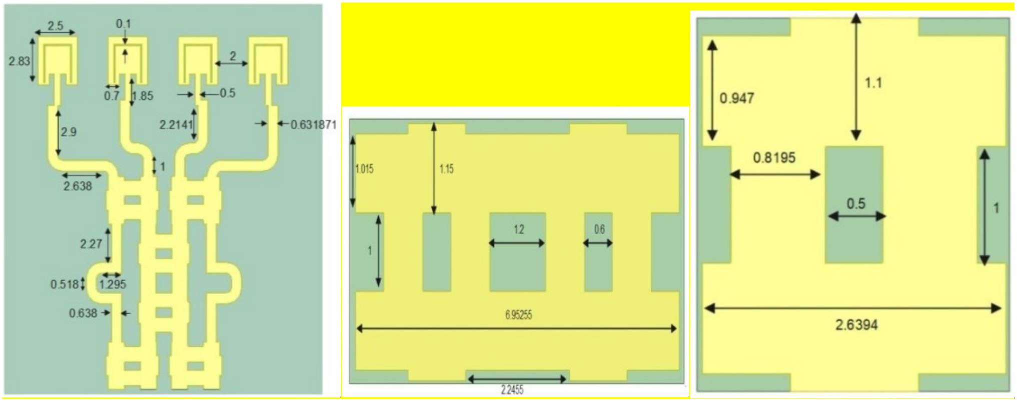


**Figure 3.17 : The schematic of the 5G multi-beam antenna proposed**

## 3.6 Ports-Controlled Beamforming Network Designed for Intelligent Antenna Arrays by Control Chips

Following the integration of the antenna and Butler Matrix on the same layer, the complete adaptive system, encompassing both transmission and reception capabilities, was meticulously designed. This holistic system amalgamates a 5G multi-beam antenna operating at 28 GHz, a 4x4 modified Butler Matrix, a 1x4 linear array antenna, and employs machine learning techniques—specifically, the Random Forest Decision Algorithm. The algorithm is implemented on an embedded control chip.

In this section, a modeling approach for an intelligent antenna is presented, centered around an embedded control chip employing the Random Forest Decision (AI) algorithm [104]. The primary objective of the research is to establish an integrated system wherein the most suitable signal is selected by the receiver, minimizing return losses and maximizing gain. Signal degradation, often encountered in traditional antenna systems due to reflections, interference, and variable signal strengths [105], is targeted for resolution through intelligent antenna technology.

Challenges associated with reception quality optimization are addressed within the proposed system, with a pivotal role played by the embedded control chip in enabling real-time decision-making [106].

Responsibility for data collection and processing related to signal parameters, including signal strength, interference levels, and frequency bands, lies with the control chip in our proposed system. The Random Forest Decision algorithm, recognized for its robustness and accuracy in classification tasks [107], is employed to analyze this information. Through the power of AI, the system intelligently determines the optimal signal for reception, with a dual emphasis on minimizing return losses and maximizing gain.

Furthermore, the modeling approach incorporates power conservation mechanisms to address concerns surrounding energy efficiency [108]. In traditional antenna systems, substantial power consumption is observed, irrespective of the actual receiver requirements. By employing the embedded control chip and AI algorithm, the system is empowered to dynamically adjust the antenna configuration and power consumption based on the receiver's needs [109]. This adaptive power management approach ensures efficient energy utilization, minimizing wastage and contributing to sustainability.

### 3.6.1 Intelligent Antenna Design

The primary objective of this part is to create a feed network for an antenna array that enables the control of input ports, allowing them to be turned on or off as needed by subscribers. Figure 3.18 provides an illustration of the proposed feed network.

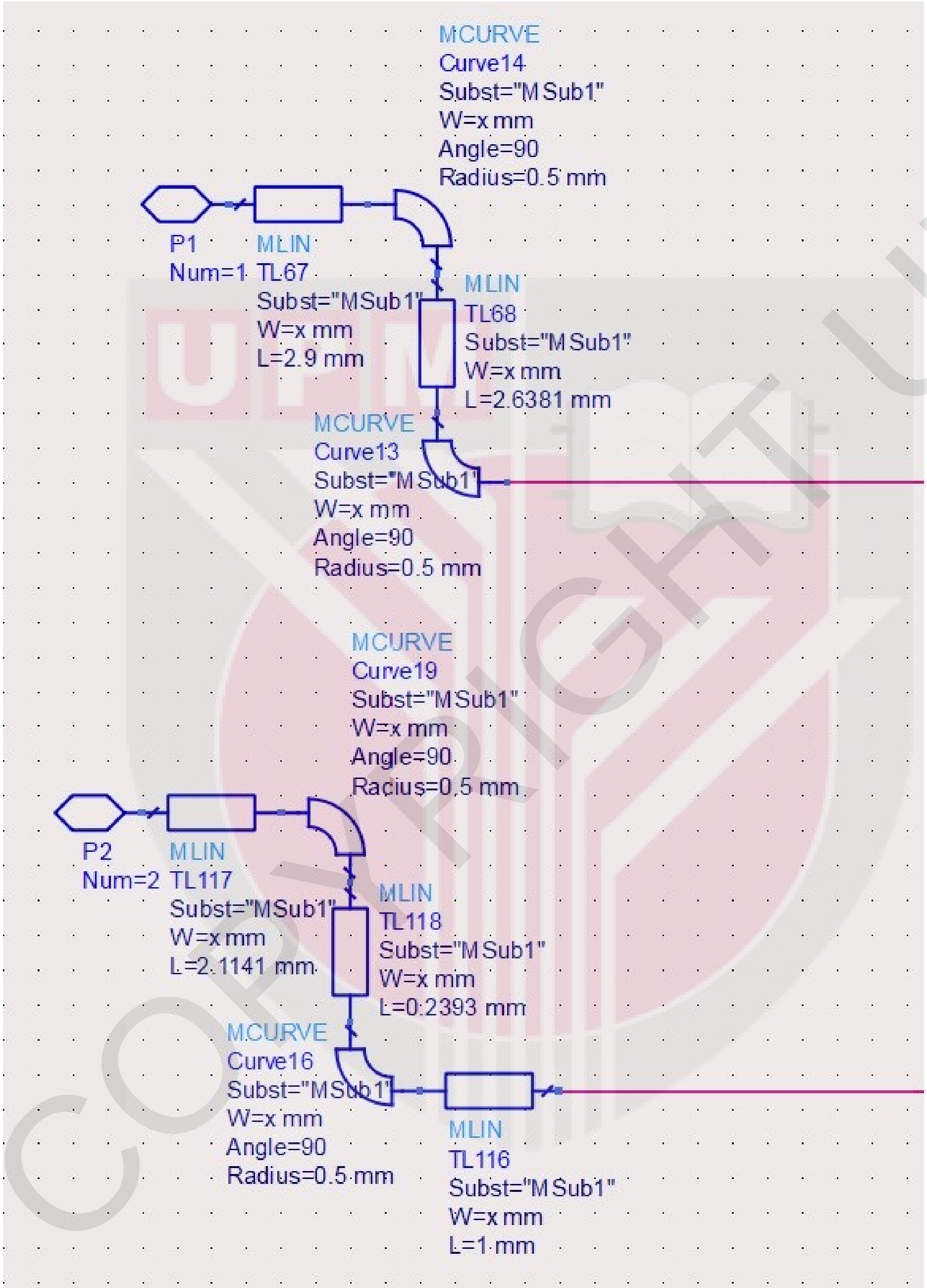


**Figure 3.18 : The proposed feed network**

The intended function of this feed network, as found for the Butler Matrix (BM), is to distribute equal amplitudes and induce phase shifts that vary equally among all elements in the antenna array. When different input ports are excited, this results in theoretically different phase shifts, specifically [-135º, -45º, 45º, and 135º]. Consequently, this capability allows for the steering of the beam in various directions. The complete adaptive system, which facilitates both sending and receiving functions, combines several components. These include a 1x4 linear 5G multi-beam array antenna operating at 28GHz, a modified 4x4 Butler Matrix, and the utilization of machine learning techniques, specifically the Random Forest Decision algorithm, which is implemented on an embedded control chip. Figure 3.2 illustrates the three controllers involved in this system:

- FPGA chip 1: Return Loss Estimator (in which the return losses are placed to calculate the error rate).

To reduce power consumption, a strategy is proposed wherein the initial control chip serves as a table for subscribers. It collects data from subscribers and return losses data for error rate calculations.

- FPGA chip 2: The AI control unit is implemented in hardware by projecting it on an FPGA chip.

Given knowledge of the optimal gain for peak performance, it has been included in the algorithm for comparison. If the gain falls within the specified range, additional port operations are unnecessary. Conversely, the algorithm triggers commands to the third chip to activate another port when required.

- FPGA chip 3: Beam selector switches are controlled by the output of the AI control to turn on the required antenna beam that gave the lowest return loss and highest gain.

The proposed approach depends basically on the classification of the estimated return loss to select the highest gain port with less power consumption. Therefore, the AI model will switch the ports on and off automatically based on the estimated return loss, as simplified in the following algorithm:

Algorithm: Deep Learning Process for Random Forest Decision

*Step 1:* *Load data*

*Step 2:* *Read the subscriber table from the receiver antenna*

*Step 3:* *If the gain <= 4.4 dB then:*

*Step 4:* *Input return loss from the table to the Random Forest (RF) model*

*Step 5:* *The RF model selects port numbers to be ON to increase the transmission power.*

*Step 6:* *The beam selector is activated based on the selected port numbers in Step 5.*

*Step 6* *Else: Go to Step 1*

Figure 3.19 summaries the algorithm for random forest decision making for the proposal.

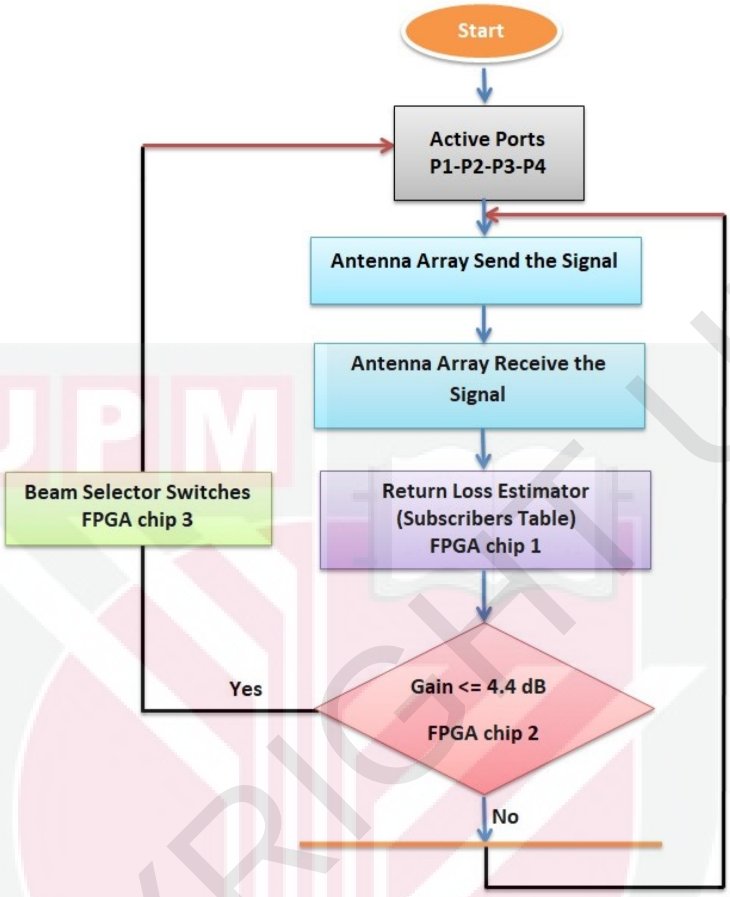


**Figure 3.19 : Deep Learning Algorithm for Random Forest Decision**

Figure 3.20 displays the layout of the proposed feed network. The input ports (P1, P2, P3, P4) are linked to a control chip, which functions as a beam selector switch. The signals from the control chip then enter the 4x4 matrix, where the required output ports are activated.

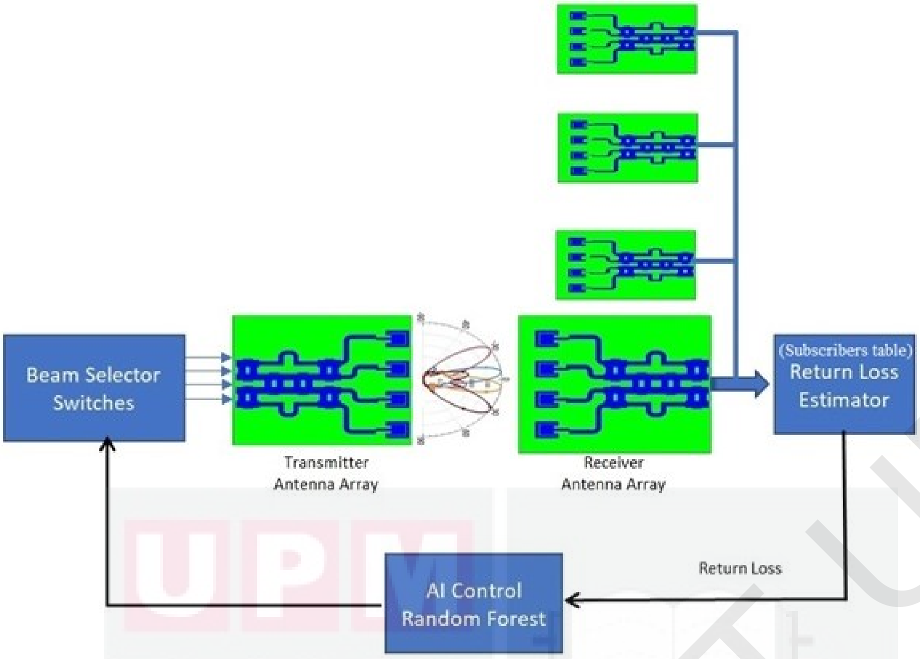


**Figure 3.20 : The Proposed Closed Loop Control Model**

## 3.7 Summary

Chapter 3 of the thesis outlines the comprehensive methodology employed in the study, detailing the development, implementation, and testing of various antenna designs. Firstly, the microstrip patch antenna (MLA) for 2.5GHz is thoroughly examined using CST Microwave Studio 2014. Parametric studies explore the effects of varying substrate, feed line, and ground diameters, with the incorporation of a defective ground structure successfully minimizing the antenna size.

The chapter then introduces a new compact planar antenna design supporting a wide range of mobile services, ISM applications, DVB, and wireless communication services. This antenna boasts a more compact size compared to previously published designs.

Following this, a novel compact planar monopole antenna configuration with U-slots for WiFi/Bluetooth LTE and 5G frequency bands is presented. The impact of varying slot dimensions on antenna performance is investigated, revealing optimal parameters for achieving low reflection coefficient, high gain, and omni-directional radiation patterns at 28 GHz. The versatility of this antenna structure is highlighted for applications in multi-functional wireless communication systems.

The methodology proceeds with the design, simulation, optimization, and characterization of a four-element linear planar monopole antenna array using a unit antenna. The array, implemented on a RogerRo4003 substrate, demonstrates close correlation between reflection coefficient and mutual coupling measurements with design simulations. This array is intended for integration into a smart antenna system, with plans to measure radiation properties alongside the feeding network and phase shifters. The main beam scanning angles are also demonstrated through HFSS simulations.

Finaly, the chapter introduces a novel modeling approach for intelligent antennas utilizing an embedded control chip and the Random Forest Decision algorithm. This system dynamically adjusts the antenna settings to conserve power based on receiver requirements, ensuring real-time decision-making. The algorithm analyzes signal parameters such as strength, interference, and frequency bands to intelligently identify the most suitable signal for reception, optimizing performance while minimizing return losses. Incorporating power conservation mechanisms, the intelligent antenna system prevents unnecessary energy wastage.

# CHAPTER 4

# RESULTS AND DISCUSSION

## 4.1 Introduction

This chapter includes the results and discussion of the proposed methodology for designing an intelligent antenna system amalgamating a multi-beam antenna for 5G at 28 GHz, a 4x4 modified Butler Matrix, a 1x4 linear array antenna, and the Random Forest Decision algorithm implemented on an embedded control chip. The ensuing results encapsulate the performance, efficacy, and synergies achieved by this integrated system, shedding light on its capabilities in the realm of advanced wireless communication.

## 4.2 Simulation Results of MLA for Operating Frequency at 2.5 GHz based on Defected Ground Structure

The following stages are performed to investigate the effect on return loss for various parameter values:

First step: Change the ground height (G) from 17 mm to 23 mm with step 3 mm increments while keeping the other settings the same. Figure 4.1 depicts the return loss characteristic. The best return loss S11 value is found when (G) equals 23 mm, at 2.5 GHz resonant frequency, and bandwidth of 62 MHz. This indicates that the ground height has an impact on the operating frequency and bandwidth. Table 4.1 shows the various simulation results achieved for altering the ground width height.

**Table 4.1 : Simulations for different heights of the ground (G)**

| G | F-start | F-stop | BW |
|---|---|---|---|
| 23 mm | 2.439 GHz | 2.501 GHz | 62 MHz |
| 20 mm | 2.457 GHz | 2.517 GHz | 60 MHz |
| 17 mm | 2.492 GHz | 2.551 GHz | 59 MHz |

Second step: Change the feed line's height (H) from (13-17 mm) with step 2 mm, and without any change in the other parameters. Figure 4.2 depicts the return loss characteristic. The best value of return loss S11 is determined when (H) equals 13 mm and the bandwidth is 57 MHz. Table 4.2 shows the various simulation results achieved with different ground width heights.

**Table 4.2 : Simulations for different heights of the feed line (H)**

| H | F-start | F-stop | BW |
|---|---|---|---|
| 13 mm | 2.469 GHz | 2.526 GHz | 57 MHz |
| 15 mm | 2.459 GHz | 2.512 GHz | 53 MHz |
| 17 mm | 2.439 GHz | 2.501 GHz | 62 MHz |

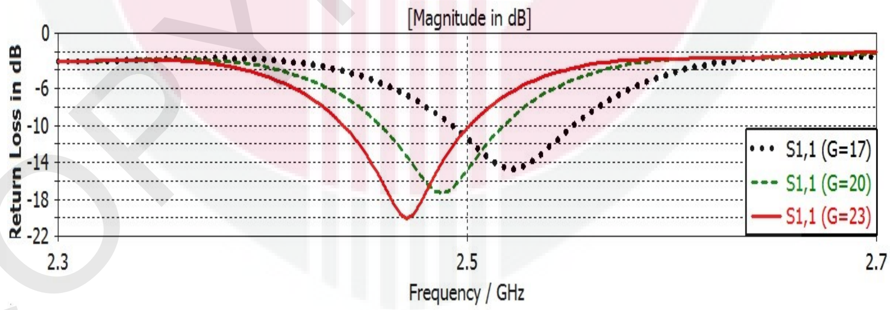


**Figure 4.1 : Return Loss (S11) for Different Ground Heights (G)**

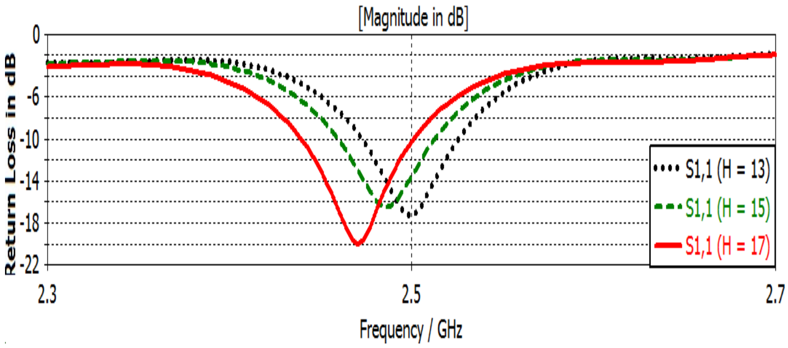


**Figure 4.2 : Effect of Different Feed Line Heights (H)**

Figure 4.3 shows the Omnidirectional radiation pattern of MLA with gain calculations at main lobe of 3.21 dB which is very suitable for offered applications.

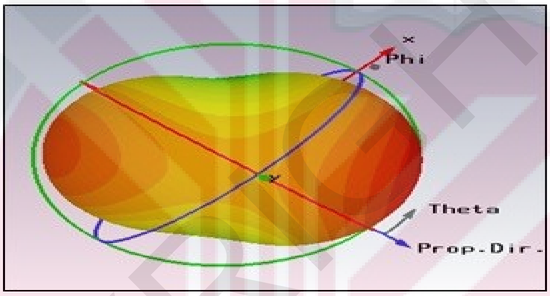


**Figure 4.3 : 3D pattern of MLA at 2.5 GHz**

## 4.3 Simulation Results of Multiband Hand Held Antenna with E-Shaped Monopole Feeding

The proposed antenna is simulated using the CST Microwave Studio 2014. The first and the second resonant frequency are controlled by adjusting the total length of the third, second, and first lines and the third and fourth resonances are controlled by adjusting the dimensions of the monopole radiators and branch lines.

The current distribution on the antenna is simulated as shown in Figure 4.4.

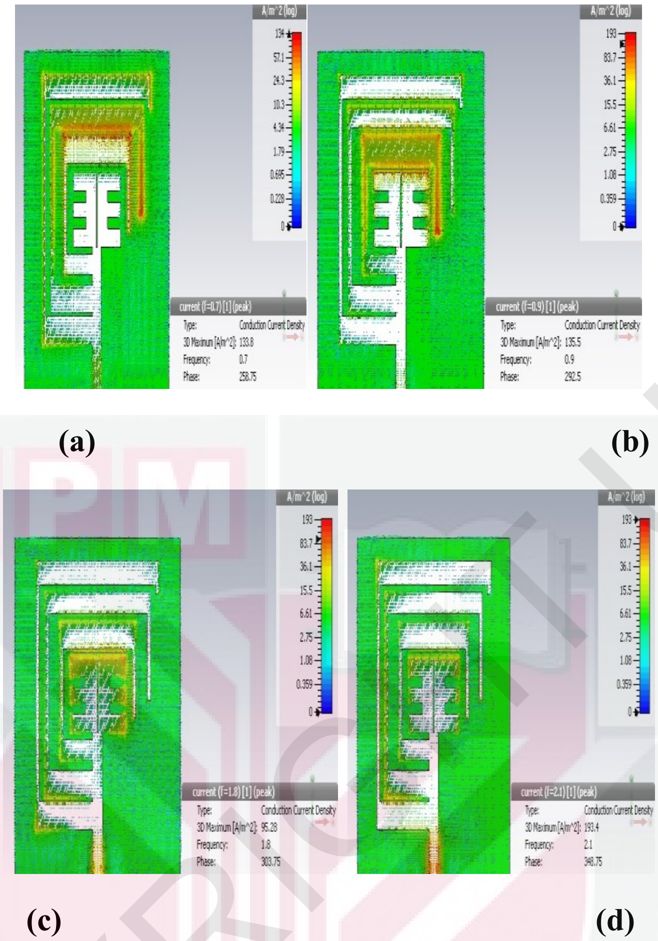


**Figure 4.4 : Current Distribution of the Antenna at Different Frequencies (a) 0.7 GHz, (b) 0.9 GHz, (c) 1.8 GHz, and (d) 2.1 GHz**

It is seen that the current distribution is concentrated consecutively on the branch lines at 0.7GHz, 0.9 GHz, and 1.8 GHz frequencies, respectively, and on the monopole at 2.1 GHz. These phenomena mean that the position of the first, second, and third resonant frequencies are controlled by adjusting the total length of the corresponding line while the fourth band from 1.4 MHz to 3.13 GHz is controlled by adjusting the dimensions of the monopole radiators.

A prototype of the antenna is fabricated over FR4 substrate ($\varepsilon_r$= 4.5) with 1.5 mm thickness and loss tangent of 0.025 as shown in Figure 4.5.

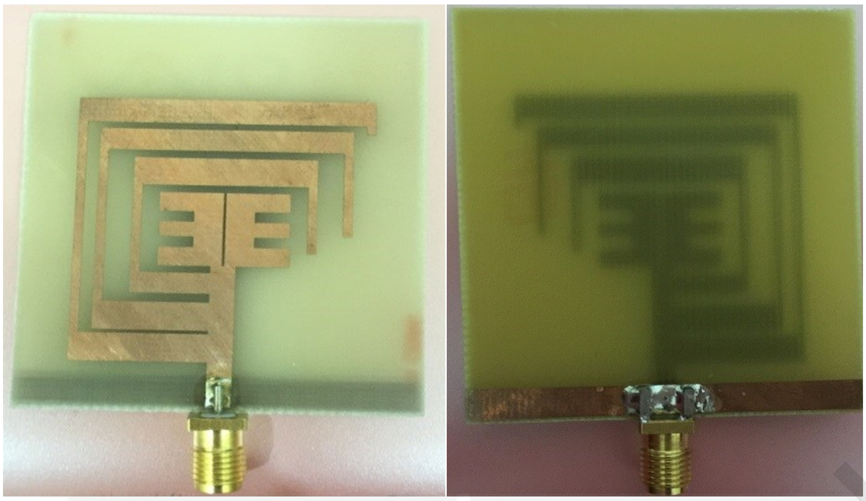

(a) Front (b) Back

**Figure 4.5 : A Photo of the Fabricated Antenna (a) Front and (b) Back**

Figure 4.6 shows a comparison between the simulated and measured results of the return loss. The simulated and the experimental results ensure that the antenna covers many of the aforementioned mobile and wireless applications bands. Taking the -10 dB return loss reference, the antenna operates in the three bands from 650 to 750MHz, from 872MHz to 1 GHz, and from 1.4 to 3.13 GHz. One of the very important parameters that should to be considered is the size of the ground plane.

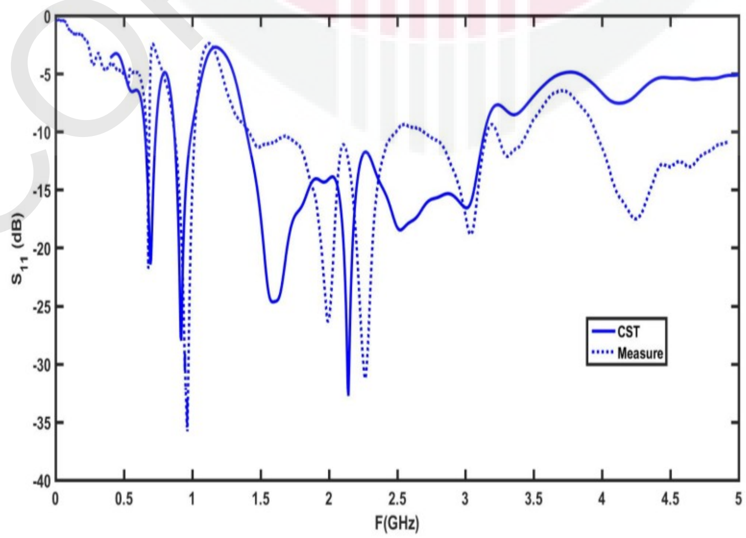


**Figure 4.6 : The Measured and Simulated Return Loss**

By simulating the antenna at different ground sizes, it is noticed that the length of the ground plane affects the matching slightly as shown in Figure 4.7, and the value of s11 is shown in Table 4.3. Figure 4.8 shows the simulated radiation patterns at frequencies 0.7, 0.9, 1.8, and 2.1GHz. Hence, the proposed design is suitable for different hand held devices with different sizes.

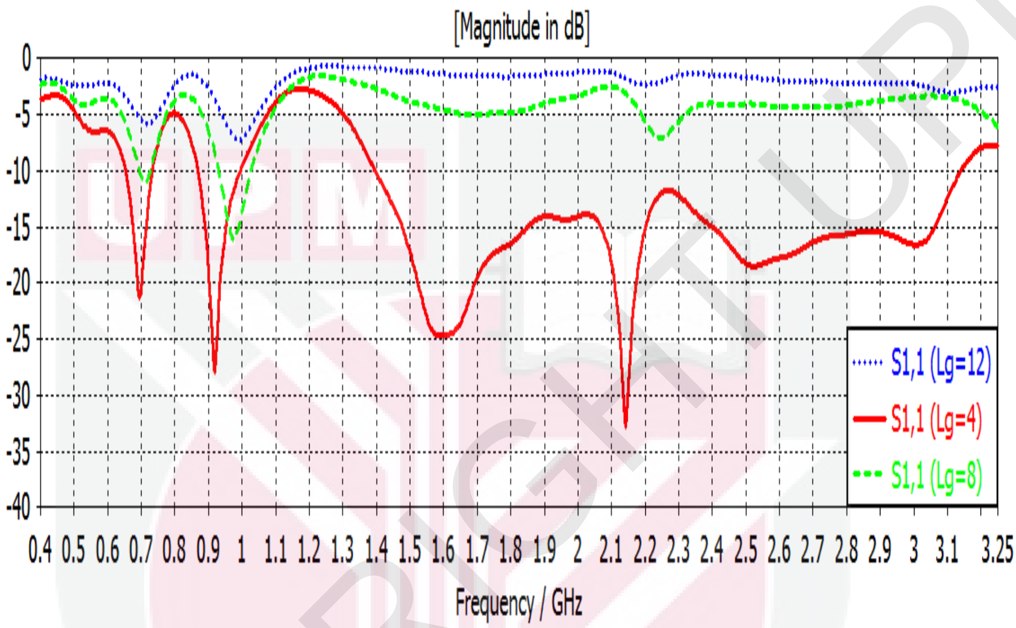


**Figure 4.7 : Return Loss by Varying the Ground Length, Lg**

**Table 4.3 : Return Loss by Varying the Ground Length, Lg**

| F In GHz | S11 by varying Lg In dB | | |
|---|---|---|---|
| | 4 mm | 8 mm | 12 mm |
| 0.7 | -19.245 | -10.784 | -5.561 |
| 0.9 | -19.406 | -6.573 | -2.704 |
| 1.8 | -16.410 | -4.810 | -1.595 |
| 2.1 | -18.875 | -2.497 | -1.319 |

| GHz) | XZ Plane | YZ Plane |
|---|---|---|
| 0.7 | 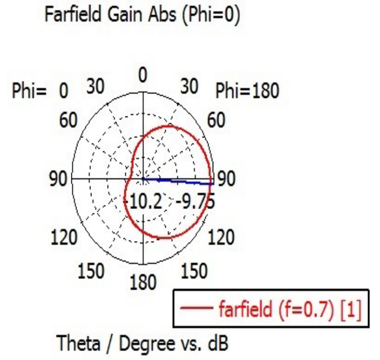 | 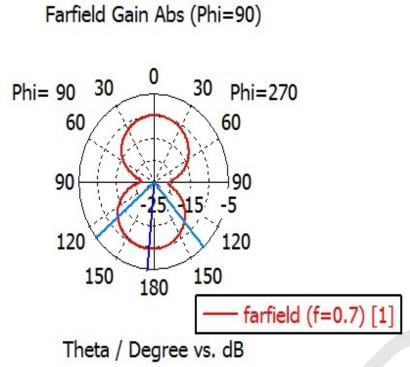 |
| 0.9 | 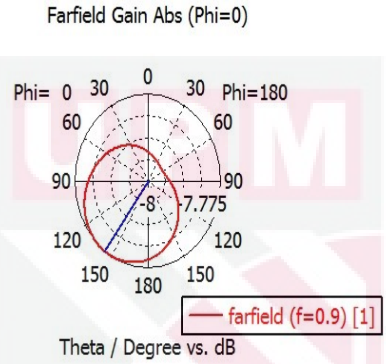 | 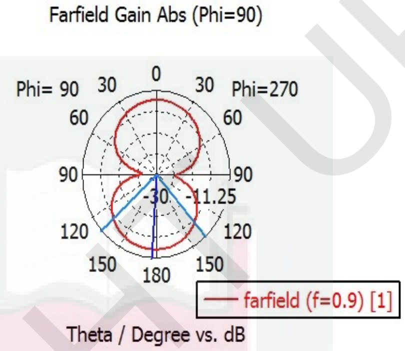 |
| 1.8 | 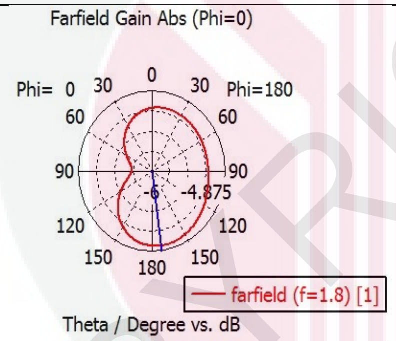 | 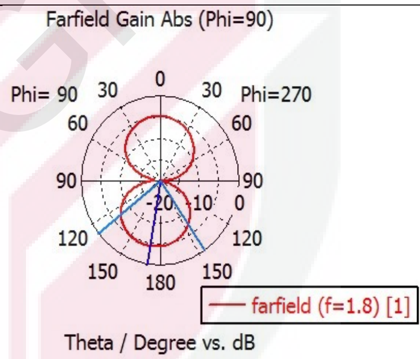 |
| 2.1 | 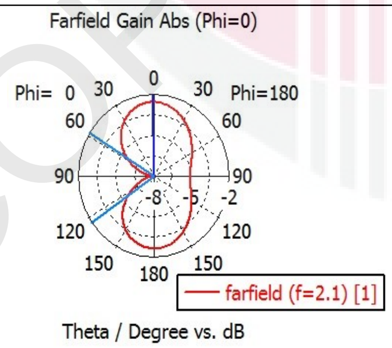 | 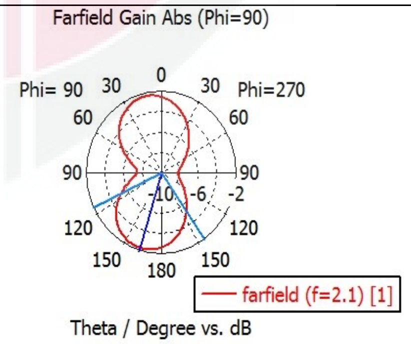 |

**Figure 4.8 : The Radiation Pattern (in dB) in the XZ and Y Z planes. The Antenna in the XY plane**

## 4.4 Simulation Results of the Novel Planar Monopole Antenna Design with U-Slots

Figure 4.9 presents the simulation results for the antenna in HFSS, which shows that the antenna operates at a frequency range of 28 GHz, and the return losses in this frequency at -33 dB. By varying the values of WS and LS, the U-slots dimensions are changed, which generates different resonate frequency performances.

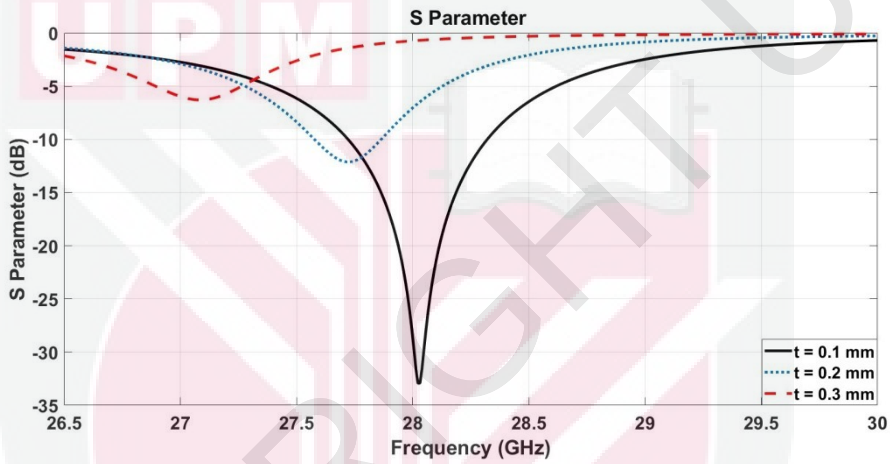


**Figure 4.9 : The antenna simulated results Return Loss (S11) with different values of t**

The antenna gain is at 28GHz 6.28 dB, so the antenna has excellent amplification capacity, which enhances its ability to efficiently direct radio signals and make the most of them in a specific direction. This means that the antenna is able to achieve high performance in receiving or transmitting wireless signals with excellent efficiency, which further improves the overall wireless system performance as shown in Figure 4.10.

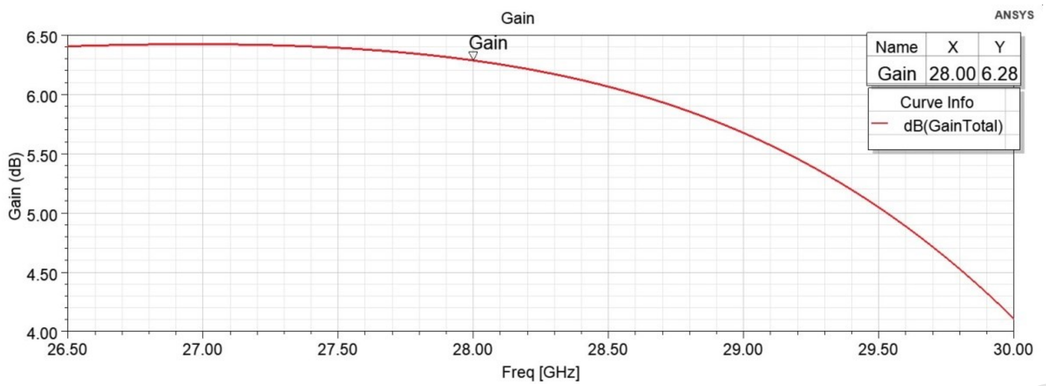


**Figure 4.10 : The antenna Gain**

The proposed antennas were compared, and the results are summarized in Table 4.4.

**Table 4.4 : Comparison of the proposed antennas**

| Section number | Freq | Substrate | Gain(dB) | Size ($\mathbf{mm^2}$) | Microstrip |
|---|---|---|---|---|---|
| 4.2 | 2.5 MHz | FR4 | 3.21 | 34 × 28 | MLA with DGS |
| 4.3 | Wade band 1.5 to 3 MHz | FR4 | 4.35 | 42×33.8 | MLA E-shape |
| 4.4 | 28 GHz | RogerRo4003 | 6.2 | 5×5 | Rectangular with U-slot |

The results show that the antenna with U-slot has a higher gain. It also has the smallest size, so it is best suited for array antenna design.

### 4.5 Simulation Results of 5G Antenna Array Design

The simulation results for the antenna are depicted in Figure 4.11(a), the reflection loss for all ports from p1 to p4 are -29, -17.5, -17.2, and -27.5 dB, respectively. The mutual coupling readings are demonstrated as follows: S21=-12.1dB, S32=-10.2dB, and S43=- 12dB. The polar sketch of antenna gain in the two planes E and H is shown in Figure 4.11(b). Figure 4.11(c) displays the antenna gain. This indicates a high-performance antenna that can be combined with a butler to obtain multiple high-efficiency beams to understand the performance of an antenna in directing radio signals in specific directions. The main difference between the E and H planes is the direction in which the antenna gain is measured, so understanding the radiation patterns in both planes provides a comprehensive view of how an antenna radiates energy in different directions.

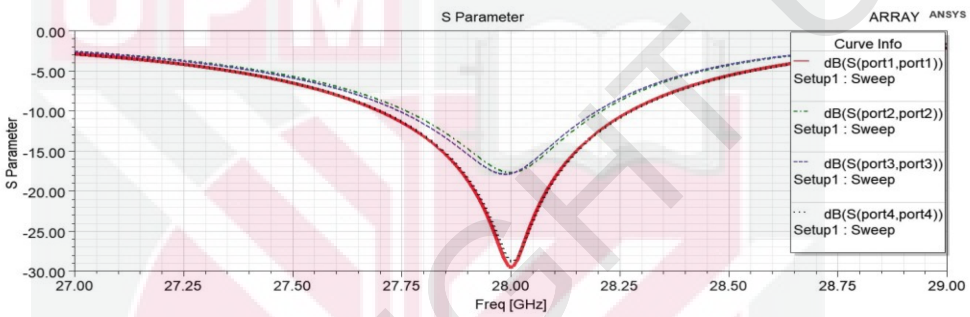


(a)

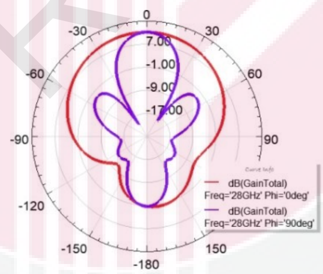


(b)


(c)

**Figure 4.11 : The antenna array simulated results (a) the S-parameters (b) 2D polar sketch for E and H planes, and (c) the total Gain**

The radiation patterns in the two plane xz-plane and the yz-plane are shown in Figure 4.12, which displays that the antenna array proposed has a directional radiation pattern and high gain (9.1 dB).

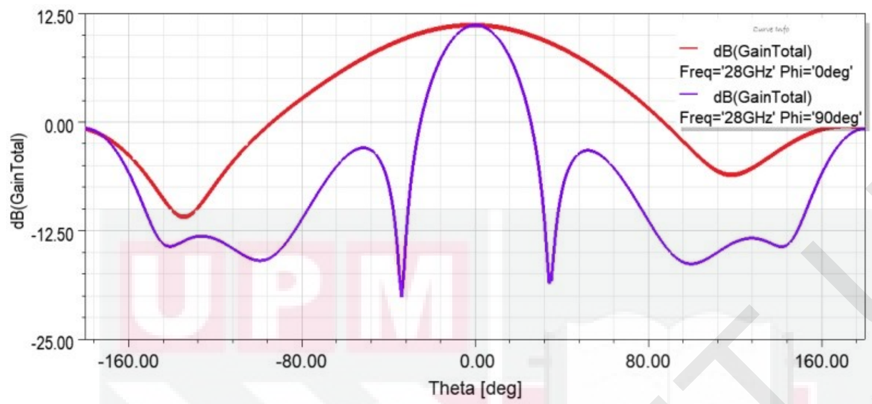


**Figure 4.12 : The radiation pattern in two plane xz-plane**

The proposed antenna has been compared with several antennas in related works. The results are summarized in Table 4.5. The proposed antenna does not have a higher gain than most of the reported antennas. However, a gain will be improved when we combined with BMN. Moreover, it is much smaller than the conventional antenna while keeping a directional radiation pattern.

**Table 4.5 : Comparison of the proposed antenna array single beam and some related designs**

| Ref.(year) | Freq.[GHz] | Gain (dB) | Size ($mm^2$) | Polarization | Microstrip Type |
|---|---|---|---|---|---|
| [110] (2018) | 2-3.1 | 2.73 | 35×50 | LP | Single slot |
| [111] (2019) | 1.8-2.5 | 11 | 200×200 | Dual polarize | 2X2 square |
| [112] (2019) | Multi-band | 10.56 | 30 X 25 | CP | 4X2 square |
| [113] (2019) | 10.4 | 9.8 | 27 X 27 | CP | 2X2 square |
| [114] (2020) | 1.7-2.9 | 9- 4.5 | 56 X 75.5 | CP | Single square loop |
| [115] (2020) | 0.91-2.55 | 5-8.3 | 165×165 | LP | 2X2 fractal |
| [116] (2021) | 27–45 | 14.8-14.1 | 16.5X 6.5 | Dual-Linear | 2×2 |
| [117] (2022) | 37 | 12.8 | 20 X 40 | LP | 1 × 4 single feed |
| **Proposed** | **28** | **9** | **5×18.5** | **CP** | **1X4 rectangular** |

## 4.6 Simulation Results of Butler Matrix

The Butler Matrix is a critical component in beamforming systems, especially in phased array antennas. It is designed to control the phase and amplitude of signals in an antenna array, enabling precise beam steering. As explained in the previous chapter, the key components of a Butler Matrix typically include hybrid couplers, phase shifters, and power dividers. Hybrid couplers split the input signals into in-phase and quadrature components, while phase shifters introduce controlled phase differences. Power dividers then distribute these phased signals to different antenna elements, forming multiple beams with distinct directions. This sophisticated network of components allows the Butler Matrix to achieve dynamic beamforming capabilities, crucial for enhancing the performance of wireless communication systems. In this section, the results of these components and the results of the proposed final design of the Butler Matrix Network will be presented.

**1- HBLC:**

The HBLC simulated results of the S parameters are shown in Figure 4.13, presented in layout window in ADS.

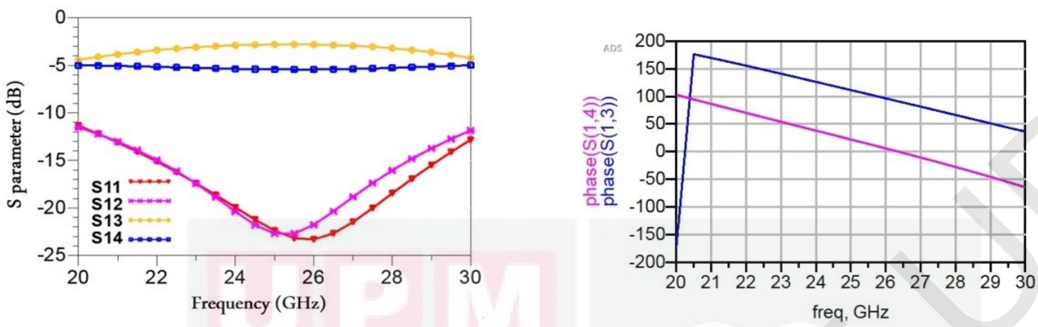


(A) (B)

**Figure 4.13 : The HBLC simulated results (a) phase difference, and (b) S-parameters of circuit**

The number of HBLC utilized in the (N X N) BFN configuration is selected according to ((N/2)×log2N) [102]. HBLC is realized by two pairs of Z0Ω and (Z0/ √ 2)Ω,λc/4 microstrip lines where Z0 is the feed line impedance [103]. The phase difference between P3 and P4 is displayed in Figure 4.13(a). The reflection coefficient (S13) and (S14) are approximately −3 dB −5 dB at resonance frequency (28GHz). In addition, the simulated S parameters are plotted in Figure 4.13(b). In the caption, the optimized design of the HBLC parameters is shown. The reflection coefficient (S11) and isolation (S212) of less than −22 dB is achieved over a wide frequency range (20GHz − 30GHz) [71].

The simulated phase difference is near to the theoretical 90o phase difference by an average of ±5o over the frequency range of (20-30) GHz.

**2- Crossover:**

The crossover is utilized to pass the signals to the second stage without loss and with 0dB insertion loss.

Figure 4.14(a) shows the phase difference of the crossover output ports. As observed in Figure 4.14(b), the simulated S-parameters the insertion loss S14 is approximately -3.9 across a wide frequency range (20-30) GHz. In addition, S11, S12, and S13 are less than -17GHz at the operating frequency. Furthermore, the phase shifter is designed.

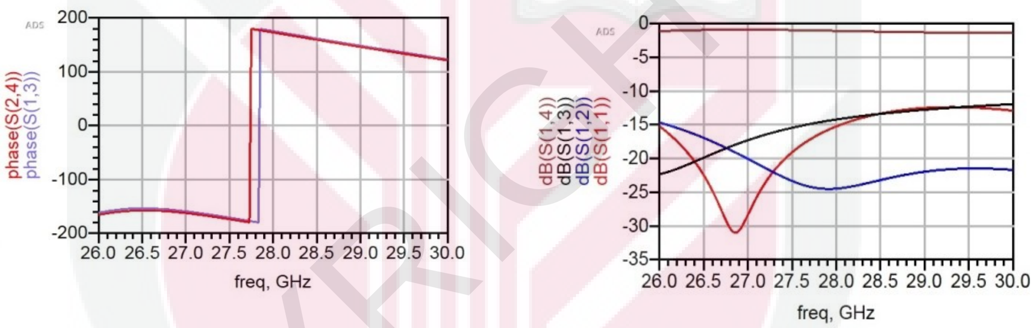


(A) (B)

**Figure 4.14 : The crossover simulated results (a) phase difference of crossover output ports, and (b) the S-parameters**

**3- Phase Shifter:**

As depicted in Figure 4.15, the phase shifter indicator closely approximated the anticipated 45 degrees. This result underscores the alignment between our theoretical model and the practical performance of the phase shifter at the designated frequency.

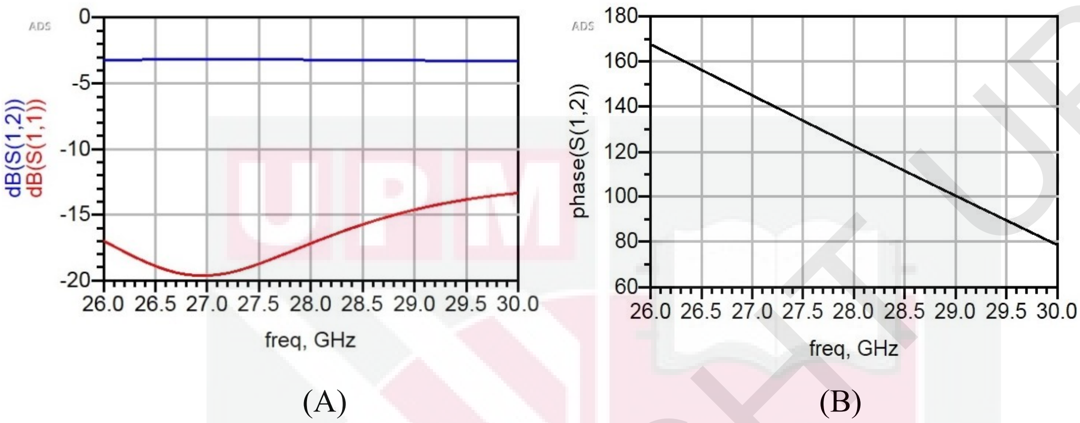


**Figure 4.15 : The phase shifter simulation result (a) the phase difference, and (b) the S-parameters**

The close approximation of the empirical results to the theoretical 45 degrees provides a significant validation of our phase shifter design and indicates its potential for reliable application in high-frequency scenarios, such as those involving 28 GHz. After that, all related components are integrated to form a modified BM network, which is implemented using a microstrip transmission line, as illustrated in Figure 4.16, the schematic structure and symbol of overall adopted 4×4 BM design in ADS schematic window.

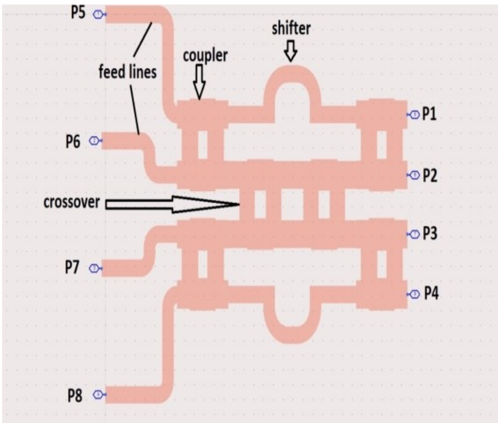


(A)

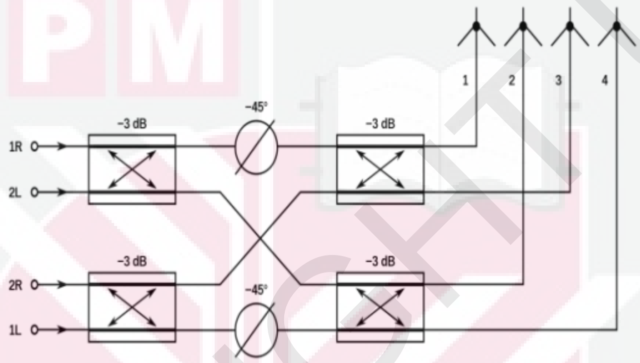


(B)

**Figure 4.16 : The layout design (a) 4X4 butler matrix proposed, and (b) Butler Matrix construction**

The insertion and isolation coefficient for each port have been analyzed as indicated in Figure 4.9. Because of the BM's symmetric nature, the excitation results of P1 are similar to P4, and P2 is similar to P3. Figure 4.17(a) shows the simulated S parameters of the proposed BM when the input ports (P1, P2) are excited. Note that a 50Ω load is utilized as a terminator when one of the four input ports is excited, and the other three input ports are terminated. As the first port is excited, the coupling and reflection coefficient is less than -15 dB through a wide frequency range of (26-30) GHz (see Figure 4.17(a)). At 28 GHz, the simulated insertion loss from P1 to output ports P5-P8 are -6.943, -8.236, -6.943, and -8.475 dB, respectively. The reflection and coupling levels when P2 is excited, across 26-30 GHz, exceed -15dB (as depicted in Figure 4.17(b)). At 28 GHz, the simulated insertion loss from P2 to P5 P8 are -8.498, -8.799, -6.579, and -9.019 dB, respectively.

Figure 4.18, shows the magnitude of the surface current distribution generated on the proposed 4×4 BM at 28 GHz, which is stimulated by the HFSS simulator, where we notice the intense density of the current distribution at the exciting input port and its decline at the other input ports. At the same time, all output ports have a strong current density. Similarly, when exciting other input ports.

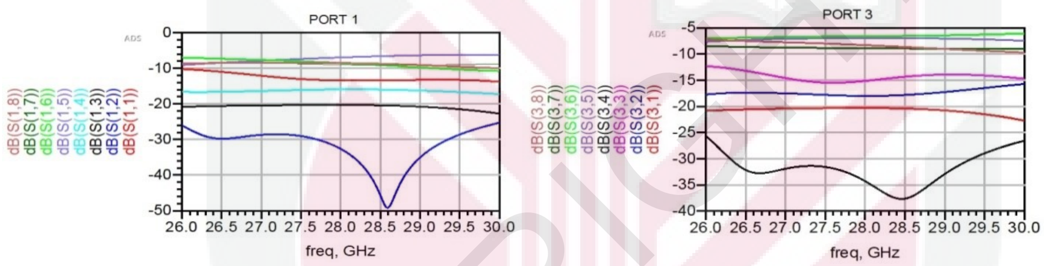


(A)

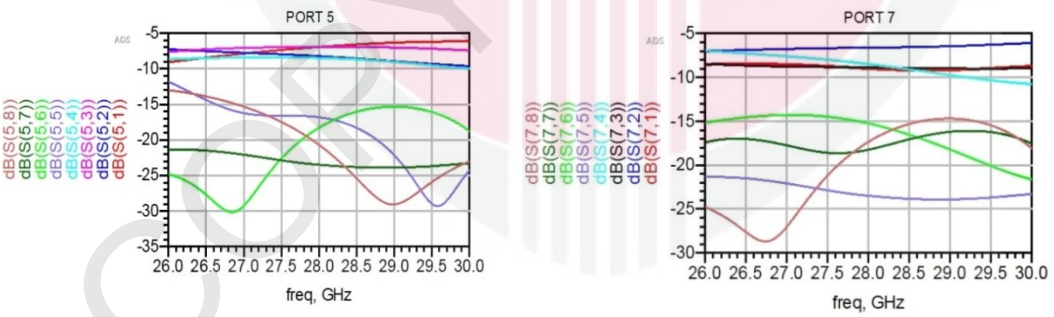


(B)

**Figure 4.17 : The insertion and reflection loss for a proposed BM when exited (a) input ports (1 or 4) (2 or 3), and (b) output ports (5 or 8) (6 or 7)**

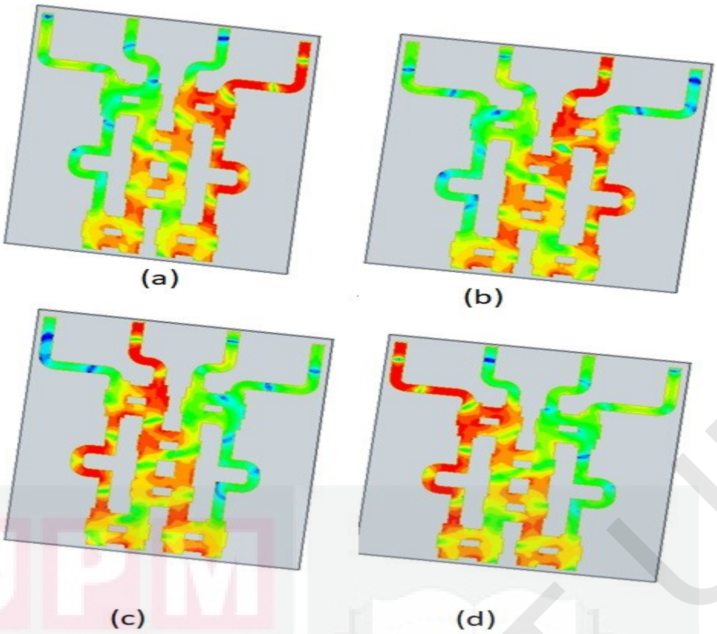


**Figure 4.18 : The current distributions for the Proposed BM when exited (a) Port-1, (b) Port-2, (c) Port-3, and (d) Port-4**

## 4.7 Simulation and Fabrication Results of 5G Beamforming Antenna Array

This section delves into the simulation and fabrication outcomes of the developed 5G beamforming antenna array, as depicted in Figure 4.19. The presented figure showcases reflection and mutual coefficients consistently below -11dB across the entire operating frequency range for all input ports. The design successfully acquires four beams, each directed differently. By allocating a specific power proportion to each input port, transmitted over the network, a constant phase difference is achieved between neighboring output ports. This systematic approach results in distinct directions for the antenna beams under each port input phase, ensuring the fulfilment of diversity in the phase difference. Notably, the simulation reveals variations within ±8° and ±33° for each input port, reflecting the precision and effectiveness of the proposed beamforming system.

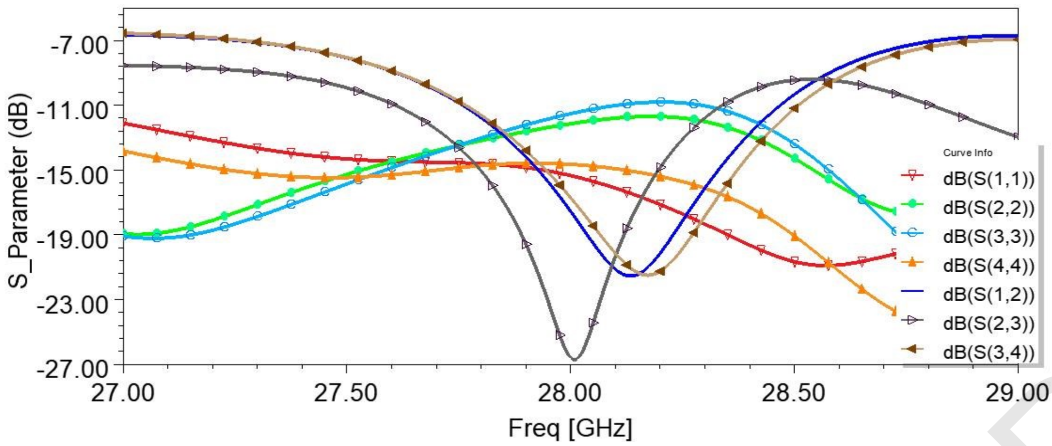


**Figure 4.19 : The S parameter of the multi-beam antenna proposed**

Figure 4.20 displays photographs of the proposed design and results after manufacturing, emphasizing the critical step of transitioning from simulation to practical realization. The primary motivation behind manufacturing was to subject the antenna to real-world testing, providing tangible proof of its simulated results. To ensure accurate testing, we adopted a meticulous approach, activating only one port at a time and studying its individual performance. This focused testing was necessitated by the substantial size difference between the SMA connector and the antenna itself, ensuring that each component's impact could be distinctly evaluated. Manufacturing, however, came with its set of challenges, ranging from material constraints and cost implications to technological limitations and stringent performance requirements. Successful management of these challenges required a delicate balance of engineering acumen, technological expertise, and a pragmatic understanding of practical constraints.

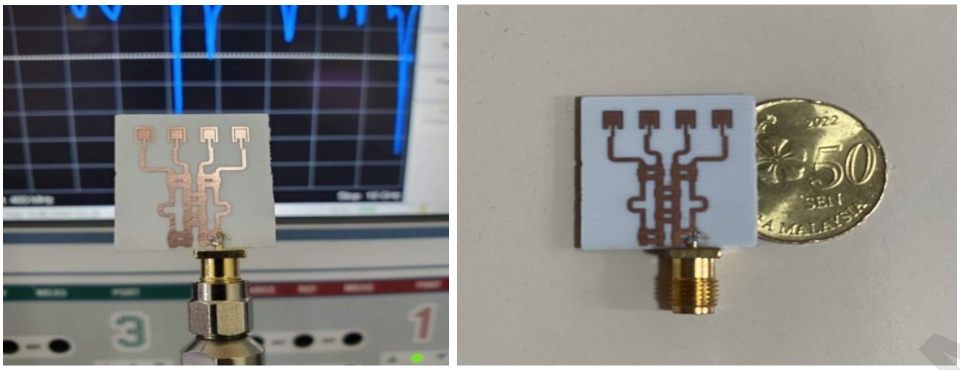

(a)

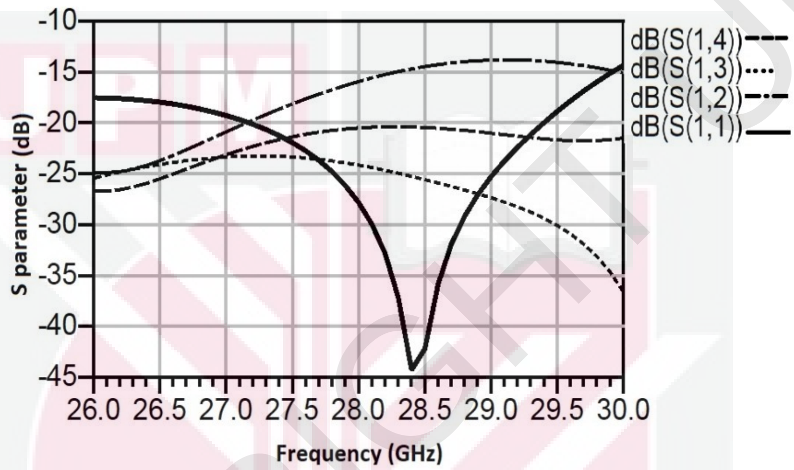


(b)

**Figure 4.20 : BFN antenna array (a) Photograph of the BFN antenna array under test, and (b) Measured S-Parameter results the BFN antenna array**

The simulated and the measured results of the antenna array show the wideband that uses a relatively wide range of frequencies. Figure 4.21 shows the simulation and measured results for a polar radiation pattern, whereby a high gain with a high directive beam can be obtained, i.e., a gain for each directed beam (4.4, 6.63, 9.01 and 9.3) db.

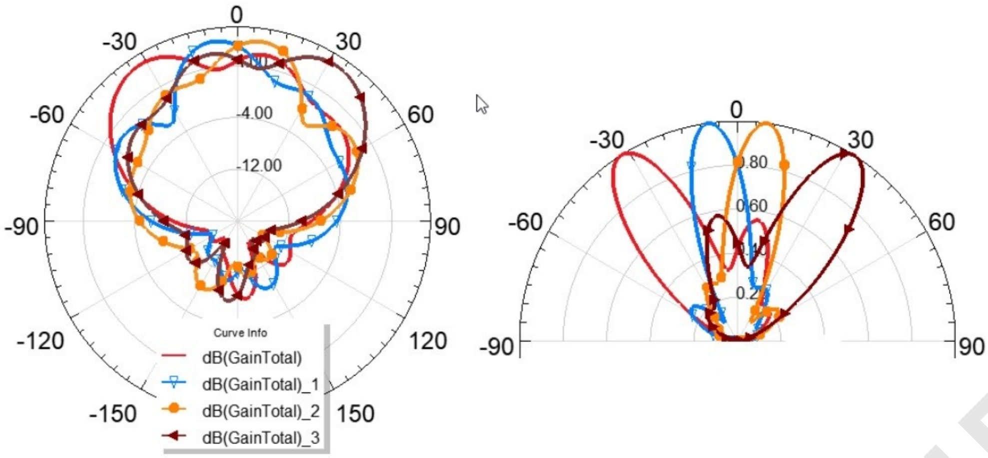


(a)

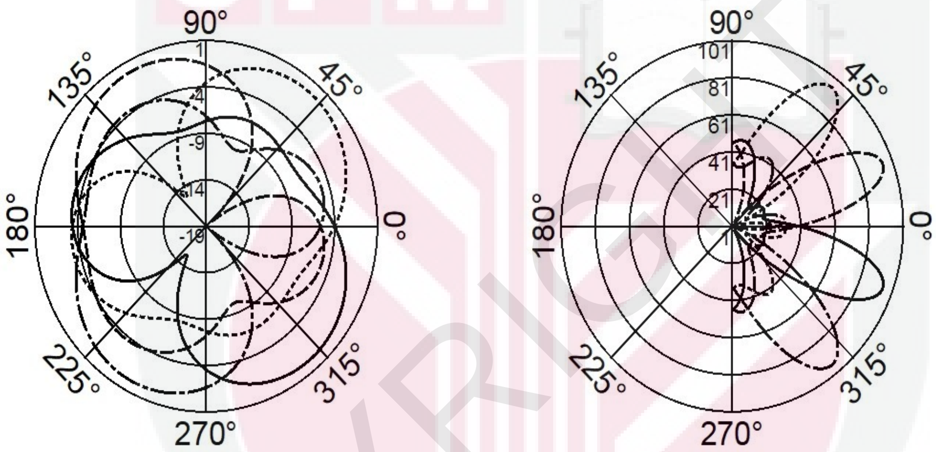


(b)

**Figure 4.21 : The 2D radiation pattern driven by the multi-beam antenna proposed (the gain for the 4 beams and normalized gain) (a) BMN with antenna, and (b) BMN without antenna**

By presenting the previous results and comparing the differences between Figure 4.21 and Figure 4.11:

- A multi-beam was obtained instead of one beam.
- The side lobe is close to fading or almost ineffective.

The distinction in beam angles becomes apparent when the BMN is integrated with the antenna array, as seen in the preceding figure, and when the BMN operates independently without an antenna.

To calculate the beam scan angle (angle) for each output port, the given equation is used:

$$\textbf{angle} = \sin^{-1}\left(\frac{\mathbf{ph\lambda}}{\mathbf{2\pi d}}\right) \qquad \textbf{(4.14)}$$

Where d represents the distance between output ports. The progressive phase difference for each port when the single input port is excited every time [-135º, -45º, 45º, and 135º].

As shown in Figure 4.22, the 3D gain radiation corresponds to the outputs. A high gain with a high directive beam can be obtained. The input ports were excited sequentially. As can be seen, the main direction is shown in Table 4.6, when port1, port2, port3, and port4 are exited, respectively, for the Butler Matrix without antenna.

**Table 4.6 : The progressive phase variation and scanning beam angle across output ports**

| Output Port No. | Progressive phase (ph) | Scan beam angle (angle) |
|---|---|---|
| Port5 | -48˚ | -20˚ |
| Port6 | -115˚ | -52˚ |
| Port7 | 115˚ | 52˚ |
| Port8 | 48˚ | 20˚ |

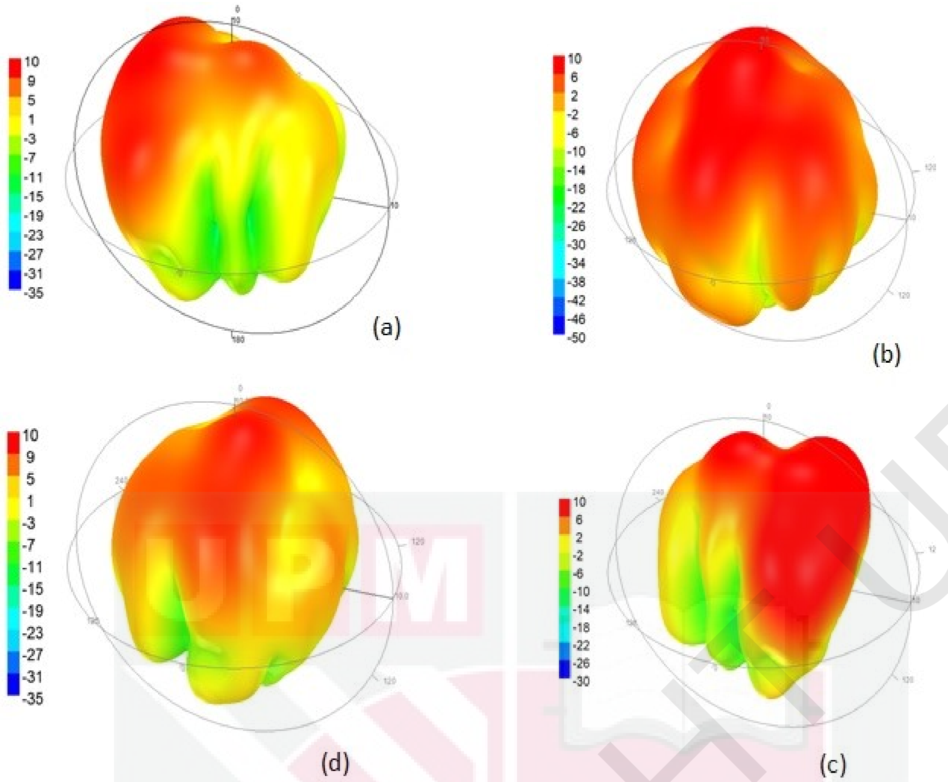


**Figure 4.22 : The simulated 3D realized gain when exited (a) Port-1, (b) Port-2, (c) Port-3, and (d) Port-4**

Figure 4.23 shows the difference in total gain for the antenna without Butler Matrix in Figure 4.23(a) and antenna with Butler Matrix in Figure 4.23(b). The improvement can be seen in the gain that describes how well the antenna converts radio waves arriving from a specified direction into electrical power, so the system performance will be high. The gain comparison between the antenna without Butler Matrix and the antenna with Butler Matrix is shown in Table 4.7.

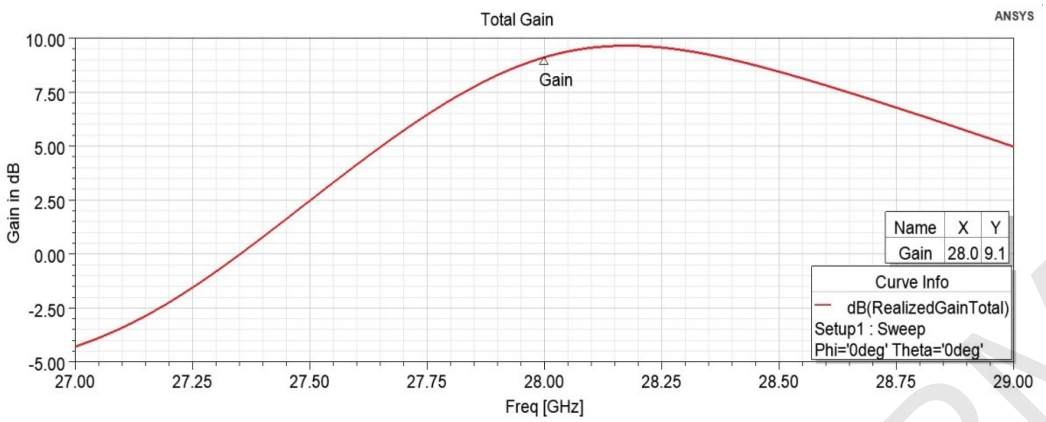


(a)

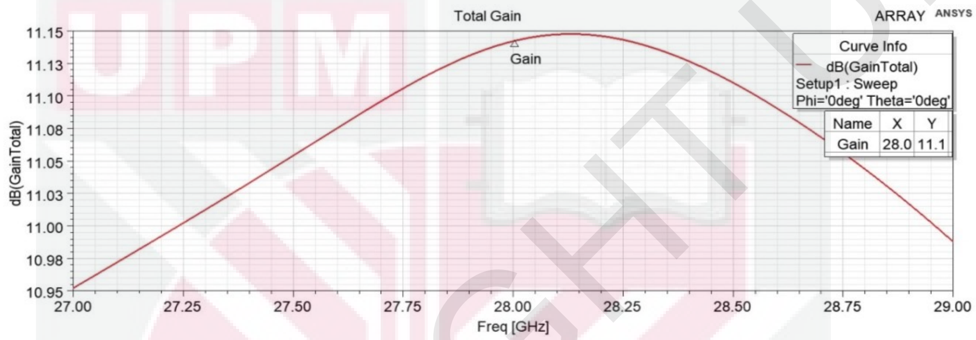


(b)

**Figure 4.23 : The realized gain for (a) the antenna without Butler Matrix, and (b) the antenna with Butler Matrix**

**Table 4.7 : Gain comparison between the antenna without Butler Matrix and the antenna with Butler Matrix**

| | |
|---|---|
| Gain in dB without Butler Matrix | 9 |
| Gain in dB with Butler Matrix | 11 |

As shown in Figure 4.24, the direction of the radiation propagation is towards the 90o plane, and in this plane, the lobes look quite different. The input ports were excited sequentially. As can be seen, the main direction is ± 8º and ± 33º when excite port1, port2, port3, and port4, respectively.

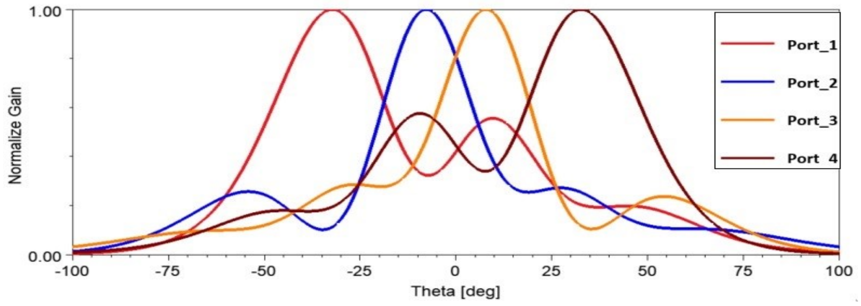


**Figure 4.24 : Simulated results showing the beam switching characteristics of the slot antenna array and the Butler Matrix from all outputs**

Table 4.8 summarizes and compares the performances of this work with that of the previous works. Our work is focused on the full integration of the antenna elements and the Butler Matrix operating at 28 GHz. Previous works [118–120] that demonstrated similar operating frequencies are chosen for comparison. [121] is not chosen because the operating frequency is at 30 GHz. Nonetheless, [120-121] are included for comparison because they, like our work, are based on the microstrip line structure. Many beamforming antennas can be found in the literature [21–29]. However, they all failed to achieve the simple inexpensive design like this work, thus they may not be appropriate for this comparison. [120] adopts a commercially available off-the-shelf packaged switch chip. This work has no integrated switch, which simplifies and improves the manufacturing process and cost. When comparing this work with the rest of the previous works, we found that it achieves an excellent balance between size and gain, which is the opposite of what we found in [119] [121] which achieved improvement gain at the expense of size. Meanwhile, we found that [118] [120] did not achieve an acceptable gain or a small size. With simplicity of design, we are able to offer the smallest, inexpensive, and easy to fabricate design, which in turn will offer many facilities in integration with other devices.

**Table 4.8 : Comparison of the proposed BM design and some related designs**

| Ref. (year) | Freq. [GHz] | Antenna | BM | Switch | Count Beam Direction | Gain [dB] | Dimension (mm $^2$) |
|---|---|---|---|---|---|---|---|
| [118] (2019) | 28 | 1 × 4 Patch | 4 × 4 Microstrip | No Switch | 4 | 5.2 | 36.2×44.3 |
| [119] (2019) | 28 | 4 × 7 Patch | 4 × 4 Microstrip | No Switch | 4 | 12 | 95 × 32 |
| [120] (2021) | 28 | 1 × 4 Patch | 4 × 4 Microstrip | Absorptive SP4T × 1 Commercial Silicon | 4 | 4.5 | 36 × 48 |
| [121] (2021) | 30 | 1 × 4 Horn | 4 × 4 Microstrip | No Switch | 4 | 9 | 50 × 52 |
| **Proposed** | **28** | **1×4 Patch** | **4 × 4 Microstrip** | **No Switch** | **4** | **11** | **23 X 20.5** |

## 4.8 Simulation Results of Intelligent Antenna Design

Adaptive array processing algorithms are employed to provide wireless power to IoT devices [122]. Various approaches to implementing these algorithms have been investigated [123]. To achieve power conservation in adaptive antenna system, it is crucial to have the right hardware setup [124].

It is possible to conserve power from being lost to no avail and use it only when needed in the case of using the Butler Matrix Network, as shown in Figure 4.18. If any of the four ports is turned on, it gives the same results as shown in Figure 4.25, and if more than one port is turned on, the change is only by increasing the power. Figure 4.25(a) presents the gain in the case of activating one port, and in the event of activating two ports, a gain can be obtained as shown in Figure 4.25(b). Figure 4.25(c) and Figure 4.25(d) present the gain value when activating three and four ports, respectively, where the gain is at its highest value of 11 dB, as shown in Table 4.9.

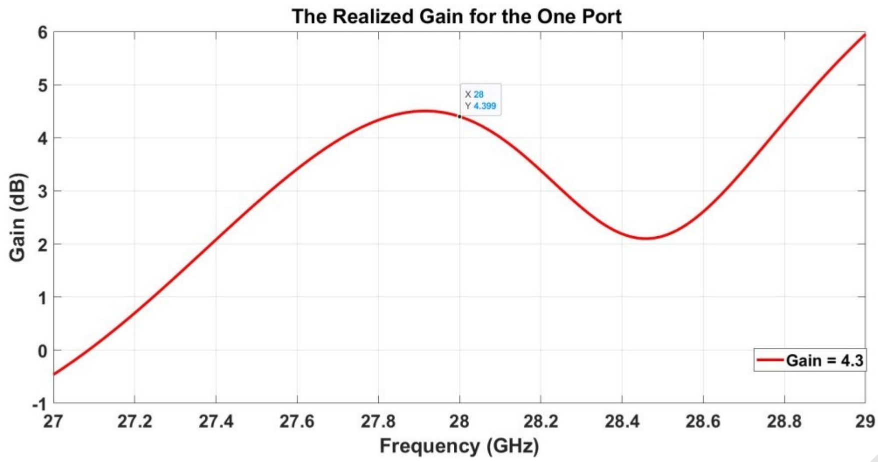
The Realized Gain for the One Port
Gain (dB)
Frequency (GHz)
X 28
Y 4.399
Gain = 4.3

(a)

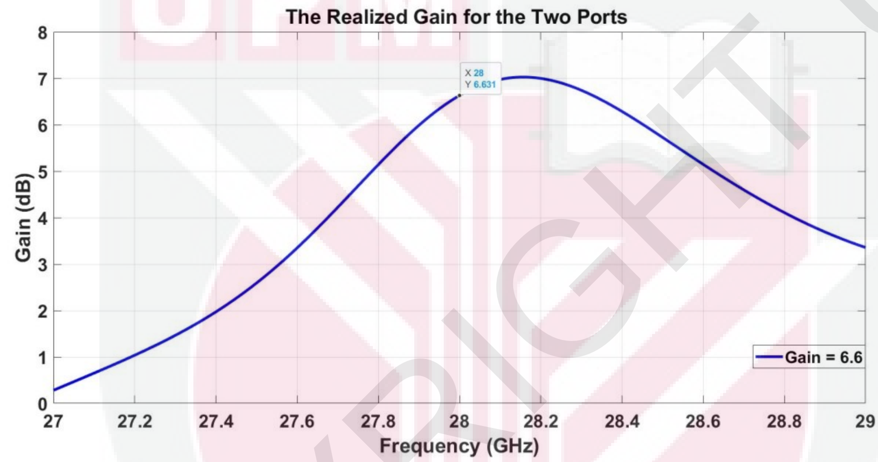
The Realized Gain for the Two Ports
Gain (dB)
Frequency (GHz)
X 28
Y 6.631
Gain = 6.6

(b)

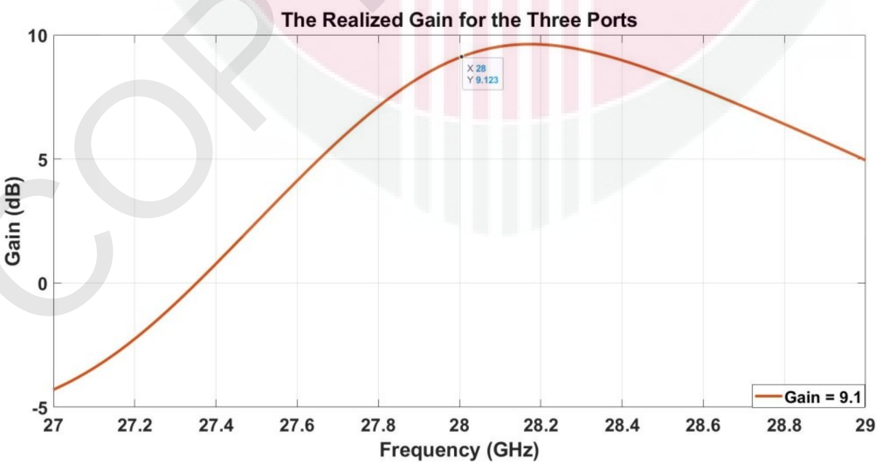
The Realized Gain for the Three Ports
Gain (dB)
Frequency (GHz)
X 28
Y 9.123
Gain = 9.1

(c)

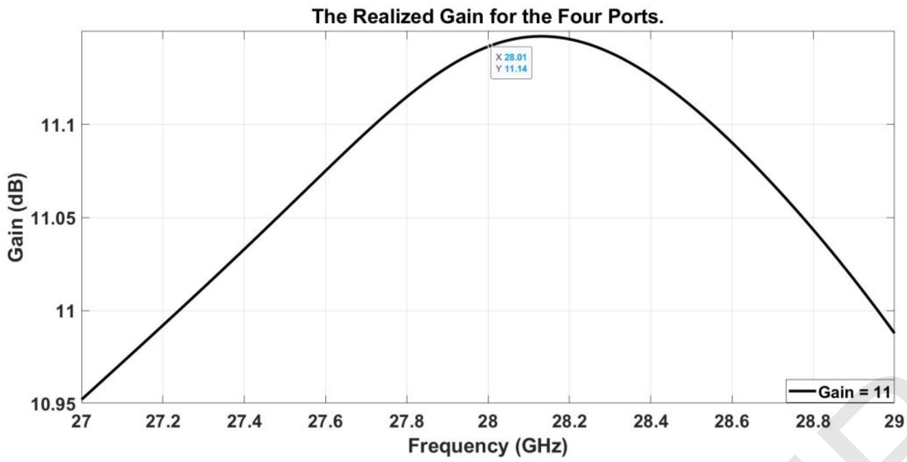


**Figure 4.25 : The realized gain for (a) one port, (b) two ports, (c) three ports, and (d) four ports**

**Table 4.9 : The realized gain for four cases**

| | | | | |
|---|---|---|---|---|
| Ports count | 1 | 2 | 3 | 4 |
| Gain in dB | 4.4 | 6.63 | 9 | 11 |

### 4.8.1 AI Automatic Beam-Selecting

This study intends to design an automatic beam-selecting at the receiver, where the selected beam-set has to achieve minimum return loss. It proposes to train an artificial intelligence (AI) model that automatically activates the best beam with high receiving quality. A set of data was collected from the suggested simulation as shown in Figure 4.19, in which different port combinations were tested under limited range of frequency. Random forest was trained to predict the best port with minimum return loss and maximum gain. There are 7 port (input port) combinations in the proposed model, which are considered as classes for the AI model, namely:

Port1

Port2

Port3

Port4

Port 2 and Port 1

Port3 and Port 2

Port4 and Port 3

Therefore, the data are supposed to have 7 classes, and the Port Selector AI has to be trained to classify the estimated return loss to one of the 7 port classes. Random Forest (RF) is the AI model in this approach, and it is based on the concept of ensemble learning and decision trees. RF divides the labelled dataset into multiple subsets, and each subset is called bootstrap sample. Then, a recursive decision tree is built for each bootstrap sample based on different features. The multiple trees are used in voting for class label, and the aggregated votes are considered in the final decision [125]. By combining the predictions of multiple decision trees and incorporating randomness in feature selection and sample selection, Random Forest improves the model's accuracy, reduces overfitting, and provides robust predictions.

After collecting the data which represent the relationship between the port combination and the return loss, it is divided into 80% training set and 20% test set. The training part of the data is used to train the Random Forest model. The trained RF model has been tested using the test part of the data to detect the final operation accuracy. Figure 4.26 shows the confusion matrix of the tested samples on the trained RF model. This matrix shows how each class can be confused by the model to be a different class, which is a misclassification error. Any number of samples in the diagonal means that the predicted class (port) is actually the same class port, estimated correctly. Other than the diagonal, classification error occurs when any sample is mapped to a different class.

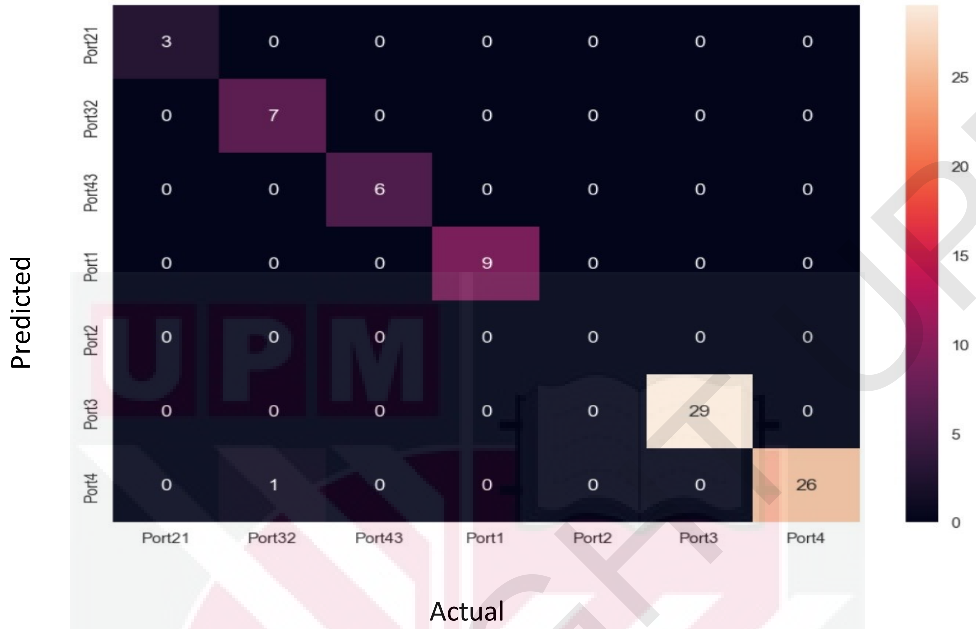


**Figure 4.26 : Confusion Matrix for the trained Random Forest AI model**

It is obvious that the trained RF model did not misclassify much of the estimated return loss test data. The proposed model has an accuracy of 98.76% based on the confusion matrix depicted in Figure 4.26.

The proposed approach basically depends on the classification of the estimated return loss to select the highest gain port with less power consumption. Therefore, the AI model will switch the ports on and off automatically based on the estimated return loss.

Table 4.10 provides a comprehensive summary of the key focus and contributions of our unique research proposal, along with a comparison to some related works. The table highlights specific aspects that differentiate each paper and offers an overview of the research areas covered in each study. Our proposal stands out for its novel approach, leveraging an embedded control chip and the Random Forest Decision algorithm for intelligent antenna selection. It emphasizes real-time decision-making and dynamic antenna adjustment for optimal signal reception and power conservation. The comparison in the table sheds light on the distinctive features of each paper and showcases the potential contributions of our proposed research to the field of intelligent antenna systems.

**Table 4.10 : Comparison of the different research papers and our proposal research paper**

| REF | Focus and Contributions |
|---|---|
| [126] | - Adaptive beamforming in mmWave systems |
| | - Utilization of Reconfigurable Intelligent Surfaces (RIS) |
| [127] | - Addressing joint localization and communication |
| | - 9 AI weight optimization algorithms for smart antennas |
| | - Application in 5G and 6G wireless systems |
| [128] | - Emphasis on antenna weight optimization |
| | - Investigation of smart antennas in 5G and 6G systems |
| | - Utilization of Linear and Non-linear Artificial Neural Networks |
| Our Proposal | - Application of Random Forest Decision algorithm |
| | - Novel modeling approach using embedded control chip |
| | - Real-time decision-making for intelligent antenna selection |
| | - Power conservation through dynamic antenna adjustment |
| | - Analysis of signal parameters for optimal signal selection |
| | - Evaluation of performance against traditional and AI techniques |

## 4.9 Summary

This chapter presents a comprehensive exploration of various antenna designs and their performance evaluations. The first section investigates the microstrip patch antenna (MLA) for 2.5GHz, revealing significant improvements in return loss (-17 dB), bandwidth (57 MHz), and gain enhancement (3.21 dB) through simulation in CST Microwave Studio 2014. The proposed MLA exhibits promising potential for integration into wireless devices like phones and tablets.

The second part introduces a Multiband Hand-Held Antenna with E-shaped Monopole Feeding, designed to cater to diverse mobile applications, including GSM, DCS, PCS, UMTS, ISM, LTE bands, and WiMAX. The antenna is meticulously simulated using the CST simulator, and the experimental results show excellent agreement with simulations, validating its versatility for a wide range of frequency bands.

Then, a novel compact planar monopole antenna configuration with U-slots for WiFi/Bluetooth, LTE, and 5G frequency bands is discussed. The study explores the effects of varying slot dimensions on the antenna's performance, revealing optimal parameters for achieving low reflection coefficient, high gain, and omni-directional radiation patterns at 28 GHz. This design holds promise for applications in multi-functional wireless communication systems.

After that, a detailed examination of a four-element linear planar monopole antenna array is presented. The array, optimized and characterized, demonstrates impressive reflection loss values and mutual coupling readings, achieving a high directivity gain of 9 dB. The integration of the designed antenna with a Butler Matrix yields four beams directed towards desired angles, showcasing the potential for practical applications.

The last part of this chapter focuses on the evaluation and validation of the proposed intelligent antenna selection system. The trained Random Forest (RF) model demonstrated remarkable accuracy, achieving a rate of 98.76% as confirmed by the confusion matrix. The primary objective of the proposed approach lies in the classification of estimated return loss to identify the port with the highest gain and minimal power consumption. This, in turn, enables the AI model to autonomously activate and deactivate ports based on the return loss estimation. The uniqueness of the proposal lies in its utilization of an embedded control chip and the Random Forest Decision algorithm for intelligent antenna selection. Emphasizing real-time decision-making, the system dynamically adjusts antennas to optimize signal reception while conserving power. The chapter concludes by highlighting the distinctive features of the proposed research through a comparative analysis, showcasing its potential contributions to the field of intelligent antenna systems.

# CHAPTER 5

# CONCLUSION AND FUTURE WORK

## 5.1 Conclusion

This research introduces four antenna types: Meander Line antennas, an E-shaped monopole-fed open slot antenna, a compact Microstrip-feed planar monopole rectangular antenna with U-slots, and a 1×4 linear antenna array of omni-directional antennas. Two Meander Line antennas are studied for LTE mobile applications in the 2.4 GHz and 2.5 GHz bands. Parametric studies are conducted, revealing enhanced gain and bandwidth, leading to optimization using HFSS.

The first Meander Line antenna design exhibits improved return loss (-38 dB), 57 MHz bandwidth, and a gain enhancement of 3.38 dB. The second design achieves return loss of -17 dB, 57 MHz bandwidth, and a gain enhancement of 3.21 dB. The MLA antennas mimic omnidirectional radiation patterns of monopole antennas. A compact planar antenna supporting various mobile services with a size of (42 × 33.8 × 1.5) $mm^3$ and a bandwidth of 1.7 GHz is introduced, showing good agreement between the simulation and experimental results.

A novel compact planar monopole antenna with U-slots for WiFi/Bluetooth LTE and 5G is presented, demonstrating low reflection coefficient (-33 dB), 6.3 dB gain, and omni-directional radiation patterns at 28 GHz. A linear array antenna with 4 elements using a Butler Matrix is designed, showing high resonance at 28 GHz and well-defined radiation patterns.

The Butler Matrix performance is demonstrated in the ADS simulator, producing four beams towards desired directions with a wide-band range from 26 to 30 GHz. The design precision is highlighted with less than 2% deviation between the simulations and fabrication results. The ultra-compact Butler Matrix design (23mmX20.5mm) represents a notable advancement in antenna array systems.

Finally, a modeling approach for intelligent antennas using an embedded control chip and the Random Forest Decision algorithm is proposed. The system dynamically adjusts antenna settings based on signal parameters, ensuring optimal performance and minimizing return losses. Power conservation mechanisms are incorporated to prevent unnecessary energy wastage, contributing to efficiency. The proposed approach surpasses traditional systems in accuracy and power conservation. Future works may explore expanding radiating elements for extended beamforming and investigating higher-order Butler Matrices for enhanced performance.

## 5.2 Future Work

Here are potential subjects for further investigation:

1- Antenna design:

Future studies can concentrate on expanding the number of radiating elements to extend the beamforming range while maintaining the miniaturized structure. We anticipate that by augmenting the array count, the antenna's overall gain will rise. As a result, we foresee potential applications for the proposed antenna in satellite communications. The above illustrates the significant potential of the proposed beamforming method for incorporation into advanced communication systems of the future. Furthermore, in this research, a linear configuration was utilized for the antenna array. Future investigations can delve into the exploration of circular, rectangular, or faceted geometries to enhance adaptive beamforming.

2- Butler Matrix Network design:

Future research can explore the utilization of higher-order Butler Matrices. While some aspects of Nth-order Butler Matrices were briefly covered, there were no specific analyses or examples provided. No recommendations were made for implementing Butler Matrices beyond the 4th order with an intelligent system. Investigating higher-order Butler Matrices holds merit, as higher orders are likely to have a comparable impact in increasing the number of elements in a conventional array.

## REFERENCES


[1] Leon-Garcia, A., & Widjaja, I. (2004). Communication networks: fundamen concepts and key architectures. McGraw-Hill.

[2] Gawas, A. U. (2015). An overview on evolution of mobile wirele communication networks: 1G-6G. International journal on recent and innovati trends in computing and communication, 3(5), 3130-3133.

[3] Bellofiore, S., Balanis, C. A., Foutz, J., & Spanias, A. S. (2002). Smart-anten systems for mobile communication networks. Part 1. Overview and anten design. IEEE Antennas and Propagation Magazine, 44(3), 145-154.

[4] Vouyioukas, D. (2013). A survey on beamforming techniques for wirele MIMO relay networks. International Journal of Antennas and Propagation, 201

[5] Bhalla, M. R., & Bhalla, A. V. (2010). Generations of mobile wirele technology: A survey. International Journal of Computer Applications, 5(4), 2 32.

[6] Scharnhorst, W., Hilty, L. M., & Jolliet, O. (2006). Life cycle assessment second generation (2G) and third generation (3G) mobile phone networ Environment international, 32(5), 656-675.

[7] Karjaluoto, H. (2006). An investigation of third generation (3G) mob technologies and services. Contemporary Management Research, 2(2), 91-91.

[8] Penttinen, J. T. (Ed.). (2016). The LTE-advanced deployment handbook: t planning guidelines for the fourth generation networks. John Wiley & Sons.

[9] Rappaport, T. S., Xing, Y., MacCartney, G. R., Molisch, A. F., Mellios, E., Zhang, J. (2017). Overview of millimeter wave communications for fif generation (5G) wireless networks—With a focus on propagation models. IE Transactions on antennas and propagation, 65(12), 6213-6230.

[10] Kitindi, E. J. (2015). Capabilities of smart antenna in tracking the desired sig in wireless communication system through non-blind adaptive algorithms.

[11] Dai, L., Wang, B., Wang, M., Yang, X., Tan, J., Bi, S., ... & Hanzo, L. (202 Reconfigurable intelligent surface-based wireless communications: Anten design, prototyping, and experimental results. IEEE access, 8, 45913-45923.

[12] Boustani, B., Baghdad, A., Sahel, A., & Badri, A. (2019). Performance analy of direction of arrival algorithms for smart antenna. International Journal Electrical and Computer Engineering, 9(6), 4873.

[13] Seker, C., Güneser, M. T., & Ozturk, T. (2018, October). A review of millime wave communication for 5G. In 2018 2nd International Symposium

Multidisciplinary Studies and Innovative Technologies (ISMSIT) (pp. 1-5). Ieee

[14] Salahdine, F., Han, T., & Zhang, N. (2023). 5G, 6G, and Beyond: Recent advances and future challenges. Annals of Telecommunications, 78(9), 525-549.

[15] Babale, S. A., Rahim, S. K. A., Barro, O. A., Himdi, M., & Khalily, M. (2018). Single Layered 4 × 4 Butler Matrix Without Phase-Shifters and Crossovers. IEEE Access, 6, 77289-77298.

[16] Vallappil, A. K., Rahim, M. K. A., Khawaja, B. A., Murad, N. A., & Mustapha, M. G. (2020). Butler matrix based beamforming networks for phased array antenna systems: A comprehensive review and future directions for 5G applications. IEEE Access, 9, 3970-3987.

[17] Matsuo, S., Miyamoto, S., Nakajo, H., & Fujii, T. (2023, January). Beam Pattern Estimation of 5G Millimeter-Wave Base Station Based on Radio Map and Multi-Beam Antenna Model at 28GHz. In 2023 International Conference on Information Networking (ICOIN) (pp. 7-12). IEEE.

[18] Liu, X., Yan, Z., Wang, E., Zhao, X., Zhang, T., & Fan, F. (2023). Multibeam Forming With Arbitrary Radiation Power Ratios Based on a Conformal Amplitude–Phase-Controlled Metasurface. IEEE Transactions on Antennas and Propagation, 71(4), 3707-3712.

[19] Han, K., Li, W., & Liu, Y. (2019). Flexible phase difference of 4× 4 Butler matrix without phase-shifters and crossovers. International Journal of Antennas and Propagation, 2019, 1-7.

[20] Sarker, N., Podder, P., Mondal, M. R. H., Shafin, S. S., & Kamruzzaman, J. (2023). Applications of Machine Learning and Deep Learning in Antenna Design, Optimization and Selection: A Review. IEEE Access.

[21] Kim, S., Yoon, S., Lee, Y., & Shin, H. (2019). A miniaturized Butler matrix based switched beamforming antenna system in a two-layer hybrid stackup substrate for 5G applications. Electronics, 8(11), 1232.

[22] Ojaroudi Parchin, N., Alibakhshikenari, M., Jahanbakhsh Basherlou, H., A. Abd-Alhameed, R., Rodriguez, J., & Limiti, E. (2019). MM-wave phased array quasi-yagi antenna for the upcoming 5G cellular communications. Applied Sciences, 9(5), 978.

[23] Campo, M. A., Carluccio, G., Blanco, D., Litschke, O., Bruni, S., & Llombart, N. (2020). Wideband circularly polarized antenna with in-lens polarizer for high-speed communications. IEEE Transactions on Antennas and Propagation, 69(1), 43-54.

[24] Lu, R., Yu, C., Zhu, Y., & Hong, W. (2020). Compact millimeter-wave endfire dual-polarized antenna array for low-cost multibeam applications. IEEE Antennas and Wireless Propagation Letters, 19(12), 2526-2530.

[25] Imani, A., & Bayati, M. S. (2021). A novel design of compact broadband 4× Butler matrix-based beamforming antenna array for C-Band applications. AE International Journal of Electronics and Communications, 138, 153901.

[26] Md Jizat, N., Yusoff, Z., A/L Nallasamy, A., & Yamada, Y. (2021). 5 Millimeter-Wave Beamforming System using Substrate Integrated Wavegui F1000Research, 10, 1311.

[27] Jeon, M., Seo, Y., Cho, J., Lee, C., Jang, J., Lee, Y., ... & Kahng, S. (202 Investigation on beam alignment of a microstrip-line Butler matrix and an SI Butler matrix for 5G beamforming antennas through RF-to-RF wireless sensi and 64-QAM tests. Sensors, 21(20), 6830.

[28] Alsirhani, A., Ezz, M., & Mostafa, A. M. (2022). Advanced Authenticati Mechanisms for Identity and Access Management in Cloud Computir Computer Systems Science & Engineering, 43(3).

[29] Temga, J., Shiba, T., & Suematsu, N. (2022, September). A Compact 2-D Phas Array Fed by 4×4 Butler Matrix Without Crossover in Broadside Coupl Stripline For Sub-6GHz 5G Applications. In 2022 52nd European Microwa Conference (EuMC) (pp. 540-543). IEEE.

[30] Nam, S., Choi, S., Ryu, J., & Lee, J. (2022). Compact 28 GHz folded But matrix using low-temperature co-fired ceramics. Journal of Electromagne Engineering and Science, 22(4), 452-458.

[31] Abdulbari, A. A., Rahim, S. K. A., Tan, K. I. M., Hanoosh, H. O., & Jawad, M. (2023). Compact 4× 4 Butler matrix design-based switch beamformi antenna array for 5G applications. Authorea Preprints.

[32] Temga, J., Edamatsu, K., Furuichi, T., Motoyoshi, M., Shiba, T., & Suematsu, (2023). 1-D and 2-D Beam Steering Arrays Antennas Fed by a Compa Beamforming Network for Millimeter-Wave Communication. IEI Transactions on Communications, 106(10), 915-927.

[33] Azad, M. M., & Ahmed, A. H. (2010). Development of smart antenna for futu generation wireless internet connection. IJCSNS Int. J. Comput. Sci. Net Secur, 10, 212-222.

[34] Wu, Q., Cao, Y., Wang, H., & Hong, W. (2020). Machine-learning-assist optimization and its application to antenna designs: Opportunities a challenges. China Communications, 17(4), 152-164.

[35] León, O., Hernández-Serrano, J., & Soriano, M. (2010). Securing cognitive rac networks. international journal of communication systems, 23(5), 633-652.

[36] Hamdi, B., Limam, S., & Aguili, T. (2016). Uniform and concentric circu antenna arrays synthesis for smart antenna systems using artificial neural netwo algorithm. Progress In Electromagnetics Research B, 67, 91-105.

[37] El Misilmani, H. M., & Naous, T. (2019, July). Machine learning in anten design: An overview on machine learning concept and algorithms. In 20 International Conference on High Performance Computing & Simulati (HPCS) (pp. 600-607). IEEE.

[38] Masood, U., Farooq, H., & Imran, A. (2019, December). A machine learni based 3D propagation model for intelligent future cellular networks. In 20 IEEE Global Communications Conference (GLOBECOM) (pp. 1-6). IEEE.

[39] Maeurer, C., Futter, P., & Gampala, G. (2020, March). Antenna desi exploration and optimization using machine learning. In 2020 14th Europe Conference on Antennas and Propagation (EuCAP) (pp. 1-5). IEEE.

[40] Wei, P., & Geyi, W. (2021). Design of MIMO/smart antenna arrays usi different array modules for handheld device. Prog. Electromagn. Res. C, 1 111-126.

[41] Mohsin, A. I., Daghal, A. S., & Sallomi, A. H. (2021). Sidelobe lev minimization for uniform circular smart antenna array using cultu algorithm. Indonesian Journal of Electrical Engineering and Compu Science, 24(2), 930-936.

[42] Chen, J., & Yeh, L. T. (2021). Adaptive array processing based wireless ener transmission for IOT applications. IRO Journal on Sustainable Wirel Systems, 2(3), 128-132.

[43] Pirapaharan, K., Ajithkumar, N., Sarujan, K., Fernando, X., & Hoole, P. (2022). Smart, Fast, and Low Memory Beam-Steering Antenna Configuratio for 5G and Future Wireless Systems. Electronics, 11(17), 2658.

[44] El-Khamy, S. E., El-Sayed, H. F., & Eltrass, A. S. (2022). Synthesis of wideba thinned Eisenstein fractile antenna arrays with adaptive beamforming capabil and reduced side-lobes. IEEE Access, 10, 122486-122500.

[45] Senapati, A., Patro, B. S., & Roy, J. S. (2023). Design of Smart Antenna for Network Using Array Synthesis Methods and Leaky LMS Algorithm. Wirel Personal Communications, 129(4), 2829-2841.

[46] Huang, Y. (2021). Antennas: from theory to practice. John Wiley & Sons.

[47] L. V. Blake and M. W. (2009) .Long, Antennas: WITH MATHCA Fundamentals, design, measurements, 3rd ed. Norwich, CT: SciTech Publishin

[48] Balanis, C. A. (2016). Antenna theory: analysis and design. John wiley & sons.

[49] Wong, K. L. (2003). Planar Antennas for Wireless Communications. Microwa Journal, 46(10), 144-145.

[50] Balanis, C. A. (1997). Traveling wave and broadband antennas. Antenna Theo

Analysis and Design, 488-540.

[51] Collaboration, A. (2004). HFSS online help version 9.2. American: Ansoft Inc.

[52] Pandey, A. (2019). Practical microstrip and printed antenna design. Arte House.

[53] Jais, M. I., Jamlos, M. F., Malek, M. F., Jusoh, M., Adam, I., Iliyes, N. I., Saad, P. (2012, February). Design Analysis of 2.45 GHz Meander Line Anten (MLA). In 2012 Third International Conference on Intelligent Systems Modelli and Simulation (pp. 628-631). IEEE.

[54] Huynh, M. C., & Stutzman, W. (2003). Ground plane effects on planar inverted antenna (PIFA) performance. IEE Proceedings-Microwaves, Antennas a Propagation, 150(4), 209-213.

[55] Garg, R. (2001). Microstrip antenna design handbook. Artech house.

[56] Kumar, G., & Ray, K. P. (2002). Broadband microstrip antennas. Artech house.

[57] Waterhouse, R. (2018). Microstrip patch antennas. In Handbook of Antennas Wireless Communications (pp. 6-1). CRC Press.

[58] Nakar, P. S. (2004). Design of a compact microstrip patch antenna for use wireless/cellular devices.

[59] Wang, F., Du, Z., Wang, Q., & Gong, K. (2004). Enhanced-bandwidth PIFA w T-shaped ground plane. Electronics Letters, 40(23), 1.

[60] Kim, B. C., Yun, J. H., & Do Choi, H. (2004, May). Small wideband PIFA f mobile phones at 1800 MHz. In 2004 IEEE 59th Vehicular Technolo Conference. VTC 2004-Spring (IEEE Cat. No. 04CH37514) (Vol. 1, pp. 27-2 IEEE.

[61] Rowell, C. R., & Murch, R. D. (1998). A compact PIFA suitable for du frequency 900/1800-MHz operation. IEEE Transactions on antennas a propagation, 46(4), 596-598.

[62] Wheeler, H. A. (1947). Fundamental limitations of small antennas. Proceedin of the IRE, 35(12), 1479-1484.

[63] Vardaxoglou, Y. C., & James, J. R. (2007). Mobile handset antennas. Anten Engineering Handbook, 36.

[64] McLean, J. S. (1996). A re-examination of the fundamental limits on t radiation Q of electrically small antennas. IEEE Transactions on antennas a propagation, 44(5), 672.

[65] Yang, C. W., Jung, Y. B., & Jung, C. W. (2011). Octaband internal antenna f 4G mobile handset. IEEE Antennas and Wireless Propagation Letters, 10, 81

819.

[66] Sten, J. E., Hujanen, A., & Koivisto, P. K. (2001). Quality factor of electrically small antenna radiating close to a conducting plane. IEI Transactions on antennas and propagation, 49(5), 829-837.

[67] Balanis, C. A. (2016). Antenna theory: analysis and design. John wiley & sons.

[68] Butler, J. (1961). Beam-forming matrix simplifies design of electronica scanned antennas. Electron. Des., 9(8), 170-173.

[69] Mailloux, R. J. (2005). Phased array antenna handbook. Artech house.

[70] He, G., Gao, X., Sun, L., & Zhang, R. (2021). A review of multibeam phas array antennas as LEO satellite constellation ground station. IEEE Access, 147142-147154.

[71] Pozar, D. M. (2011). Microwave engineering. John wiley & sons.

[72] Luo, Q., Gao, S., Izquierdo, B. S., Yang, X., Ren, X., & Wu, J. (2019, Octobe Low-cost smart antenna using active frequency selective surfaces. In 20 International Symposium on Antennas and Propagation (ISAP) (pp. 1-3). IEEE.

[73] Celik, N., Iskander, M. F., Emrick, R., Franson, S. J., & Holmes, J. (200 Implementation and experimental verification of a smart antenna syste operating at 60 GHz band. IEEE Transactions on Antennas a Propagation, 56(9), 2790-2800.

[74] Zhou, W. (2015). Autonomous smart antenna systems for future mobile devices

[75] Bakhar, M., & Vani, R. M. (2016). Robust blind beam formers for smart anten system using window techniques. Procedia Computer Science, 93, 713-720.

[76] Mulay, G., Patil, N., Pawar, D., & Mainkar, P. M. (2015). Optimizing Adapti Beam-forming Method in Smart Antennas. International Journal of Electroni Electrical and Computational System IJEECS, 4(4), 77-82.

[77] Roy, J. S., Senapati, A., & Convergence, D. (2016). Hybrid beam-formi algorithms for planar adaptive antenna array. International Journal of Informati Communication Technology and Digital Convergence, 1(1), 5-14.

[78] Sharma, Y. (2020). Machine Learning and Additive Manufacturing Bas Antenna Design Techniques (Doctoral dissertation, The University of Arizona).

[79] Shcherbakov, M. V., Brebels, A., Shcherbakova, N. L., Tyukov, A. P., Janovsk T. A., & Kamaev, V. A. E. (2013). A survey of forecast error measures. Wo applied sciences journal, 24(24), 171-176.

[80] Talbi, E. G. (2021). Machine learning into metaheuristics: A survey a

taxonomy. ACM Computing Surveys (CSUR), 54(6), 1-32.

[81] Wang, J., Sung, C., Raghothaman, M., & Wang, C. (2021, May). Data-driv synthesis of provably sound side channel analyses. In 2021 IEEE/ACM 43 International Conference on Software Engineering (ICSE) (pp. 810-822). IEEE

[82] Choudhury, S., & Bhowal, A. (2015, May). Comparative analysis of machi learning algorithms along with classifiers for network intrusion detectic In 2015 International Conference on Smart Technologies and Management f Computing, Communication, Controls, Energy and Materials (ICSTM) (pp. 8 95). IEEE.

[83] Luo, Q., Gao, S., & Zhang, L. (2015, May). Millimeter-wave smart antennas f advanced satellite communications. In 2015 IEEE MTT-S Internatioı Microwave Symposium (pp. 1-4). IEEE.

[84] Vu, T. B. (2018). Smart antenna system architecture and hardwa implementation. In Handbook of antennas in wireless communications (pp. 22- CRC Press.

[85] Rappaport, T. S., Xing, Y., Kanhere, O., Ju, S., Madanayake, A., Mandal, S., & Trichopoulos, G. C. (2019). Wireless communications and applications abo 100 GHz: Opportunities and challenges for 6G and beyond. IEEE access, 78729-78757.

[86] Anabuki, M., Okumura, S., Sato, T., Sakamoto, T., Saho, K., Yoshioka, M., ... Sakai, H. (2017). Ultrawideband radar imaging using adaptive array and Dopp separation. IEEE Transactions on Aerospace and Electronic Systems, 53(1), 19 200.

[87] de Lange, L., Ludick, D. J., & Grobler, T. L. (2019, September). Detecting fail elements in an arbitrary antenna array using machine learning. In 20 International Conference on Electromagnetics in Advanced Applicatic (ICEAA) (pp. 1099-1103). IEEE.

[88] Sudha, S., & Sasirekha, N. (2016, March). Design of smart antenna array of 2× MIMO for 4G-LTE. In 2016 International Conference on Wirele Communications, Signal Processing and Networking (WiSPNET) (pp. 161 1615). IEEE.

[89] Sudha, S., & Sasirekha, N. (2016, March). Design of smart antenna array of 2× MIMO for 4G-LTE. In 2016 International Conference on Wirele Communications, Signal Processing and Networking (WiSPNET) (pp. 161 1615). IEEE.

[90] N. Seshu Kumar and U. D. Yalavarthi. (2021) "A comprehensive review machine learning based optimization algorithms for antenna design," J. Phy Conf. Ser., vol. 1964, no. 6, p. 062098.

[91] Gampala, G., & Reddy, C. J. (2020, July). Fast and intelligent antenna desi optimization using machine learning. In 2020 International Appli Computational Electromagnetics Society Symposium (ACES) (pp. 1-2). IEEE.

[92] Roy, R. H. (1997, December). An overview of smart antenna technology and application to wireless communication systems. In 1997 IEEE Internatio Conference on Personal Wireless Communications (Cat. No. 97TH8338) (p 234-238). IEEE.

[93] Mahdi, M. N., Ahmad, A. R., Qassim, Q. S., Natiq, H., Subhi, M. A., Mahmoud, M. (2021). From 5G to 6G technology: meets energy, internet-o things and machine learning: a survey. Applied Sciences, 11(17), 8117.

[94] Liu, Q., Reniers, A. C., Johannsen, U., van Beurden, M. C., & Smolders, A. (2018). Improved probing reliability in antenna-on-chip measurements. IE Antennas and Wireless Propagation Letters, 17(9), 1745-1749.

[95] Geers, J. P. (2019). Smart antenna system management utilising multi-age systems. University of Johannesburg (South Africa).

[96] Patel, S. K., & Kosta, Y. P. (2011, December). E-shape microstrip patch anten design for GPS application. In 2011 Nirma University International Conferen on Engineering (pp. 1-4). IEEE.

[97] Lin, C. C., Kuo, S. W., & Chuang, H. R. (2005). A 2.4-GHz printed meander-li antenna for USB WLAN with notebook-PC housing. IEEE Microwave a Wireless Components Letters, 15(9), 546-548.

[98] Sah, S., Tripathy, M. R., & Mittal, A. (2018). Multiband and Miniaturized du layer Antenna incorporated with FSS and DGS. Advanc Electromagnetics, 7(1), 1-6.

[99] Ibrahim, K. M., Elkattan, M., & Eldamak, A. R. (2018, September). Design Low Frequency Meander Line Antenna with Efficient Size Reduction. In 20 IEEE International Conference on Aerospace Electronics and Remote Sensi Technology (ICARES) (pp. 1-5). IEEE.

[100] Mo, L., Zhang, H., & Zhou, H. (2008). Broadband UHF RFID tag antenna wit pair of U slots mountable on metallic objects. Electronics Letters, 44(20), 117 1174.

[101] Kara, M. (1996). Formulas for the computation of the physical properties rectangular microstrip antenna elements with various substra thicknesses. Microwave and Optical Technology Letters, 12(4), 234-239.

[102] Kim, S., Yoon, S., Lee, Y., & Shin, H. (2019). A miniaturized Butler mat based switched beamforming antenna system in a two-layer hybrid stack substrate for 5G applications. Electronics, 8(11), 1232.

[103] BARRO, O. A., & HIMDI, M. Single Layered 4× 4 Butler Matrix Witho Phase-Shifters and Crossovers.

[104] Silva, D. H., Ribeiro, D. A., Ramírez, M. A., Rosa, R. L., Chaudhary, S., Rodríguez, D. Z. (2022, May). Selection of Beamforming in 5G MIMO scenari using Machine Learning approach. In 2022 19th International Conference Electrical Engineering/Electronics, Computer, Telecommunications a Information Technology (ECTI-CON) (pp. 1-4). IEEE.

[105] Ma, X., Chen, Z., Li, Z., Chen, W., & Liu, K. (2019, May). Low complex beam selection scheme for terahertz systems: A machine learning approach. 2019 IEEE International Conference on Communications Workshops (IC Workshops) (pp. 1-6). IEEE.

[106] Zardi, F., Nayeri, P., Rocca, P., & Haupt, R. (2020). Artificial intelligence f adaptive and reconfigurable antenna arrays: A review. IEEE Antennas a Propagation Magazine, 63(3), 28-38.

[107] Kurniawati, N., Putri, D. N. N., & Ningsih, Y. K. (2020, October). Random for regression for predicting metamaterial antenna parameters. In 2020 2 International Conference on Industrial Electrical and Electronics (ICIEE) (p 174-178). IEEE.

[108] Lavdas, S., Gkonis, P. K., Zinonos, Z., Trakadas, P., Sarakis, L., Papadopoulos, K. (2022). A machine learning adaptive beamforming framewo for 5G millimeter wave massive MIMO multicellular networks. IEEE Access, 1 91597-91609.

[109] Lorincz, J., Capone, A., & Wu, J. (2019). Greener, energy-efficient a sustainable networks: State-of-the-art and new trends. Sensors, 19(22), 4864.

[110] Shi, Y., Fan, Y., Li, Y., Yang, L., & Wang, M. (2018). An efficient broadba slotted rectenna for wireless power transfer at LTE band. IEEE transactions Antennas and Propagation, 67(2), 814-822.

[111] Shen, S., Zhang, Y., Chiu, C. Y., & Murch, R. (2019). A triple-band high-ga multibeam ambient RF energy harvesting system utilizing hybrid combinin IEEE Transactions on Industrial Electronics, 67(11), 9215-9226.

[112] Alam, S., Surjati, I., Ningsih, Y. K., Sari, L., Syukriati, E., & Safitri, A. (201 October). Design of Truncated Microstrip Antenna with Array 4× 2 f Microwave Radio Communication. In 2019 IEEE Conference on Anten Measurements & Applications (CAMA) (pp. 1-4). IEEE.

[113] Zou, Y., Li, H., Xue, Y., & Sun, B. (2019). A high-gain compact circular polarized microstrip array antenna with simplified feed network. Internation Journal of RF and Microwave Computer-Aided Engineering, 29(12), e21964.

[114] Du, Z. X., Bo, S. F., Cao, Y. F., Ou, J. H., & Zhang, X. Y. (2020). Broadba circularly polarized rectenna with wide dynamic-power-range for efficie

wireless power transfer. IEEE Access, 8, 80561-80571.

[115] Fakharian, M. M. (2020). A wideband rectenna using high gain fractal plar monopole antenna array for rf energy scavenging. International Journal Antennas and Propagation, 2020, 1-10.

[116] Sun, W., Li, Y., Chang, L., Li, H., Qin, X., & Wang, H. (2021). Dual-band du polarized microstrip antenna array using double-layer gridded patches for ; millimeter-wave applications. IEEE Transactions on Antennas a Propagation, 69(10), 6489-6499.

[117] Khan, J., Ullah, S., Ali, U., Tahir, F. A., Peter, I., & Matekovits, L. (202: Design of a millimeter-wave MIMO antenna array for 5G communicati terminals. Sensors, 22(7), 2768.

[118] Kim, S., Yoon, S., Lee, Y., & Shin, H. (2019). A miniaturized Butler mat based switched beamforming antenna system in a two-layer hybrid stack substrate for 5G applications. Electronics, 8(11), 1232.

[119] Trinh-Van, S., Lee, J. M., Yang, Y., Lee, K. Y., & Hwang, K. C. (2019). Sidelobe-Reduced, Four-Beam Array Antenna Fed by a Modified 4 × 4 But Matrix for 5G Applications. IEEE Transactions on Antennas a Propagation, 67(7), 4528-4536.

[120] Lee, S., Lee, Y., & Shin, H. (2021). A 28-GHz switched-beam antenna w integrated Butler matrix and switch for 5G applications. Sensors, 21(15), 5128.

[121] Ashraf, N., Sebak, A. R., & Kishk, A. A. (2020). PMC packaged single-substra 4× 4 Butler matrix and double-ridge gap waveguide horn antenna array f multibeam applications. IEEE Transactions on Microwave Theory a Techniques, 69(1), 248-261.

[122] Javali, A., Sahoo, A., & Gupta, J. (2021, March). Machine learning algorithms smart antenna and arrays for internet of things applications. In 2021 Internatior Conference on Artificial Intelligence and Smart Systems (ICAIS) (pp. 297-30 IEEE.

[123] Shurdi, O., Ruci, L., Biberaj, A., & Mesi, G. (2021). 5G energy efficien overview. Eur. Sci. J. ESJ, 17(03), 315-327.

[124] Karthick, T., & Chandrasekaran, K. (2021). Design of IoT based smart compa energy meter for monitoring and controlling the usage of energy and pow quality issues with demand side management for a commerc building. Sustainable Energy, Grids and Networks, 26, 100454.

[125] Samigulina, G. A., & Samigulina, Z. I. (2019). Modified immune netwc algorithm based on the Random Forest approach for the complex obje control. Artificial Intelligence Review, 52(4), 2457-2473.

[126] He, J., Wymeersch, H., Sanguanpuak, T., Silvén, O., & Juntti, M. (2020, Apri Adaptive beamforming design for mmWave RIS-aided joint localization a communication. In 2020 IEEE Wireless Communications and Networki Conference Workshops (WCNCW) (pp. 1-6). IEEE.

[127] Hoole, P. R. (2020). 9 Real-and Complex-Valued Artificial Intelligence Weig Optimization Algorithms for Smart Antennas in 5/6G Wireless Systems: Line and Nonlinear Arrays.

[128] Herath, H. M. C. J., Herath, H. M. G. G. J. G., Ranaweera, K. M. U. Uduwawala, D. N., & Hoole, P. R. P. (2022). 5/6G, Smart Antennas and Codi the Algorithms: Linear ANN, Non-linear ANN, and LMS. In Smart Antennas a Electromagnetic Signal Processing in Advanced Wireless Technology (pp. 36 383). River Publishers.

# APPENDICES

## Appendix A

## Algorithm Code

```
In [ ]: import numpy as np
import pandas as pd
from pycaret.classification import *
In [ ] : df = pd.read_csv('AllData.csv')
In [ ] : df.head()
Out[ ]:
```

| | Freq [GHz] | S [dB] | | | | | | | Labe l |
|---|---|---|---|---|---|---|---|---|---|
| | | (port2,port1) | (port3,port2) | (port4,port3) | (port1,port1) | (port2,port2) | (port3,port3) | (port4,port4) | |
| 0 | 27.000 | -6.642706 | -8.537461 | -6.564469 | -12.098631 | -18.917763 | -19.046103 | -13.815381 | NaN |
| 1 | 27.005 | -6.646184 | -8.540800 | -6.568911 | -12.125327 | -18.928712 | -19.066829 | -13.843123 | NaN |
| 2 | 27.010 | -6.649757 | -8.544182 | -6.573449 | -12.152075 | -18.937797 | -19.086046 | -13.870827 | NaN |
| 3 | 27.015 | -6.653426 | -8.547610 | -6.578085 | -12.178871 | -18.945013 | -19.103735 | -13.898486 | NaN |
| 4 | 27.020 | -6.657195 | -8.551087 | -6.582822 | -12.205712 | -18.950357 | -19.119880 | -13.926098 | NaN |

In [ ] **:** df**.**describe()
Out[ ]:

| | Freq [GHz] | S [dB] | | | | | | | Label |
|---|---|---|---|---|---|---|---|---|---|
| | | (port2,port1) | (port3,port2) | (port4,port3) | (port1,port1) | (port2,port2) | (port3,port3) | (port4,port4) | |
| count | 401 | 401.000000 | 401.000000 | 401.000000 | 401.000000 | 401.000000 | 401.000000 | 401.000000 | 0.0 |
| mean | 28 | -10.792732 | -12.467772 | -10.999504 | -16.446961 | -15.013919 | -15.405158 | -17.345065 | NaN |
| std | 0.57 | 4.541358 | 4.531605 | 4.583776 | 2.789254 | 2.366626 | 3.448891 | 3.792028 | NaN |
| min | 27 | -21.507139 | -26.662653 | -21.460189 | -20.871446 | -18.955436 | -21.560745 | -26.023911 | NaN |

| | | | | | | | | | |
|---|---|---|---|---|---|---|---|---|---|
| 25% | 27.5 | -13.472230 | -13.355841 | -13.846460 | -19.310807 | -17.225271 | -18.588270 | -19.054779 | NaN |
| 50% | 28 | -8.799555 | -10.711812 | -9.028234 | -15.334269 | -14.956879 | -15.082454 | -15.368085 | NaN |
| 75% | 28.5 | -7.101835 | -9.447719 | -7.231478 | -14.304857 | -12.700886 | -12.092996 | -14.806747 | NaN |
| max | 29 | 6.642706 | -8.537461 | -6.564469 | -12.098631 | -11.687429 | -10.802069 | -13.815381 | NaN |

```
In [ ]:
# get the index of min of each Row and put it in the last column

new_columns = {'Freq [GHz]': "Freq",
'dB(S(port2,port1)) []': "Port21",
'dB(S(port3,port2)) []': "Port32",
'dB(S(port4,port3)) []': "Port43",
'dB(S(port1,port1)) []': "Port1",
'dB(S(port2,port2)) []': "Port2",
'dB(S(port3,port3)) []': "Port3",
'dB(S(port4,port4)) []': "Port4",
'Label': "minReturnLoss"}


df.rename(columns=new_columns, inplace=True)
df["minReturnLoss"] = df.iloc[:, 1:].min(axis=1)
df["portName"] = df.iloc[:, 1:].idxmin(axis=1)
```

In [ ] : df.head()
Out[ ]:

| | Freq | Port21 | Port32 | Port43 | Port1 | Port2 | Port3 | Port4 | Min return loss | Port name |
|---|---|---|---|---|---|---|---|---|---|---|
| 0 | 27.000 | -6.64270 | -8.537461 | -6.564469 | -12.098631 | -18.917763 | -19.046103 | -13.815381 | -19.046103 | Port3 |
| 1 | 27.005 | -6.64618 | -8.540800 | -6.568911 | -12.125327 | -18.928712 | -19.066829 | -13.843123 | -19.066829 | Port3 |
| 2 | 27.010 | -6.64975 | -8.544182 | -6.573449 | -12.152075 | -18.937797 | -19.086046 | -13.870827 | -19.086046 | Port3 |
| 3 | 27.015 | -6.65342 | -8.547610 | -6.578085 | -12.178871 | -18.945013 | -19.103735 | -13.898486 | -19.103735 | Port3 |
| 4 | 27.020 | -6.65719 | -8.551087 | -6.582822 | -12.205712 | -18.950357 | -19.119880 | -13.926098 | -19.119880 | Port3 |

In [ ]:

```
# convert the portName to a number
df["portName"] = df["portName"].map({"Port21": 0, "Port32": 1, "Port43": 2,"Port1": 3, "Port2": 4, "Port3": 5, "Port4": 6})
```

In [ ]:

```
x = df.iloc[:, 1:-2]
y = df.iloc[:, -1]
```

In [ ]:

```
# to categorical one hot encoding
from keras.utils import to_categorical

y = to_categorical(y, num_classes=7)
```

In [ ]: x.head()

Out[ ]:

| | Port21 | Port32 | Port43 | Port1 | Port2 | Port3 | Port4 |
|---|---|---|---|---|---|---|---|
| 0 | -6.642706 | -8.537461 | -6.564469 | -12.098631 | -18.917763 | -19.046103 | -13.815381 |
| 1 | -6.646184 | -8.540800 | -6.568911 | -12.125327 | -18.928712 | -19.066829 | -13.843123 |
| 2 | -6.649757 | -8.544182 | -6.573449 | -12.152075 | -18.937797 | -19.086046 | -13.870827 |
| 3 | -6.653426 | -8.547610 | -6.578085 | -12.178871 | -18.945013 | -19.103735 | -13.898486 |
| 4 | -6.657195 | -8.551087 | -6.582822 | -12.205712 | -18.950357 | -19.119880 | -13.926098 |

In [ ]: y[0:5]

Out[ ]:

```
array([[0., 0., 0., 0., 0., 1., 0.],
       [0., 0., 0., 0., 0., 1., 0.],
       [0., 0., 0., 0., 0., 1., 0.],
       [0., 0., 0., 0., 0., 1., 0.],
       [0., 0., 0., 0., 0., 1., 0.]], dtype=float32)
```

In [ ]:

```
from sklearn.model_selection import train_test_split
X_train, X_test, y_train, y_test = train_test_split(x,y, test_size=0.2, random_state=42)
```

In [ ]:

```
from sklearn.ensemble import RandomForestClassifier
from sklearn.metrics import accuracy_score
from sklearn.metrics import classification_report
```

**Train the model**

In [ ]:

```
model = RandomForestClassifier()
model.fit(X_train, y_train)
```

Out[ ]: RandomForestClassifier
RandomForestClassifier()

**Test the models**

```
In [ ]: predictions = model.predict(X_test)
   In [ ]: print("Accuracy score for RandomForestClassifier: ", accuracy_score(y_test,
                                                                                    predictions))
        Accuracy score for RandomForestClassifier:  0.9876543209876543
In [ ]: print("Classification report for RandomForestClassifier: ")
        print(classification_report(y_test, predictions))
        Classification report for RandomForestClassifier:
           precision    recall  f1-score   support

         0      1.00      1.00      1.00         3
         1      0.88      1.00      0.93         7
         2      1.00      1.00      1.00         6
         3      1.00      1.00      1.00         9
         4      0.00      0.00      0.00         0
         5      1.00      1.00      1.00        29
         6      1.00      0.96      0.98        27

   micro avg      0.99      0.99      0.99        81
   macro avg      0.84      0.85      0.84        81
weighted avg      0.99      0.99      0.99        81
 samples avg      0.99      0.99      0.99        81
```

**Print the confusion matrix**

```
In [ ]: from sklearn.metrics import confusion_matrix
        import seaborn as sns
        import matplotlib.pyplot as plt
        import pandas as pd
 ports = ['Port21', 'Port32', 'Port43', 'Port1', 'Port2', 'Port3', 'Port4']
y_test_index = np.array([ports[i] for i in np.argmax(y_test, axis=1)])
y_pred_index = np.array([ports[i] for i in np.argmax(predictions, axis=1)])
cm = confusion_matrix(y_test_index, y_pred_index, labels=ports)
df_cm = pd.DataFrame(cm, index = ports, columns = ports)
plt.figure(figsize = (10,7))
sns.heatmap(df_cm, annot=True, fmt='g')
 plt.show()
```

## Appendix B

**The schematic structure for a proposed design in ADS**

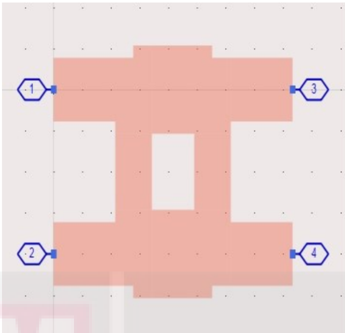

(a)

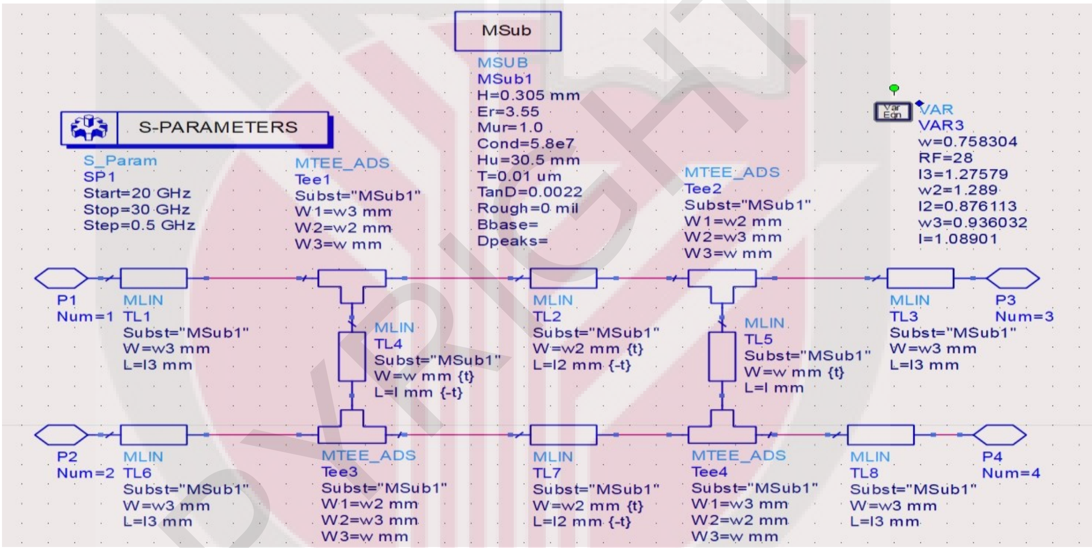


(b)

**Figure 1 : Hybrid Branch Line Coupler proposed in ADS (a) symbol (b)The schematic structure**

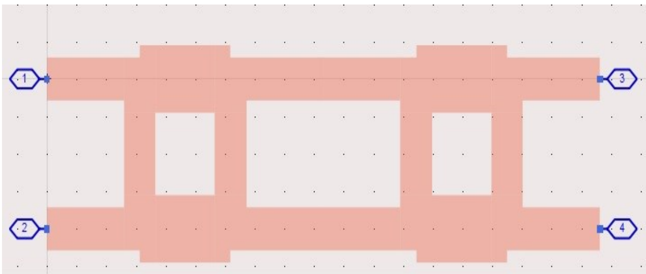


(a)

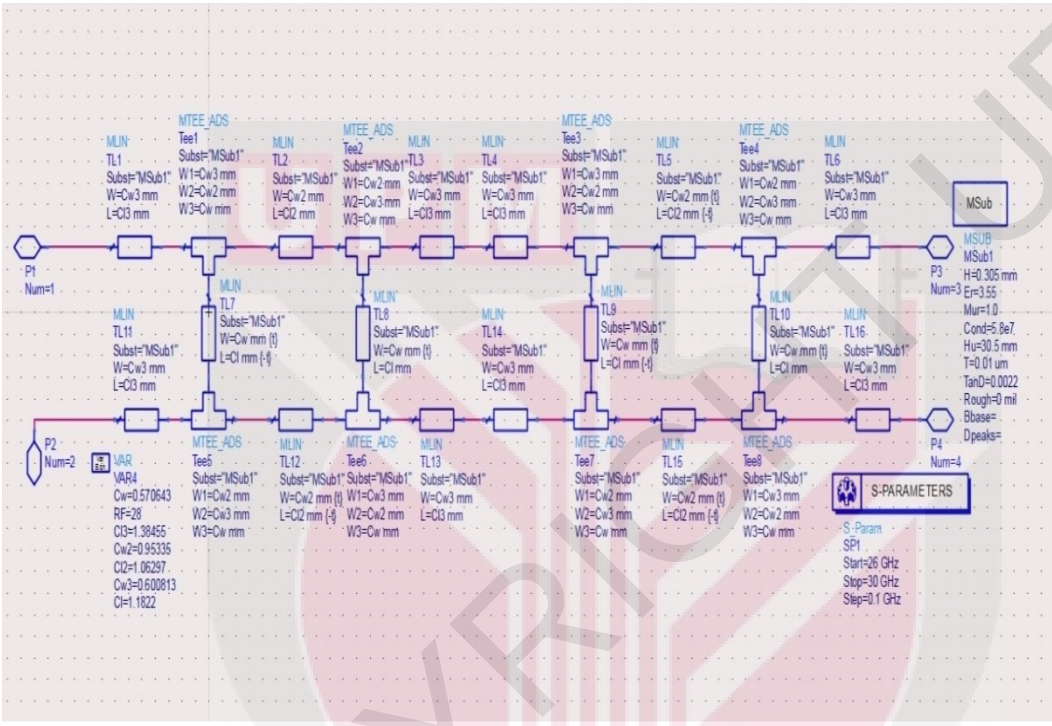


(b)

**Figure 2 : The crossover structure proposed in ADS (a) symbol (b)The schematic structure**

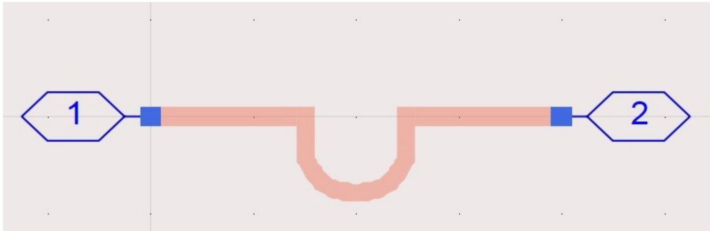


(a)

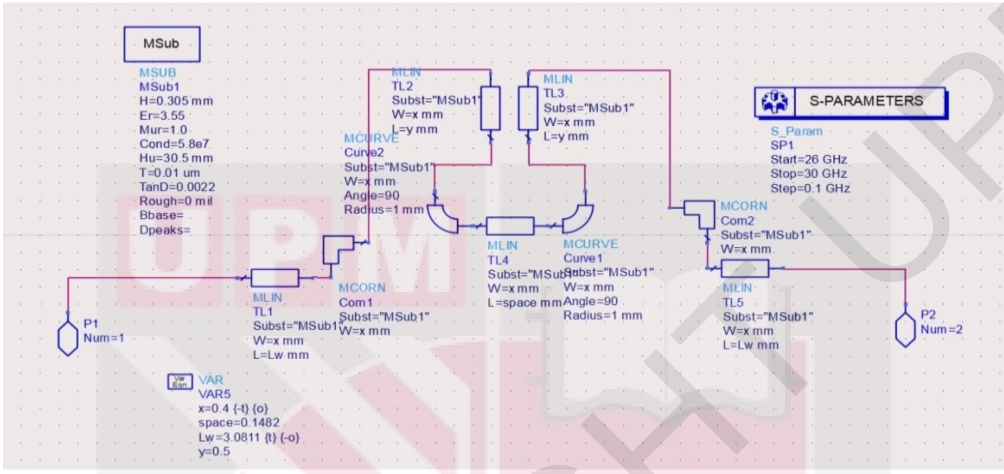


**(b)**

**Figure 3 : The phase shifter proposed in ADS (a) symbol (b)The schematic structure**

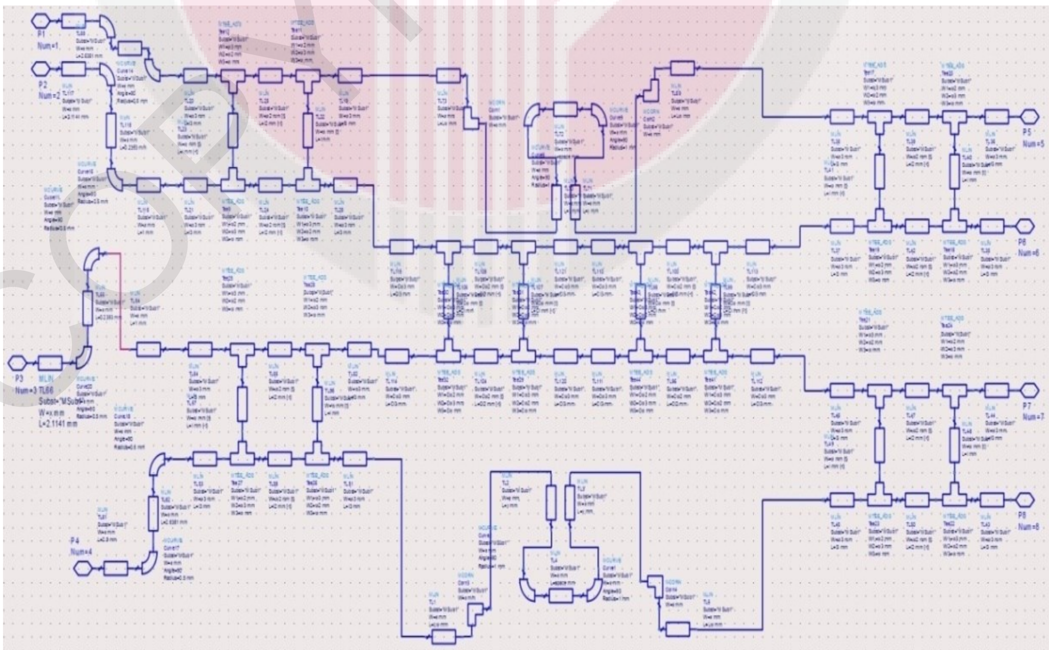

**Figure 4 : The schematic of an schematic 4X4 butler matrix proposed**

# LIST OF PUBLICATIONS

Sadiq, M., bin Sulaiman, N., Isa, M. M., & Hamidon, M. N. (2022). A Review on Machine Learning in Smart Antenna: Methods and Techniques. TEM Journal, 11(2), 695.

Sadiq, M., Sulaiman, N. B., Mohd, M. B., & Hamidon, M. N. (2022). Design and Simulation of Meander Line Antenna for Operating Frequency at 2.5 GHz Based on Defected Ground Structure. In Next Generation of Internet of Things: Proceedings of ICNGIoT 2022 (pp. 359-367). Singapore: Springer Nature Singapore.

Sadiq, M., Sulaiman, N. B., Mohd, M. B., & Hamidon, M. N. (2022). Multiband Handheld Antenna with E-shaped Monopole Feeding. In Next Generation of Internet of Things: Proceedings of ICNGIoT 2022 (pp. 391-398). Singapore: Springer Nature Singapore.

**Submitted paper :**

1. A Miniaturized Multi-Beam Wideband High Gain-5G Antenna Based on a Novel Design of Compact 4x4 Butler Matrix.

Submitted in : APPLIED COMPUTATIONAL ELECTROMAGNETICS SOCIETY JOURNAL.
Publisher: APPLIED COMPUTATIONAL ELECTROMAGNETICS SOC, UNIV MISSISSIPPI, DEPT ELECTRICAL ENGINEERING, UNIVERSITY, USA, MS, 38677.

2. Modelling for Intelligent Antenna Based on Embedded Control Chip.

Submitted in : Cybernetics and Information Technologies.
Publisher: Institute of Information and Communication Technologies, Bulgarian Academy of Sciences.